CAPACITANCE RESISTANCE MODEL IN A CONTROL SYSTEMS FRAMEWORK: A TOOL FOR DESCRIBING AND CONTROLLING WATERFLOODING RESERVOIRS

A Thesis

by

RAFAEL WANDERLEY DE HOLANDA

Submitted to the Office of Graduate and Professional Studies of
Texas A&M University
in partial fulfillment of the requirements for the degree of

MASTER OF SCIENCE

Chair of Committee,	Eduardo Gildin
Committee Members,	Shankar P. Bhattacharyya
	Thomas A. Blasingame
Head of Department,	A. Daniel Hill

August 2015

Major Subject: Petroleum Engineering

ABSTRACT

The Capacitance Resistance Model (CRM) is a fast way for modeling and simulating gas and waterflooding recovery processes, making it a great tool for improving flood management in real time. CRM is an input-output and material balance-based model, and uses only the most reliable data gathered throughout the production life of a flooded reservoir, which are bottom-hole pressures and production/injection rates. In this work, the CRM input-output relationship is explored by representing CRM in a control systems framework with state-space (SS) equations and transfer functions. Systems identification is applied for history matching using only production data to characterize the reservoir, evaluating interwell connectivities, time constants and productivity indices.

A linear system SS equations define the relationship between inputs, outputs and states to completely describe system dynamics. We estimate the CRM parameters using a grey-box system identification algorithm, where production rates are computed simulating the system with SS-CRM instead of using ODE solutions as in prior works. The matrix form of the CRM history matching and a sensitivity analysis to the CRM parameters estimates are presented. Minimal realizations and reduced order models are easily obtained with the SS-CRM approach. The performance of three types of CRM formulations are analyzed: integrated (ICRM), producer based (CRMP), injector-producer based (CRMIP). Also, the methodology developed here are tested in three different reservoir setups: 1) homogeneous with flow barriers; 2) channelized; 3) shoreface environment.

The new formulation in terms of state-space allows to write the CRM in a matrix representation, this provides more insight into reservoir behavior and is computa-

tionally faster. SS-CRM facilitates closed loop reservoir management by enabling CRM's use for linear control algorithms, which can improve tracking performance and predictability, and is amenable to real time optimization. Expressing the history matching problem using matrices provides structure and facilitates its implementation. CRM represented as a multi-input multi-output model is easier to apply in fields with large number of wells.

DEDICATION

Since I was born, I'm continuously receiving support, motivation and inspiration from several people around the globe, which led me to live this international masters experience. I'm really thankful to all of them.

This thesis is specially dedicated to:

- My parents, for their unconditional love and support, as well as for encouraging me to do my best;
- My siblings, for being the best partners throughout my life, for their friendship and inspiration;
- My relatives and friends, for the good memories, making life more enjoyable;
- Kokel and Rosofsky families, for the love, support, delicious food and english assistance;
- My roommates (Gorgonio Fuentes, Sardar Afra and Andre de Moraes), for being part of my family in the USA;
- My advisor (Dr. Gildin) and officemates, for the insightful and collaborative work environment, and friendship;
- The reader, who is the focus of this work and the one capable of using the knowledge developed here to improve industry practices.

ACKNOWLEDGEMENTS

I gratefully acknowledge the guidance and suggestions of Dr. Eduardo Gildin, who was always very helpful, inspiring and considerate since the beginning of my journey at Texas A&M University in 2012 as an undergraduate intern.

I also want to extend special thanks to the following individuals: Dr. Thomas Blasingame (Texas A&M University), for encouraging me to do a comprehensive review on CRM and its applicability to unconventional reservoirs; Dr. Jerry Jensen (University of Calgary) and Dr. Shah Kabir (Hess Corporation), for being available to share their knowledge on CRM; Dr. Wolfgang Bangerth (Texas A&M University), for teaching me numerical optimization, and improving my understanding of the history matching problem; Dr. Shankar Bhattacharyya (Texas A&M University), for teaching me control theory; Dr. Mauro Becker (Petrobras) and Dr. Ibere Alves (Texas A&M University, previously in Petrobras) for my internship experience, contributing to my knowledge on the reservoir simulation's role to overcome the energy challenges worldwide; my officemates, specially Mohammadreza Ghasemi, Gorgonio Fuentes-Cruz, Sardar Afra and Mohammadali Tarrahi, for the constant and uncountable assistance, such as concepts clarification and Matlab tutoring; Dr. Bernardo Horowitz (Federal University of Pernambuco, UFPE), Dr. Leonardo Guimaraes (UFPE) and M.S. Manuel Fragoso (Petrobras) for continuously encouraging me to gain knowledge in reservoir simulation since my undergraduate program at UFPE.

I also want to thank and highlight the importance of the following institutions: Fundation CMG (FCMG), for funding this research and providing a good learning environment for reservoir simulation; Texas A&M University, for providing excellent infrastructure and resources to maximize knowledge; UFPE, PRH(Human Resources

Program)-26, PRH-28 for introducing me to the oil industry during my undergraduate program.

TABLE OF CONTENTS

Page

LIST OF FIGURES

FIGURE Page

LIST OF TABLES

TABLE Page

1. INTRODUCTION

1.1 Problem Statement

The ultimate goal of reservoir modeling and simulation is to obtain a model that can reliably predict the reservoir behavior and be used to achieve the best management strategy in a timely manner. Usually, it involves an integration of several disciplines and can become a quite complex task to be performed in a timely manner. Besides the physical complexity of the porous media flow phenomena itself, the fact that petroleum reservoirs are data poor environments makes the process even more challenging. Few reservoir properties are directly measured, and many of them have to be inferred, which frequently results in complex models with high uncertainty. Furthermore, acquiring data can be quite expensive in the oil industry. Thus, it is very important to ensure that the data acquired significantly contribute to the improvement of the decision making process. Another problem is that data analysis is time consuming, since data from different sources have to be examined and interpreted to be incorporated in a reservoir model, and very often the industry is pressed to make decisions in a daily basis with limited amount of resources.

Simplified reservoir models emerge as an attempt to overcome the problems previously mentioned. In this context, the capacitance resistance model (CRM) characterizes a flooded reservoir by estimating interwell connectivities, time constants and productivity indices using only the producers' bottom hole pressure (BHP) and production/injection rates for history matching. This results in fast and cheap reservoir modeling and simulation [62, 46, 59], which can be used for optimization in real time. Similarly, other simplified models for waterflooding reservoirs have been proposed in the literature, as for example the flow-network model [32], and interwell numerical

simulation model (INSIM) [64].

In 1942, when the first capacitor resistor circuit was used to mimic the reservoirs behavior under waterflooding, the experiment was mainly justified by the lack of computational power to solve the large scale problem of reservoir simulation [3]. Nowadays, the oil industry tackles another paradigm, namely the real-time recovery and optimization. Even though the computational power is available to run large reservoir grid-based models and support the decision making process, optimization algorithms require running numerous simulations, which is unfeasible in many cases. Furthermore, due to the high uncertainty related to some important parameters (e. g. porosity and permeability), robust mathematical solutions still can be very doubtful for managerial decisions, requiring many realizations for the geologic model and estimates of worst and best case scenarios. In this context, reduced complexity models are the best alternative for optimization purposes, because they are much faster to run, provide a good physical understanding of the reservoir, and usually present an objective function with smoother surface, which keeps the optimization algorithm from getting stuck in a local minima. For these reasons, CRM has been applied as flooding management tool in many fields [47, 45].

The underlying idea of CRM is that the reservoir can be thought out as a simple data-driven input-output model governed by linear material balance differential equations. The inputs, injection rates and bottomhole pressures, are the variables that can be manipulated to control the outputs, which are production rates, the variables with economical value. This input-output representation uses only the most accurate information from the system. In this context, the actual literature misses a valuable point of view that is to use the linear control theory to improve CRM's applicability, since it provides a very consistent basis to represent CRM in a control systems framework. Also, the CRM equations have been written individually for

each well, instead of using a matrix format to represent the reservoir behavior, as it is done in grid-based reservoir simulation.

1.2 Chapter Layouts

In chapter 2, we document the progression of CRM since its inception by doing a comprehensive literature review. Even though the underlying physical analogy between electrical circuits and petroleum reservoirs is still the same [3], formulations and applications considerably evolved with time.

Since CRM is an input-output model with the dynamics governed by linear material balance differential equations, we see a great potential for applying linear control theory algorithms. In chapter 3, we derived the state space equations for CRMT, CRMP, CRMIP, and the transfer functions for CRMT, CRMP, CRMIP, CRMIP-Block and the CRM for unconventional reservoirs [52]. Such approach improves the understanding of the input-output relationship, allows fast computation and analysis of CRM in a reservoir scale, instead of a well by well basis, and facilitates real-time optimization.

In chapter 4, the history matching problem is described as a grey-box system identification algorithm. The physical meaning of the CRM parameters and their deviations from the assumption of being constant are also discussed. Data preprocessing for the experiments done in this thesis are also explained. The history matching with its constraints was also formulated in a matrix format, which is suitable to implement with optimization algorithms. The production rates for the history matching objective function were computed by simulating the system with the state space equations, instead of the ODE analytical solution as in previous works [63, 47, 60].

In chapter 5, the state-space equations with grey-box system identification is val-

idated with three reservoirs with different geological environments: 1) homogeneous with flow barriers; 2) channelized; 3) shoreface environment. The performance of ICRM, CRMP and CRMIP are assessed. Minimal realizations and reduced order models are easily obtained from CRMIP, which means that it is possible to obtain simpler models than CRMIP that are capable to preserve its dynamics.

2. CAPACITANCE RESISTANCE MODEL BACKGROUND

This chapter covers several formulations for the Capacitance Resistance Model (CRM), presenting the equations and highlighting the applicability of each one. It is a comprehensive literature review of what has been done in this topic of research.

2.1 First Lab Experiments and Underlying Analogy

Oil has been commercially produced much earlier than the first computer's invention. Even though reservoir simulation has been used to facilitate the decision making process in the last decades, there was always a need to have tools that could support such a process. In 1942, Bruce [3] developed a capacitor resistor circuit to mimic the fluid flow behavior in a water-drive reservoir.

The basic idea was to explore the similarities between fluid flow in a porous media (such as a reservoir rock) and electrons flow (current) in a conductor (such as a wire). In the electrical circuit, a potential difference (ΔE) in a conductor generates a current (I). According to Ohm's Law, I is proportional to ΔE and inversely proportional to the resistance (R). Analogously, fluid flow in a reservoir (q) results from a pressure difference (Δp). According to Darcy's law, flowrate is proportional to pressure difference. From a macroscopic point of view, Darcy's law can be applied to obtain the well deliverability equation ($q = J\Delta p$, where $\Delta p = \bar{p} - p_{wf}$), therefore one can see that the resistance (R) is equivalent to the inverse of the well index ($R = \frac{1}{J}$). In both systems (circuit and reservoir), resistance is a function of cross-sectional area and length, as well as another intrinsic properties of the system (resistivity in the electrical circuit and mobility in the reservoir, $\frac{k}{\mu}$) [52].

In an electrical circuit, a capacitor stores energy in the form of an electrical charge. Capacitance is defined as ratio of the stored energy to the voltage (ΔE) applied to

such capacitor. If a constant current is applied to a pure capacitance, the voltage will change linearly over time, i. e. $I = C\frac{dE}{dt}$. Similarly in a reservoir, capacitance can be thought out as the ability of the system to supply energy (pressure). Thus, it is the ratio of cumulative fluid produced to the pressure depletion (difference) caused by the displacement of such fluids, i. e. $q = -C\frac{dp}{dt}$. According to the compressibility equation, capacitance can be expressed as the product of the total system compressibility and the reservoir volume being depleted. Table 2.1 summarizes the analogies between these two systems [52]:

Table 2.1: CRM's underlying analogies (adapted from [52]).

	Capacitor Resistor Circuit	Reservoir and Wells System
Driving force:	voltage difference, ΔE	pressure difference, Δp
Flow equation:	Ohm's law, $I = \frac{\Delta E}{R}$	deliverability eq., $q = J\Delta p$
Storage equation:	Faraday eq.	compressibility eq.
Resistance, R:	f_1(material property, A_c,L)	f_2(fluid/rock properties, A_c,L)
Capacitance, C:	$C = \frac{Idt}{dE}$	$C = -\frac{qdt}{dp}$

Based on these analogies, Bruce [3] was able to history match his apparatus by controlling potential (pressure) difference and currents (flowrates). An experiment based on the same concepts was conducted in 1962, when an extremely large capacitor-resistor circuit with a control equipment was built to simulate the production of four of the most prolific Saudi Arabian fields. The history matching was based in a trial and error procedure, where the authors adjusted resistances and capacitances until the voltage history of each controller in the circuit agreed with the pressure history of the wells in the fields. Then, this huge network was used to forecast oil production [57]. The next sections present the evolution of the mathematical models based on the capacitance resistance analogy, which have been applied to real

fields.

2.2 Correlating Injection and Production Rates

Albertoni and Lake [1] suggested two simplified models to predict liquid rates in waterflooding and infer interwell connectivity based on injection rates. The first model accounts for unbalanced waterflooding, that is when the field injection rate is significantly different from the field production rate. In such case, the production rate (q_j) of producer j is given by the linear combination of the injection rates (i), plus a constant (f_{0j}) that accounts for the unbalance, as follows:

$$q_j(t) = f_{0j} + \sum_{i=1}^{N_{inj}} f_{ij} i_i(t) \qquad (j = 1, 2, ..., N_{prod}) \tag{2.1}$$

where N_{inj} is the total number of injectors, N_{prod} is the total number of producers, and f_{ij} are the weighting coefficients correlating injector i to producer j. The system of equations above is a multivariate linear regression (MLR), similar to a simple kriging problem. Thus, the unknowns (weighting coefficients, f_{ij}, and constant term, f_{0j}) are determined exactly as in a simple kriging: minimizing the variance to obtain f_{ij}'s and computing the expected values of the known variables to obtain f_{0j}. The weighting coefficients (f_{ij}) are equivalent to injector-producer connectivity.

The second model proposed was applicable to balanced waterflooding, that is when total injection rate and total production rate are approximately equal. In this case, the constant term is zero, as shown below [1]:

$$q_j(t) = \sum_{i=1}^{N_{inj}} f_{ij} i_i(t) \tag{2.2}$$

This system of equations was called balanced multivariate linear regression (BLMR), and it has the same structure and solution as the ordinary kriging.

Equations 2.1 and 2.2 account for incompressible fluids. Actually, for the case of compressible fluids there is a time delay and attenuation in the production rates' response when the injection rates vary. In order to account for such dissipation in the stimulus signal (injection), diffusivity filters were applied to the injection rates as shown in the following equations for BLMR [1]:

$$q_j(t) = \sum_{i=1}^{N_{inj}} f_{ij} i_{ij}^c(t) \tag{2.3}$$

where $i_{ij}^c(t)$ are the transformed injection rates for the effect of compressibility, which are computed as follows:

$$i_{ij}^c(t) = \sum_{n=0}^{N_t} \alpha_{ij}^{(n)} i_i(t-n) \tag{2.4}$$

Basically, the coefficients $\alpha_{ij}^{(n)}$ quantify the influence of previous injection rates in the actual production rate, N_t is the number of time steps considered in the diffusivity filters. These filters are used to transform the response of the compressible system in an incompressible system.

2.3 CRM: A Material Balance Based Model

The MLR and BMLR models were not material balance based models. Moreover, they could not account for the effects of bottom hole pressure (p_{wf}) variation, and the diffusivity filters required the evaluation of many coefficients to account for the time lag. Thus, based on the analogies first presented by Bruce [3], Yousef et al. [63] proposed a Capacitance Resistance Model (CRM) to describe the production behavior of waterflooding reservoirs. The material balance equation can be written as follows:

$$\text{accumulation within system} = \text{flow in} - \text{flow out} \tag{2.5}$$

$$c_t V_p \frac{d\bar{p}}{dt} = i(t) - q(t) \tag{2.6}$$

where c_t is total compressibility, V_p is pore volume, $\bar{p}$ is average pressure, $i(t)$ is injection rate and $q(t)$ is total production rate (oil and water). The deliverability equation is given by:

$$q = J(\bar{p} - p_{wf}) \tag{2.7}$$

Thus, $\bar{p}$ can be expressed in terms of q, p_{wf} and J (productivity index):

$$\bar{p} = \frac{q}{J} + p_{wf} \tag{2.8}$$

Substituting equation 2.8 in 2.6, the following expression is obtained:

$$\tau \frac{dq}{dt} + q(t) = i(t) - \tau J \frac{dp_{wf}}{dt} \tag{2.9}$$

where τ is the time constant given by:

$$\tau = \frac{c_t V_p}{J} \tag{2.10}$$

The time constant was incorporated into the model to capture the time lag and attenuation of the systems' response (production rates) to the stimulus (injection rates and BHP variation). Thus, it substituted the use of diffusivity filters in the previous model.

In order to have more accurate results and describe pressure and saturation propagation in the models, grid-based reservoir simulators can generate fine grids to obtain more resolution. Likewise, the reservoir domain can also be discretized in several ways when using CRM. Superposition in time and space is used to extend the material balance equation 2.9 to cases with multiple injectors and producers as done in

[63, 62, 48, 46, 33]. In the following subsections four CRM discretization schemes will be presented: CRMT (single tank representation), CRMP (producer based representation), CRMIP (injector-producer pair based representation), and CRM-block (blocks in series representation).

2.3.1 CRMT: Single Tank Representation

The control volume for CRMT is the drainage volume of the entire reservoir (figure 2.1). A material balance is computed by assuming only two wells: 1) a single pseudo-producer, that sums all the production rates, and 2) single pseudo-injector, that sums all the injection rates. So, the whole reservoir has only one time constant and one productivity index. The parameter f (connectivity or gain) is introduced in the differential equation to account for effective injection, in other words, the effects of leakage ($f < 1$) or aquifer pressure support ($f > 1$), as described by Weber [59]. Therefore, the differential equation for CRMT is given by:

$$\tau \frac{dq(t)}{dt} + q(t) = fi(t) - \tau J \frac{dp_{wf}(t)}{dt} \tag{2.11}$$

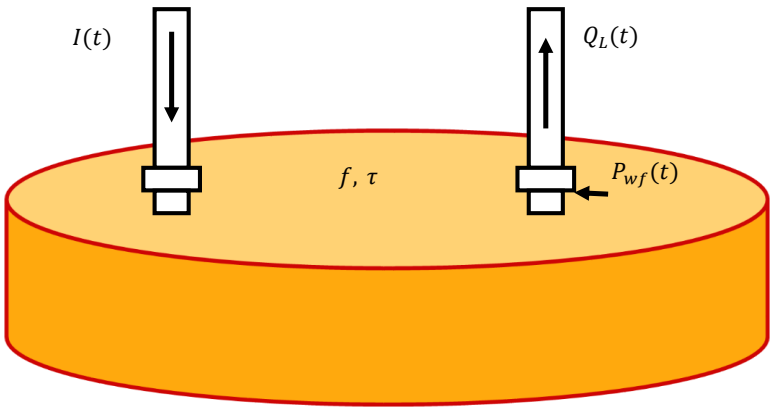

Figure 2.1: Single tank representation (CRMT).

This formulation is similar to the classical chemical engineering control problem of a first-order tank, where the inlet rate is used to predict and control the level of an incompressible fluid in the tank and outlet rate [50]. For such reason, CRMT is called a *single tank representation* of the whole reservoir control volume.

Assuming that injection rate varies as a step and bottom hole pressure varies linearly in a discrete time interval, the ordinary differential equation 2.11 can be solved analytically by integrating over a discrete time step (Δt), giving the following solution [46]:

$$q_k = q_{(k-1)} e^{-\frac{\Delta t}{\tau}} + \left(1 - e^{-\frac{\Delta t}{\tau}}\right) \left(fi_k - J\tau \frac{p_{wf}^{(k)} - p_{wf}^{(k-1)}}{\Delta t} \right), \tag{2.12}$$

where k indicates the k^{th} time step. As one can see, the solution of the differential equation 2.11 is the superposition in time of three factors:

1. primary production $\left(q_{(k-1)} e^{-\frac{\Delta t}{\tau}}\right)$;
2. injection $\left(\left(1 - e^{-\frac{\Delta t}{\tau}}\right) fi_k\right)$;
3. BHP variation $\left(\left(1 - e^{-\frac{\Delta t}{\tau}}\right) \left(-J\tau \frac{p_{wf}^{(k)} - p_{wf}^{(k-1)}}{\Delta t}\right)\right)$.

The CRMT representation can rapidly history match and predict total field production rates, and its estimated parameters are an useful initial guess for other more robust representations. CRMT is not suitable for optimization because it does not estimate the production rates of each producer separately.

2.3.2 CRMP: Producer Based Representation

It is usually important to analyze and predict well rates separately. More resolution can be obtained if instead of considering pseudo-injectors and pseudo-producers as in CRMT, the actual well rates can be computed individually. As shown in fig-

ure 2.2, the producer based representation (CRMP) divides the reservoir in control volumes ("conceptual grid blocks") based on each producer and including all of the injectors that influences its production rate, which usually are all of them, unless some assumptions are made, such as an specified maximum interwell distance. This formulation was originally introduced in [33].

CRMP considers one time constant (τ_j) for each producer and one connectivity (f_{ij}) for each injector(i)-producer(j) pair, therefore, the continuity equation for producer j becomes:

$$\tau_j \frac{dq_j}{dt} + q_j(t) = \sum_{i=1}^{N_{inj}} f_{ij} i_i(t) - \tau_j J_j \frac{dp_{wf}^{(j)}}{dt} \tag{2.13}$$

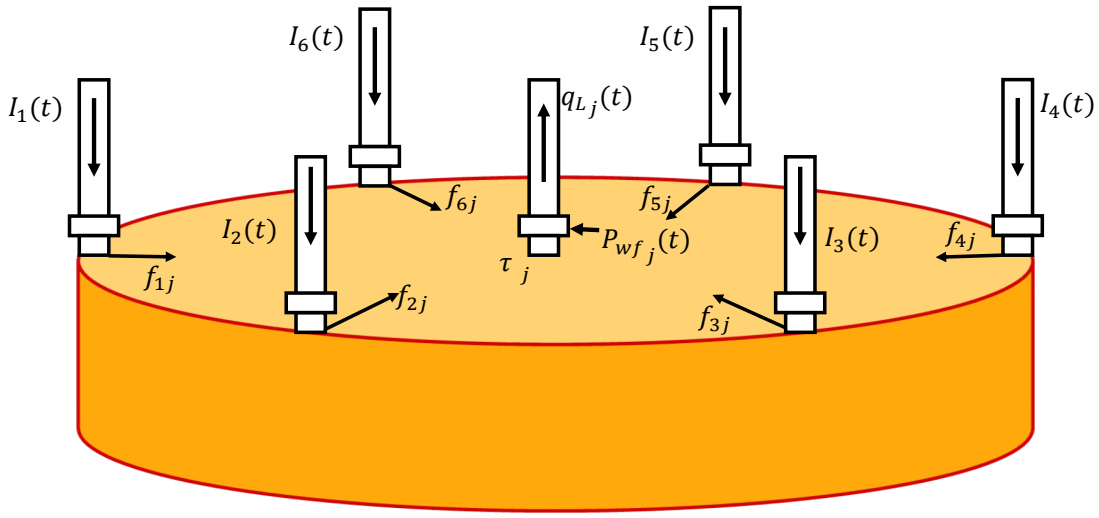

Figure 2.2: Producer based representation (CRMP).

The production rates for a producer j is obtained by integrating equation 2.13 over a discrete time step (Δt) and assuming that injection rates vary as a step and

bottom hole pressures vary linearly in a discrete time interval [46]:

$$q_{jk} = q_{j(k-1)} e^{-\frac{\Delta t}{\tau_j}} + \left(1 - e^{-\frac{\Delta t}{\tau_j}}\right) \left(\sum_{i=1}^{N_{inj}} f_{ij} i_{ik} - J_j \tau_j \frac{p_{wf}^{(jk)} - p_{wf}^{(j(k-1))}}{\Delta t} \right) \tag{2.14}$$

The CRMP representation works better when the reservoir properties are mostly homogeneous around each producer because it considers only one time constant per producer.

2.3.2.1 ICRM: Integrated Capacitance Resistance Model

Nguyen et al. [43] generated the Integrated Capacitance Resistance Model (ICRM) by integrating the simplified continuity material balance equation for the CRMP control volumes in the cases of primary and secondary recovery. Integrating equation 2.13 in time from t_0 to t_k, one gets the model for secondary recovery:

$$\int_{q_{j0}}^{q_{jk}} dq_j + \frac{1}{\tau_j} \int_{t_0}^{t_k} q_j dt = \frac{1}{\tau_j} \sum_{i=1}^{N_{inj}} \left(f_{ij} \int_{t_0}^{t_k} i_i dt \right) - J_j \int_{p_{wf,j}^0}^{p_{wf,j}^k} dp_{wf,j} \tag{2.15}$$

$$N_{p,j}^k = (q_{j0} - q_{jk})\tau_j + \sum_{i=1}^{N_{inj}} \left(f_{ij} CWI_i^k \right) + J_j \tau_j (p_{wf,j}^0 - p_{wf,j}^k) \tag{2.16}$$

where $N_{p,j}^k$ is the cumulative total liquid production of producer j at t_k, and CWI_i^k is the cumulative volume of water injected in injector i at t_k.

As it will be presented in chapter 4, the ICRM representation is easier to history match because it results in a constrained linear regression for the cumulative production. The implications of this approach will be further discussed in chapter 5.

Kim et al. [29] also highlighted the advantages of ICRM by applying it to three synthetic fields. Besides this, they proposed a linear regression to estimate connectivities between new injectors and existing producers in homogeneous reservoirs based

only on the interwell distance and connectivities of existing wells. Even though this estimation of connectivities for new injectors does not present a very good correlation, the error related to it might not be so large when analyzing field production data so it might be a valid approach under very restricted situations.

2.3.3 CRMIP: Injector-Producer Pair Based Representation

Depending on the heterogeneity of the reservoir in study, different injectors can impact the production rates of a certain producer with different velocities. So, assuming only one time constant for each producer, as in CRMP, will no longer be a reliable model. In such case, it is better to write one continuity equation for each injector-producer pair, obtaining the *injector-producer pair based representation* (CRMIP), as shown in figure 2.3, which assigns one time constant (τ_{ij}) and connectivity (f_{ij}) for each injector(i)-producer(j) pair. Then, the governing differential equation for each control volume is given by:

$$\tau_{ij}\frac{dq_{ij}}{dt} + q_{ij}(t) = f_{ij}i_i(t) - \tau_{ij}J_{ij}\frac{dp_{wf}^{(j)}}{dt} \tag{2.17}$$

Where q_{ij} is the production rate in producer j relative to the injector(i)-producer(j) pair control volume, as well as J_{ij} is the productivity index associated with such control volume. Thus, the total production rate of producer j is simply the sum of all of its control volumes production rates:

$$q_j(t) = \sum_{i=1}^{N_{inj}} q_{ij}(t) \tag{2.18}$$

The ordinary differential equation 2.17 can be integrated analytically over a discrete time step (Δt) to obtain production rates for each control volume, and assuming that injection rates vary as a step and bottom hole pressures vary linearly in each

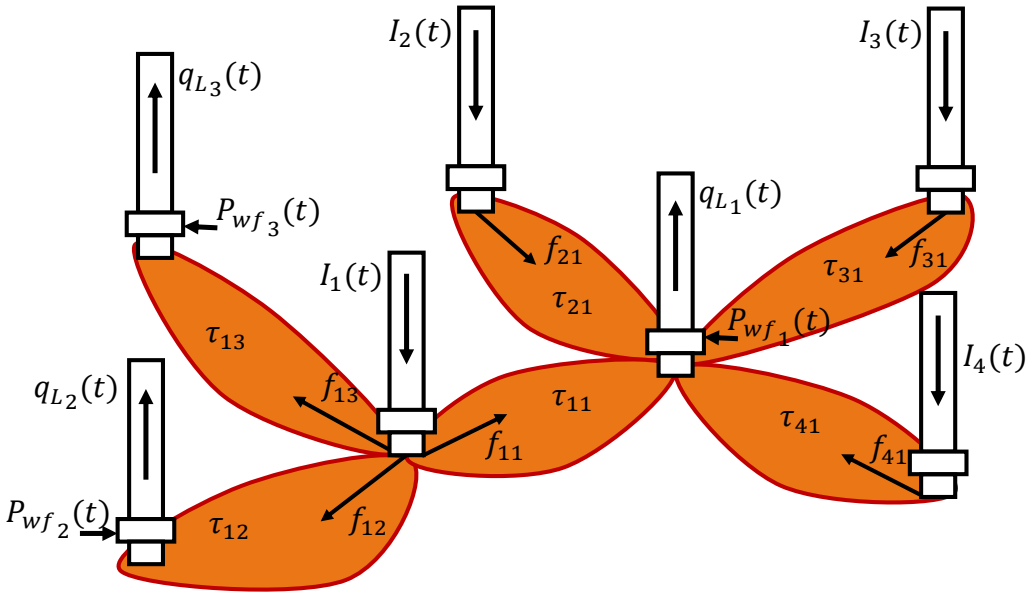

Figure 2.3: Injector-producer pair based representation (CRMIP).

discrete time step [46]:

$$q_{ijk} = q_{ij(k-1)} e^{-\frac{\Delta t}{\tau_{ij}}} + \left(1 - e^{-\frac{\Delta t}{\tau_{ij}}}\right) \left(\sum_{i=1}^{N_{inj}} f_{ij} i_{ik} - J_{ij} \tau_{ij} \frac{p_{wf}^{(jk)} - p_{wf}^{(j(k-1))}}{\Delta t} \right) \tag{2.19}$$

The production rates for each producer can be calculated by substituting Equation 2.19 in 2.18:

$$q_j(t) = \sum_{i=1}^{N_{inj}} \left(q_{ij(k-1)} e^{-\frac{\Delta t}{\tau_{ij}}} + \left(1 - e^{-\frac{\Delta t}{\tau_{ij}}}\right) \left(\sum_{i=1}^{N_{inj}} f_{ij} i_{ik} - J_{ij} \tau_{ij} \frac{p_{wf}^{(jk)} - p_{wf}^{(j(k-1))}}{\Delta t} \right) \right) \tag{2.20}$$

2.3.4 CRM-Block: Block Refinement Representation

Sayarpour [46] extended the CRMT and CRMIP to consider the time delay in the producers response because the first-order tank formulation assumes immediate response to variations in the input signals. Hence, the injector-producer control volume

was divided in several blocks, as a tanks in series model (figure 2.4). This representation was called CRM-Block and is recommended for cases with low permeability, high frequency injection signal, and/or distant injector-producer pairs.

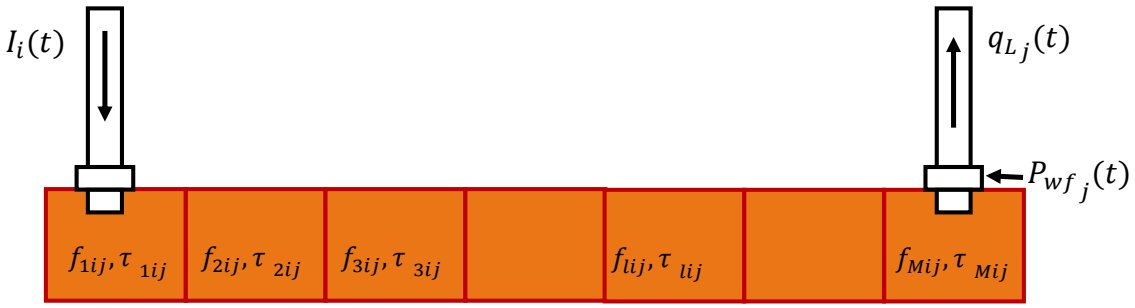

Figure 2.4: Block representation (CRM-Block).

Originally, the CRM-Block formulation was derived from the analytical solution and neglecting the effects of bottom hole pressures variation [46]. Here, the derivation from the differential equations is presented and BHP variation is included, assumptions are discussed as well. Each "conceptual" block l between injector i and producer j represents one reservoir control volume and its dynamics is governed by the same differential equation as CRMIP:

$$\tau_{lij}\frac{dq_{lij}}{dt} + q_{lij}(t) = f_{lij}i_{lij}(t) - \tau_{lij}J_{lij}\frac{dp_{wf}^{(lj)}}{dt} \tag{2.21}$$

If we consider that the total control volume between producer and injector is defined by the streamlines from injector i that arrive to producer j, then it is reasonable to assume that the connectivities are equal to one for all of the blocks, except for the first one:

$$f_{lij} = 1, \quad l = 2, \ldots, M \tag{2.22}$$

$$f_{1ij} = f_{ij} \tag{2.23}$$

where M is the total number of blocks between each injector-producer pair. Following the same assumption, each the production rate for a given block is equal to the injection rate of the next block:

$$i_{lij} = q_{(l-1)ij}, \quad l = 2, \ldots, M \tag{2.24}$$

Indeed the only value of bottom hole pressure ($p_{wf}^{(lj)}$) that is known is the one for the block of the producer well ($p_{wf}^{(Mj)}$), this is the reason why it was totally neglected in a previous work [46]. Here, since BHP is controlled only in the producers and, obviously, impacts the pressure much more in the near wellbore region, $\frac{dp_{wf}^{(lj)}}{dt}$ is assumed to be zero, except in the block M:

$$\frac{dp_{wf}^{(lj)}}{dt} = 0, \quad l = 1, \ldots, M-1 \tag{2.25}$$

This is an empirical assumption, which results in a semi-empirical formulation for CRMIP-Block that is capable to account for the time lag in the response to injection rates variation and also considers BHP variation.

2.3.5 Other CRM Models and Applications

CRM relies on field data to properly estimate connectivities, time constants, and productivity indices by history matching. Once such parameters were estimated, the model can be used for forecasting production. Even though injection and production rates are readily available in the history data, producers' BHP might be missing in a significant amount of practical cases, which leads to an unreliable history matching. In order to address this issue, Kaviani et al. [26] proposed a model to keep track

of the effects of non-measured BHP's. The segmented CRM adds a constant to the analytical solution obtained by Yousef et al. [63] to account for the unknown BHP variation effect in the production rate. The time is always segmented when the BHP of some producer changes. The constants need to be reevaluated to account for the shift that this BHP variation causes to the production rates.

Another problem arises when there are long shut-in time for producers. In such cases, there is a significant change in the flow pattern, causing different allocation of the injected fluids in the reservoir, in other words, connectivity changes. Based on superposition, the compensated CRM treats shut-in producers by keeping it as an open producer and re-injecting all the produced fluid at the same spot. In this sense, connectivities between producers (or producer-virtual injector) is also defined [26].

As discussed before, Sayarpour [46] obtained analytical solutions for CRMT, CRMP, CRMIP and CRM-Block. Taking consecutive data points in the production history, he considered injection rates varying linearly or stepwise between those points while BHP varies only linearly. Even though these material balance equations are capable to forecast the total liquid production rates quite well under specified circumstances, due to economic values, reservoir engineers are more interested in the oil and water production rates separately. Thus, fractional flow models were included in the model to calculate the oil rate from the total production rate for waterflooding and CO_2 flooding; the parameters were obtained by matching the oil production history. Coupling CRM and fractional flow models, an optimal injection strategy to develop fields can be determined, such as defining water reallocation in the reservoir to maximize cumulative oil production.

Since CRM predicts production rates solving the pressure propagation equation for much less control volumes than in the traditional reservoir simulation scheme,

it is expected to incredibly speed up the computational time in optimization problems. Weber et al. [60] defined the main problems regarding CRMs applicability and optimization to reservoir with hundreds of wells. In such cases, hundreds to thousands of parameters have to be estimated, which requires thousands of data points. Therefore, first, it is necessary to be very cautious in the data processing stage, removing outliers, determining shut-in periods, producers that become injectors, and even relaxing some constraints when needed. Additionally, the number of connectivities can be drastically reduced by removing inactive wells, where the flowrates are zero, setting up an upper limit for the interwell distance above which connectivities are considered to be zero, and selecting a cutoff value for connectivities below which they are automatically fixed at zero. This approach was validated by optimizing net present value for two reservoirs, using an empirical fractional flow model to calculate oil rates from the total rates. The results showed that it was possible to obtain significantly more profitable injection strategies using fewer injector than in patterned schemes.

The classical CRM solves only the pressure propagation equation in the reservoir, disregarding saturation effects. To compute the oil production rates, the fractional flow models used earlier were restricted to mature waterflooding (large water cut). Cao et al. [7, 8] developed a fully coupled two-phase flow CRM, which extends CRMs applicability to immature waterflooding cases (low water cut). For this purpose, the oil material balance equation was included in the formulation. It is proved that time constants are actually a function of total mobility, and therefore a function of saturation, and can vary significantly at low water cuts. Since the coupled CRM take such effects into account, it is a more physically based tool, which is expected to perform better for injection strategy optimization [7, 8].

Studying the stratigraphy of a generic reservoir, one may note that it is comprised

of a sequence of several layers, and the rock properties may vary a lot from one layer to the subsequent one such that it is common to have completely some sealing layers. In such case, flow patterns may be also quite different in the several regions of the reservoir that are delimited by sealing layers. So, a better representation of the reservoir would be to compute the material balance equation for each of the permeable layers separately.

A version of CRM to compute the contribution of different layers in the reservoir and the impact of completion status in each layer was proposed by Moreno [39]. This model assigns connectivities for each layer of the reservoir and recalculates them by history matching always that there is a flow pattern change due to opening or shutting-in the completion. Therefore, it assumes dynamic parameters for CRM, but the limitation is that they can only be determined when history data is available, so it is not possible to re-estimate connectivities in each layer for future events.

The adaptiveness of the CRM concept to complex reservoirs was also illustrated by Salazar et al. [45] when CRM was combined with an exponential decline curve model to history match and predict the behavior of a deep highly fractured carbonated field under hydrocarbon gas and nitrogen injection. It was also necessary to consider the water encroachment from the aquifer. Due to the existence of several components and their implications in the field operations, a fractional flow model was developed using multivariate linear regression to compute separately flowrates for water, oil, hydrocarbon gas and nitrogen. The decline curve model was used for the primary depletion period and propagated for the enhanced oil recovery period, when CRM was also used to determine the incremental response to the injection rates.

In order to demonstrate CRMs practicality and reliability, Sayarpour et al. [47] published multiple field examples covering waterflooding and CO_2 flooding projects.

Reservoir description is provided for each case. The good quality of the results for different geological environments, such as carbonate reservoirs and low permeability turbidite, illustrates the applicability of CRM to different levels of heterogeneity. Furthermore, CRM can be used as precursor for grid-based simulation since transmissibility trends, response time and fluids allocation can be easily assessed with this tool.

2.4 CRM for Unconventional Reservoirs

2.4.1 Primary Production

Due to the early exploitation of unconventional resources, it is still a mystery which methods are the best at forecasting their production. Indeed, many different models have been created in order to try to explain the behavior of such reservoirs. In this context, this section also discusses the CRM formulations for unconventional reservoirs.

The CRM-Block analytical solution for primary production derived by Sayarpour [46] was used by Kabir and Lake [21] to represent the decline production behavior of unconventional reservoirs. The reservoir was divided in several concentric conceptual blocks (or "compressibility elements") around a horizontal well. Assuming only primary production, the analytical solution for a well considering M blocks (the well is in the M-th block) becomes:

$$q_M(t) = q_M(t_0)e^{-\frac{t-t_0}{\tau_M}} + \sum_{b=1}^{M-1}\left\{q_b(t_0)e^{-\frac{t-t_0}{\tau_b}}\prod_{a=1}^{M-b}\left(1-e^{-\frac{t-t_0}{\tau_b}}\right)\right\} \tag{2.26}$$

If the time constants for all of the blocks are equal ($\tau_1 = \tau_2 = \cdots = \tau_M = \tau^*$), the

solution is:

$$q_M(t_1) = q_M(t_0)e^{-\frac{\Delta t_1}{\tau^*}} + \sum_{b=1}^{M-1} q_b(t_0)e^{-\frac{\Delta t_1}{\tau^*}} \left(1 - e^{-\frac{\Delta t_1}{\tau^*}}\right)^{M-b}$$

$$= \sum_{b=1}^{M} q_b(t_0)e^{-\frac{\Delta t_1}{\tau^*}} \left(1 - e^{-\frac{\Delta t_1}{\tau^*}}\right)^{M-b} \quad (2.27)$$

In this formulation it is possible to quantify the flowrate of each block at a specific time. The fractional contribution of distant blocks from the well is very low in the beginning and increases with time, so they are like a source. The blocks close to the well have high fractional contribution in the beginning and decrease with time. In this model, the time constant governs the fluid transfer between blocks. Since unconventional reservoirs have very low permeability (in the scale of micro to nano-Darcy), they have high values for time constants, which results in slow signal propagation away from the producer. Major events, e. g. pump installation or restimulation, require another history matching to define the model's time constants again.

The results in [21] are consistent in the fact that blocks far away from the well will have increasing contribution with time to the total production. In other words, as the pressure breakthrough advances and the reservoir's investigated volume grows, the distant regions will start to flow an increasing amount of fluids due to the increasing pressure difference. On the other hand, the reservoir is depleting, so pressure drawdown decreases affecting first the blocks close to the well, because it is where the pressure wave started. Therefore, blocks close to the well have decreasing contribution with time.

Even though Kabir and Lake [21] state that this is a more flexible formulation because BHP variation can be included, there is no analytical solution in the litera-

ture including varying BHP for CRM-Block, not even in the work done by Sayarpour [46]. Here, this issue has been discussed in this chapter and the transfer function for CRMIP-Block will be derived in the next chapter, which accounts for BHP variation. In Sayarpour's [46] equation, an initial flowrate is assumed for every block since the stimulus (injection) comes from the first block (block of the injector) and travels through the reservoir until the M-th block (block of the producer). In other words, stimulus and response are physically located at the extremes of the reservoir control volume. For primary production, it is different; stimulus (BHP) and response (production rate) are in the same spot (producer well); however, the stimulus still will travel through the reservoir (pressure wave) to obtain the response. So, initial flowrates of blocks other than the well block should be zero. For this reason, it is fair to judge that Kabir and Lake [21] representation is reasonable in providing insight of how flow develops in the reservoir, but it comes from an unphysical assumption.

As documented by Mohaghegh [38], full field modeling of shale formations using analytical and numerical methods has been impractical or provided poor results, so data-driven models seems to be the most reasonable alternative. Also, decline curve analysis is simple and easy to implement, providing good results when used appropriately. Other decline curve models are comparable to the CRM presented by Kabir and Lake [21], such as stretched exponential decline model [55], two-tank model [51], three-tank model [4], and variable pressure drop model [17].

Shahamat et al. [52] coupled three simple concepts to predict the declining production behavior of unconventional reservoirs: material balance (compressibility equation), boundary dominated flow (deliverability equation) and distance of investigation. Doing the same analogy to electrical engineering as Bruce [3], the concepts

of capacitance (C) and resistance (R) can be applied to the reservoir giving:

$$q = -C\frac{dp}{dt} \tag{2.28}$$

$$q = \frac{\Delta p}{R} = \frac{p - p_{wf}}{R} \tag{2.29}$$

Substituting reservoir pressure (p) from 2.29 in 2.28, one obtains the following continuity equation:

$$q = -C\left(R\frac{dq}{dt} + \frac{dp_{wf}}{dt}\right) \tag{2.30}$$

Due to transient flow, the investigated reservoir volume increases with time, hence the reservoir's capacitance and resistance vary. So, capacitance and resistance are dynamic variables for transient flow; it violates the assumptions from the classical CRM. Shahamat et al. [52] defined two parameters that describe the reservoir and are not time dependent: capacity and resistivity.

Capacity and resistivity can be calculated analytically for simple flow geometries. The inverse of the multiplication of capacity by resistivity gives hydraulic diffusivity. Using hydraulic diffusivity and capacity resistivity ratio it is possible to calculate the distance of investigation. Once the distance of investigation was defined, capacitance and resistance can be calculated. Assuming a succession of pseudo-steady states with the size of the investigated reservoir increasing during transient flow and constant during boundary dominated flow, the values of flowrates or BHP can be predicted. Linear flow is considered in their work. Flowcharts of the calculation procedure are provided, making it very easy to understand how the three concepts mentioned above are coupled. There are examples for liquid and gas reservoirs, considering two different production scenarios: constant pressure production and constant rate production.

2.4.2 Flooding Processes in Unconventional Reservoirs

Unconventional reservoirs have a very low recovery factor and rapid decline in production. Flooding processes are commonly used in conventional reservoirs to enhance oil recovery. On the other hand, re-fracking has been the most used alternative to increase well flowrates in unconventional reservoirs. Flooding processes are a challenging subject for low permeability reservoirs due to their low injectivity, but it has not gained enough academic and industrial efforts to judge their feasibility, especially due to the fact that unconventional reservoirs are at an early developmental stage. However, few works have pointed out that flooding processes could leverage oil production in such reservoirs.

Morsy et al. [40] tested the impact of brines composition and pH at core samples from Eagle Ford, Marcellus, Barnett and Mancos, proving that these are major factors in the waterflooding efficiency and can significantly affect shale stability. Morsy et al. [42] did a simulation study indicating that the recovery factor in the Eagle Ford could increase from 12% (natural depletion) to 18% by secondary recovery. In this case, key factors in the project design are fracture half-length, fracture spacing between producer and injector, and vertical to horizontal permeability; which are determined by sensitivity analysis. Using core samples, Morsy et al. [41] showed that it is possible to significantly improve the waterflooding performance in shale formations by optimizing fracture orientation and using low pH fracturing fluids.

According to Kurtoglu and Kazemi [30], secondary permeability and porosity (interconnected micro-fractures) are necessary to explain the drive mechanism for waterflooding in the Bakken formation. Even though the matrix contribution is negligible in a short-term, it is significant in a long-term. Numerical experiments done by Fakcharoenphol et al. [12] indicate that waterflooding changes the formation in-situ

stress due to the pressure increase and temperature decrease, which opens macrofractures and creates new microfractures. Therefore, oil production of shale formations is improved by the new paths created and additional interface area between fractures and matrix.

Kurtoglu et al. [31] provided a detailed geologic description to analyze CO_2 flooding potential for a Bakken reservoir. Comparing to water, CO_2 has the advantage that it is more miscible, dissolving in oil easily; it reduces the mixture viscosity, expands the oil, and diffuses across the fracture-matrix interface. Wells are recommended to be placed in areas with more macro and micro-fractures, where the connectivity is higher, because of the greater fracture-matrix interface area, allowing CO_2 to penetrate the matrix. Wang et al. [58] also demonstrated that CO_2 has much better injectivity than water in tight formations and can provide much higher recovery factors, several injection strategies are considered in this study. CO_2 injection in the Bakken formation was also studied by Liu et al. [34], who estimated that oil production could increase by 43% to 58%. They point out that the results are very sensitive to fracture and matrix relative permeability, thus it is fundamental to have accurate relative permeability models to define fracture and matrix flow contributions.

Traditionally, CRM has been mostly applied to flooding processes. Even though unconventional reservoirs have been developed by primary depletion, the previous works mentioned above have indicated that secondary and tertiary recovery are attractive solutions to significantly enhance oil recovery in some reservoirs. Moreover, some unconventional oil plays can have some areas with richer permeability, not in the micro to nano-Darcy scale, where flooding processes are feasible. An example is the pilot waterflooding plant operating in Bakken since 2006 [61]. Since there is a very high number of well in such reservoirs, CRM might be a good model to approach

them due to its simplicity.

A sophisticated approach to evaluate interwell connectivity analytically in tight formations was developed by Soroush [53]. He applied for transient flow a similar method to the one used by Kaviani and Jensen [25] to derive analytical connectivities for boundary dominated flow using multiwell productivity index [56]. Due to the transient flow nature of tight formations, connectivities between injectors and producers are time dependent. In the beginning, all connectivities are equal, because producers cannot feel the influence of injectors. As transient flow evolves, increasing the investigated size of the reservoir, the connectivities will tend smoothly to their constant values at boundary dominated flow. Therefore, the low permeability reservoirs' transient flow behavior results in a linear time-variant system because connectivities and time constants are time dependent.

Furthermore, as mentioned before the porous media suffers significant changes over time, changing the connectivities not only due to the transient flow behavior, but also due to structural transformations in the fracture system [12], which may require several history matching windows to fit the model taking into account such effects.

Because unconventional reservoirs are slow systems, the signals may take too long to reach the producer, or be dissipated on their way; parameters such as permeability and interwell distance are crucial to analyze this. Therefore, closed-loop reservoir management has limited applicability, but real time history matching is still encouraged, since parameters such as capacity and resistivity can be inferred from the transient response.

Soroush [53] also adapted CRM to heavy oil reservoirs, where the non-unit mobility ratio is an important violation of the original assumptions. Using his formulation it was possible to detect the existence of wormhole, as well as its equivalent skin and

rate of growth.

3. CRM IN A CONTROL SYSTEMS FRAMEWORK

CRM describes the flow behavior in a flooded reservoir through a system of linear differential equations. Thus, the reservoir can be thought out as linear system (figure 3.1), where injection rates and producers' BHP are manipulated variables, i. e. inputs, used to control the production rates, i. e. outputs. Since the reservoirs outputs depend only on the past and present input values, it is also classified as a causal system [22, 9]. This chapter describes the process for obtaining CRM state space equations and transfer functions, which represent the reservoir as a multiple-input/multiple-output (MIMO) system.

3.1 State-Space Equations

A simple way to represent a linear system, such as CRM representations, is through state space equations, which converts higher order linear differential equations to a set of first order differential equations. The state space representation defines the relationship between the states of the system, $\mathbf{x}(t)$, the inputs, $\mathbf{u}(t)$, the outputs, $\mathbf{y}(t)$, and the future states of the system, represented by the time derivative $\dot{\mathbf{x}}(t)$, as follows:

$$\dot{\mathbf{x}}(t) = \mathbf{A}(t)\mathbf{x}(t) + \mathbf{B}(t)\mathbf{u}(t) \tag{3.1}$$

$$\mathbf{y}(t) = \mathbf{C}(t)\mathbf{x}(t) + \mathbf{D}(t)\mathbf{u}(t) \tag{3.2}$$

Supposing that the system has n states, m inputs and r outputs, $\mathbf{A}(t)$ is the state matrix $(n \times n)$, $\mathbf{B}(t)$ is the input matrix $(n \times m)$, $\mathbf{C}(t)$ is the output matrix $(r \times n)$, and $\mathbf{D}(t)$ is the feedforward matrix $(r \times m)$. Formulating CRM in this matrix format provides structure to the CRM representations, simulates the production rates simul-

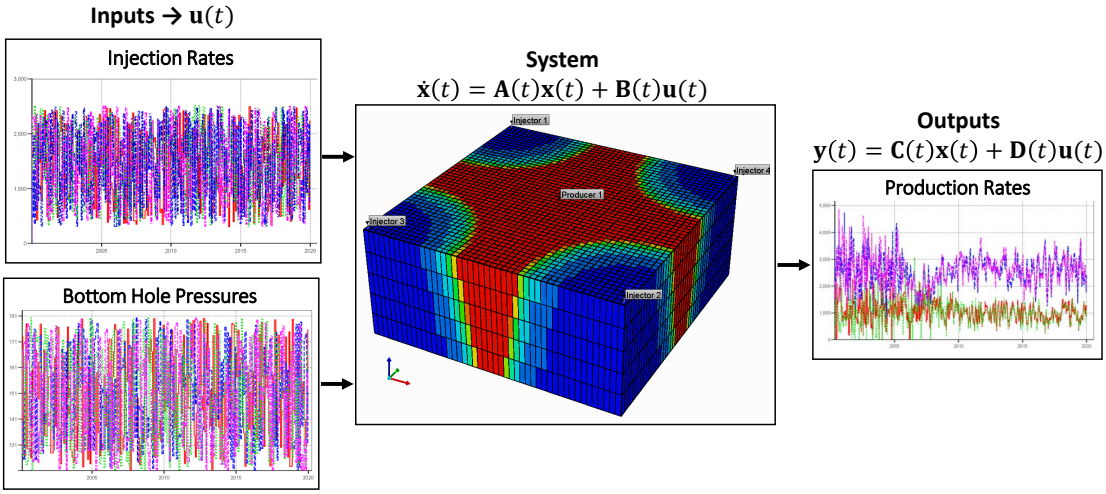

Figure 3.1: Input-output representation of the reservoir system.

taneously, saving computational time, and enables the use of several linear control algorithms that can improve CRM's performance [22, 9]. State-space equations are also amenable for real-time optimization. Because of these advantages, state-space equations has already been developed and applied for grid-based reservoir simulation by Jansen [19] . In the following subsections the state space equations for the CRM representations will be derived.

3.1.1 CRMT

As previously discussed, CRMT is the simplest representation, where all the injector wells are replaced by one pseudo-injector that sums up all of the injection rates, and the producers are replaced by a pseudo-producer that sums up all of the production rates. Such simplification results in a system with two inputs $\left(i(t), \frac{dp_{wf}(t)}{dt}\right)$ and one output $(q(t))$ as shown in equations 3.3 and 3.4, respectively. Since 2.11 is a first-order ordinary differential equation and there is only one control volume to represent the whole system, one state is enough. The choice of the states is arbitrary. For the sake of simplicity, the states are defined as the production rate of each control

volume (equation 3.4) in this work.

$$\mathbf{u}(t) = \begin{bmatrix} i(t) \\ \frac{dp_{wf}(t)}{dt} \end{bmatrix}, \quad \mathbf{u}(t) \in \Re^{2\times 1} \tag{3.3}$$

$$\mathbf{y}(t) = \mathbf{x}(t) = q(t) \tag{3.4}$$

Once the inputs, outputs and states of the system have been defined, equation 2.11 can be rearranged to provide the time derivatives of the states of the system in a very straightforward way:

$$\frac{dq(t)}{dt} = -\frac{1}{\tau}q(t) + \frac{f}{\tau}i(t) - J\frac{dp_{wf}(t)}{dt} \tag{3.5}$$

Comparing equation 3.5 to 3.1, the matrices $\mathbf{A}$ and $\mathbf{B}$ are obtained as

$$\mathbf{A} = -\frac{1}{\tau}; \quad \mathbf{B} = \begin{bmatrix} \frac{f}{\tau} & -J \end{bmatrix}. \tag{3.6}$$

$\mathbf{C}$ and $\mathbf{D}$ are obtained from equation 3.4 as

$$\mathbf{C} = 1; \quad \mathbf{D} = 0. \tag{3.7}$$

Indeed, the values of total injection and production rates are known. On the other hand, the values of BHP for the pseudo-producer is unknown, and it is very often assumed to be constant; however, in this work it is assumed to be the arithmetic mean of the BHP of all producer wells.

3.1.2 CRMP

For CRMP, the input vector is defined by all of the injection rates ($i_i(t)$) and the time derivative of the BHP of all producers $\left(\frac{dp_{wf}^{(j)}(t)}{dt}\right)$:

$$\mathbf{u}(t) = \begin{bmatrix} i_1(t) \\ i_2(t) \\ \vdots \\ i_{N_{inj}}(t) \\ \frac{dp_{wf}^{(1)}(t)}{dt} \\ \frac{dp_{wf}^{(2)}(t)}{dt} \\ \vdots \\ \frac{dp_{wf}^{(N_{prod})}(t)}{dt} \end{bmatrix}, \quad \mathbf{u}(t) \in \Re^{(N_{prod}+N_{inj})\times 1} \tag{3.8}$$

Similarly to the CRMT formulation, the outputs are the production rates of each producer well ($q_j(t)$). Again, the states of the system are defined to be the production rate of each reservoir control volume, which is equal to the output for this representation:

$$\mathbf{y}(t) = \mathbf{x}(t) = \begin{bmatrix} q_1(t) \\ q_2(t) \\ \vdots \\ q_{N_{prod}}(t) \end{bmatrix}, \qquad \mathbf{y}(t), \mathbf{x}(t) \in \Re^{N_{prod}\times 1} \tag{3.9}$$

Thus, it is easy to rearrange equation 2.13 to get the time derivatives of the states:

$$\frac{dq_j}{dt} = -\frac{1}{\tau_j} q_j(t) + \sum_{i=1}^{N_{inj}} \frac{f_{ij}}{\tau_j} i_i(t) - J_j \frac{dp_{wf}^{(j)}}{dt} \tag{3.10}$$

The state matrix ($\mathbf{A}$) and input matrix ($\mathbf{B}$) are obtained from writing 3.10 for all the producer wells and assembling the system of equations. Organizing it algebraically, one gets:

$$\mathbf{A} = \begin{bmatrix} -\frac{1}{\tau_1} & 0 & 0 & \cdots & 0 \\ 0 & -\frac{1}{\tau_2} & 0 & & \vdots \\ 0 & 0 & -\frac{1}{\tau_3} & & \\ \vdots & & & \ddots & 0 \\ 0 & \cdots & & 0 & -\frac{1}{\tau_{N_{prod}}} \end{bmatrix}, \quad \mathbf{A} \in \Re^{N_{prod} \times N_{prod}} \tag{3.11}$$

Since there are two types of inputs (rates and pressure), it is simpler to divide input matrix ($\mathbf{B}$) in two blocks: one representing the influence of injection rates ($\mathbf{B_{inj}}$) and the other one representing the influence of the time derivative of the BHP ($\mathbf{B_{BHP}}$).

$$\mathbf{B} = \left[\begin{array}{c:c} \mathbf{B_{inj}} & \mathbf{B_{BHP}} \end{array} \right], \quad \mathbf{B} \in \Re^{N_{prod} \times (N_{prod} + N_{inj})} \tag{3.12}$$

$$\mathbf{B_{inj}} = \begin{bmatrix} \frac{f_{11}}{\tau_1} & \frac{f_{21}}{\tau_1} & \frac{f_{31}}{\tau_1} & \cdots & \frac{f_{N_{inj},1}}{\tau_1} \\ \frac{f_{12}}{\tau_2} & \frac{f_{22}}{\tau_2} & \frac{f_{32}}{\tau_2} & & \frac{f_{N_{inj},2}}{\tau_2} \\ \vdots & \vdots & \vdots & \ddots & \vdots \\ \frac{f_{1,N_{prod}}}{\tau_{N_{prod}}} & \frac{f_{2,N_{prod}}}{\tau_{N_{prod}}} & \frac{f_{3,N_{prod}}}{\tau_{N_{prod}}} & \cdots & \frac{f_{N_{inj},N_{prod}}}{\tau_{N_{prod}}} \end{bmatrix}, \quad \mathbf{B_{inj}} \in \Re^{N_{prod} \times N_{inj}} \tag{3.13}$$

$$\mathbf{B_{BHP}} = \begin{bmatrix} -J_1 & 0 & \cdots & 0 \\ 0 & -J_2 & & \vdots \\ \vdots & & \ddots & 0 \\ 0 & \cdots & 0 & -J_{N_{prod}} \end{bmatrix}, \quad \mathbf{B_{BHP}} \in \Re^{N_{prod} \times N_{prod}} \tag{3.14}$$

Since the states are equal to the output, the output matrix ($\mathbf{C}$) is an identity

matrix ($\mathbf{I}$), and the feedforward matrix ($\mathbf{D}$) is a null matrix ($\mathbf{0}$).

$$\mathbf{C} = \mathbf{I}, \quad \mathbf{C} \in \Re^{N_{prod} \times N_{prod}} \tag{3.15}$$

$$\mathbf{D} = \mathbf{0}, \quad \mathbf{D} \in \Re^{N_{prod} \times (N_{prod}+N_{inj})} \tag{3.16}$$

3.1.3 CRMIP

The inputs and outputs for CRMIP are the same as for CRMP (equations 3.8 and 3.9, respectively), however the outputs are different from the states, because the states are defined by the flowrates of each reservoir control volume as

$$\mathbf{x}(t) = \begin{bmatrix} q_{11}(t) \\ q_{12}(t) \\ \vdots \\ q_{ij}(t) \\ \vdots \\ q_{N_{inj},N_{prod}}(t) \end{bmatrix}, \quad \mathbf{x}(t) \in \Re^{N_{inj}N_{prod} \times 1}. \tag{3.17}$$

The time derivatives of the states are obtained by simply rearranging equation 2.17:

$$\frac{dq_{ij}}{dt} = -\frac{1}{\tau_{ij}} q_{ij}(t) + \frac{f_{ij}}{\tau_{ij}} i_i(t) - J_{ij} \frac{dp_{wf}^{(j)}}{dt} \tag{3.18}$$

Thus, writing 3.18 for every control volume results in a system of equations from which the state matrix ($\mathbf{A}$) and input matrix ($\mathbf{B}$) can be obtained as

$$\mathbf{A} = \begin{bmatrix} -\frac{1}{\tau_{11}} & 0 & 0 & \cdots & 0 \\ 0 & -\frac{1}{\tau_{12}} & 0 & & \vdots \\ 0 & 0 & -\frac{1}{\tau_{13}} & & \\ \vdots & & & \ddots & 0 \\ 0 & \cdots & & 0 & -\frac{1}{\tau_{N_{prod},N_{prod}}} \end{bmatrix}, \quad \mathbf{A} \in \Re^{N_{inj}N_{prod} \times N_{inj}N_{prod}}. \quad (3.19)$$

As done for CRMP, it is suitable to divide the input matrix ($\mathbf{B}$) in blocks for CRMIP as well. However, in CRMIP, the number of blocks is given by $2 \times N_{inj}$, because such matrix blocks comprise the influence of a given type of input (injection rates, $\mathbf{B_{inj,i}}$, or BHP, $\mathbf{B_{BHP,i}}$) for all the control volumes connected to an injector (i). Thus, $\mathbf{B}$ is defined as

$$\mathbf{B} = \left[\begin{array}{c|c} \mathbf{B_{inj,1}} & \mathbf{B_{BHP,1}} \\ \hline \vdots & \vdots \\ \hline \mathbf{B_{inj,i}} & \mathbf{B_{BHP,i}} \\ \hline \vdots & \vdots \\ \hline \mathbf{B_{inj,N_{inj}}} & \mathbf{B_{BHP,N_{inj}}} \end{array}\right], \quad \mathbf{B} \in \Re^{(N_{prod}N_{inj}) \times (N_{prod}+N_{inj})}, \quad (3.20)$$

$$\mathbf{B_{inj,i}} = \begin{bmatrix} 0 & \cdots & 0 & \frac{f_{i1}}{\tau_{i1}} & 0 & \cdots & 0 \\ 0 & \cdots & 0 & \frac{f_{i2}}{\tau_{i2}} & 0 & \cdots & 0 \\ \vdots & & \vdots & \vdots & \vdots & & \vdots \\ 0 & \cdots & 0 & \frac{f_{i,N_{prod}}}{\tau_{i,N_{prod}}} & 0 & \cdots & 0 \end{bmatrix}, \quad \mathbf{B_{inj,i}} \in \Re^{N_{prod} \times N_{inj}}, \quad (3.21)$$

where in $\mathbf{B_{inj,i}}$ only the i^{th} column has non-zero elements, and $\mathbf{B_{BHP,i}}$ is defined as

$$\mathbf{B_{BHP,i}} = \begin{bmatrix} -J_{i1} & 0 & \cdots & 0 \\ 0 & -J_{i2} & & \vdots \\ \vdots & & \ddots & 0 \\ 0 & \cdots & 0 & -J_{i,N_{prod}} \end{bmatrix}, \quad \mathbf{B_{BHP,i}} \in \Re^{N_{prod} \times N_{prod}}. \tag{3.22}$$

Since equation 2.18 express that the production rate of a certain producer is given by the summation of the production rates of each control volume connected to such producer, this relationship is algebraically translated to the output matrix ($\mathbf{C}$) as

$$\mathbf{C} = \left[\begin{array}{c:c:c:c} \mathbf{I} & \cdots & \mathbf{I} & \cdots & \mathbf{I} \end{array} \right], \quad \mathbf{C} \in \Re^{N_{prod} \times (N_{prod} N_{inj})}, \tag{3.23}$$

where $\mathbf{I}$ is the identity matrix of size $N_{prod} \times N_{prod}$. Thus, the feedforward matrix ($\mathbf{D}$) is also a null matrix ($\mathbf{0}$):

$$\mathbf{D} = \mathbf{0}, \quad \mathbf{D} \in \Re^{N_{prod} \times (N_{prod} + N_{inj})}. \tag{3.24}$$

3.2 Transfer Functions

The state vector , usually, does not have an evident physical meaning, however inputs and outputs do. Therefore, in many cases one is actually interested in knowing the input-output relationship directly, which is called transfer function and by definition it is in the Laplace domain. For a single-input single-output (SISO) system, the transfer function can be written as:

$$\mathbf{G}(s) = \frac{\mathbf{Y}(s)}{\mathbf{U}(s)}, \tag{3.25}$$

where s is the Laplace variable, $\mathbf{U}(s)$ and $\mathbf{Y}(s)$ are the input and output in the Laplace domain, respectively. The transfer function is directly related to the state-space representation by:

$$\mathbf{G}(s) = \mathbf{C}(s\mathbf{I} - \mathbf{A})^{-1}\mathbf{B} + \mathbf{D} \tag{3.26}$$

where $\mathbf{I}$ is the identity matrix. This equation is valid for SISO and MIMO systems [22, 9].

The transfer functions of CRMT, CRMP, CRMIP, CRMIP-Block and CRM for unconventional reservoirs are presented in the following subsections. The transfer functions derived here and the state-space equations previously presented will be not directly interchangeable because the transfer functions will consider $P_{wf}(s)$ as an input while the state-space equations considered $\frac{dp_{wf}(t)}{dt}$. Zero initial conditions are considered.

3.2.1 CRMT

The inputs of the system for CRMT representation can be defined as injection rate ($I(s)$) of the pseudo-injector and the bottom hole pressure ($P_{wf}(s)$) of the pseudo-producer, instead of its time derivative $\left(\frac{dp_{wf}(t)}{dt}\right)$ as in the state space equation. The output is still the total liquid production rate $Q(s)$.

$$\mathbf{U}(s) = \begin{bmatrix} I(s) \\ P_{wf}(s) \end{bmatrix}; \qquad \mathbf{Y}(s) = Q(s) \tag{3.27}$$

Recalling equation 2.11 and taking the Laplace transform, one gets:

$$\tau\frac{dq}{dt} + q(t) = fi(t) - \tau J\frac{dp_{wf}}{dt}$$

$$\tau s Q(s) - \tau q(0) + Q(s) = fI(s) - \tau J s P_{wf}(s) + \tau J p_{wf}(0) \tag{3.28}$$

$$(1 + \tau s) Q(s) = fI(s) - \tau J s P_{wf}(s) + \tau J p_{wf}(0) + \tau q(0) \tag{3.29}$$

In a matrix format, equation 3.29 becomes:

$$Q(s) = \begin{bmatrix} \frac{f}{1+\tau s} & -\frac{\tau J s}{1+\tau s} \end{bmatrix} \begin{bmatrix} I(s) \\ P_{wf}(s) \end{bmatrix} + \frac{\tau J p_{wf}(0) + \tau q(0)}{1 + \tau s} \tag{3.30}$$

Notice that the term $\left(\frac{\tau J p_{wf}(0) + \tau q(0)}{1+\tau s}\right)$ represents the influence of the initial conditions. It is in agreement with what has been shown in the literature, since the primary production term has an exponential decline in the analytic solutions derived in [62, 46]. Assuming zero initial conditions ($p_{wf}(0) = 0$ and $q(0) = 0$), the transfer function is given by:

$$G(s) = \begin{bmatrix} \frac{f}{1+\tau s} & -\frac{\tau J s}{1+\tau s} \end{bmatrix} \tag{3.31}$$

3.2.2 CRMP

The inputs and outputs for the transfer function of CRMP are analogous to the ones defined for CRMT, but instead of having only one pseudo-producer and one pseudo-injector, there are multiple wells. Thus, the input and output vectors become the ones shown below, respectively:

$$\mathbf{U}(s) = \begin{bmatrix} I_1(s) \\ I_2(s) \\ \vdots \\ I_{N_{inj}}(s) \\ P_{wf}^{(1)}(s) \\ P_{wf}^{(2)}(s) \\ \vdots \\ P_{wf}^{(N_{prod})}(s) \end{bmatrix}; \qquad \mathbf{Y}(s) = \begin{bmatrix} Q_1(s) \\ Q_2(s) \\ \vdots \\ Q_{N_{prod}}(s) \end{bmatrix}. \tag{3.32}$$

In order to find the transfer function, it is necessary to recall the differential equation 2.13 and transform to the Laplace domain as it was previously done for CRMT:

$$\tau_j \frac{dq_j}{dt} + q_j(t) = \sum_{i=1}^{N_{inj}} f_{ij} i_i(t) - \tau_j J_j \frac{dp_{wf}^{(j)}}{dt}$$

$$\tau_j s Q_j(s) - \tau_j q_j(0) + Q_j(s) = \sum_{i=1}^{N_{inj}} f_{ij} I_i(s) - \tau_j J_j s P_{wf}^{(j)}(s) + \tau_j J_j p_{wf}^{(j)}(0) \tag{3.33}$$

$$(1 + \tau_j s) Q_j(s) = \sum_{i=1}^{N_{inj}} f_{ij} I_i(s) - \tau_j J_j s P_{wf}^{(j)}(s) + \tau_j J_j p_{wf}^{(j)}(0) + \tau_j q_j(0) \tag{3.34}$$

$$Q_j(s) = \sum_{i=1}^{N_{inj}} \frac{f_{ij}}{1 + \tau_j s} I_i(s) - \frac{\tau_j J_j s}{1 + \tau_j s} P_{wf}^{(j)}(s) + \frac{\tau_j J_j p_{wf}^{(j)}(0) + \tau_j q_j(0)}{1 + \tau_j s} \tag{3.35}$$

Assuming $p_{wf}^{(j)}(0) = 0$ and $q_j(0) = 0$, the previous equation must be written in a matrix format to represent the transfer function for the CRMP representation:

$$\mathbf{Y}(s) = \left[\begin{array}{c:c} \mathbf{G_{inj}}(s) & \mathbf{G_{BHP}}(s) \end{array} \right] \mathbf{U}(s) \tag{3.36}$$

where, $\mathbf{G}_{inj}(s)$ and $\mathbf{G}_{BHP}(s)$ are respectively given by:

$$\mathbf{G}_{inj}(s) = \begin{bmatrix} \frac{f_{11}}{1+\tau_1 s} & \frac{f_{21}}{1+\tau_1 s} & \cdots & \frac{f_{N_{inj},1}}{1+\tau_1 s} \\ \frac{f_{12}}{1+\tau_2 s} & \frac{f_{22}}{1+\tau_2 s} & & \frac{f_{N_{inj},2}}{1+\tau_2 s} \\ \vdots & & \ddots & \vdots \\ \frac{f_{1,N_{prod}}}{1+\tau_{N_{prod}} s} & \frac{f_{2,N_{prod}}}{1+\tau_{N_{prod}} s} & \cdots & \frac{f_{N_{inj},N_{prod}}}{1+\tau_{N_{prod}} s} \end{bmatrix} \tag{3.37}$$

$$\mathbf{G}_{BHP}(s) = \begin{bmatrix} -\frac{\tau_1 J_1 s}{1+\tau_1 s} & 0 & \cdots & 0 \\ 0 & -\frac{\tau_2 J_2 s}{1+\tau_2 s} & & \vdots \\ \vdots & & \ddots & 0 \\ 0 & \cdots & 0 & -\frac{\tau_{N_{prod}} J_{N_{prod}} s}{1+\tau_{N_{prod}} s} \end{bmatrix} \tag{3.38}$$

3.2.3 CRMIP

The inputs and outputs for CRMIP are the same as in CRMP (equation 3.32). However, before obtaining the full transfer function of the system it is useful to take a secondary step by defining the outputs as being the production rates of each injector producer pair as

$$\mathbf{Y_{ij}}(s) = \begin{bmatrix} Q_{11}(s) \\ Q_{12}(s) \\ \vdots \\ Q_{ij}(s) \\ \vdots \\ Q_{N_{inj},N_{prod}}(s) \end{bmatrix}. \tag{3.39}$$

The same procedure used for CRMT and CRMP must be applied to obtain the transfer functions for CRMIP, that is to transform equation 2.17 to the Laplace

domain:

$$\tau_{ij}\frac{dq_{ij}}{dt} + q_{ij}(t) = f_{ij}i_i(t) - \tau_{ij}J_{ij}\frac{dp_{wf}^{(j)}}{dt}$$

$$\tau_{ij}sQ_{ij}(s) - \tau_{ij}q_{ij}(0) + Q_{ij}(s) = f_{ij}I_i(s) - \tau_{ij}J_{ij}sP_{wf}^{(j)}(s) + \tau_{ij}J_{ij}p_{wf}^{(j)}(0) \tag{3.40}$$

$$(1+\tau_{ij}s)Q_{ij}(s) = f_{ij}I_i(s) - \tau_{ij}J_{ij}sP_{wf}^{(j)}(s) + \tau_{ij}J_{ij}p_{wf}^{(j)}(0) + \tau_{ij}q_{ij}(0) \tag{3.41}$$

$$Q_{ij}(s) = \frac{f_{ij}}{1+\tau_{ij}s}I_i(s) - \frac{\tau_{ij}J_{ij}s}{1+\tau_{ij}s}P_{wf}^{(j)}(s) + \frac{\tau_{ij}J_{ij}p_{wf}^{(j)}(0) + \tau_{ij}q_{ij}(0)}{1+\tau_{ij}s} \tag{3.42}$$

Assuming zero initial conditions ($p_{wf}^{(j)}(0) = 0$ and $q_j(0) = 0$), the following block matrix is obtained:

$$\mathbf{G^{(ij)}}(s) = \left[\begin{array}{c|c} \mathbf{G_{inj,1}^{(ij)}}(s) & \mathbf{G_{BHP,1}^{(ij)}}(s) \\ \hline \vdots & \vdots \\ \hline \mathbf{G_{inj,i}^{(ij)}} & \mathbf{G_{BHP,i}^{(ij)}} \\ \hline \vdots & \vdots \\ \hline \mathbf{G_{inj,N_{inj}}^{(ij)}} & \mathbf{G_{BHP,N_{inj}}^{(ij)}} \end{array}\right] \tag{3.43}$$

where $\mathbf{G_{inj,i}^{(ij)}}$ is the transfer function related to injection inputs, and $\mathbf{G_{BHP,i}^{(ij)}}$ is the transfer function related to BHP inputs of the control volumes of injector i. $\mathbf{G_{inj,i}^{(ij)}}$ and $\mathbf{G_{BHP,i}^{(ij)}}$ are expressed as, respectively:

$$\mathbf{G_{inj,i}^{(ij)}} = \begin{bmatrix} 0 & \cdots & 0 & \frac{f_{i1}}{1+\tau_{i1}s} & 0 & \cdots & 0 \\ 0 & \cdots & 0 & \frac{f_{i2}}{1+\tau_{i2}s} & 0 & \cdots & 0 \\ \vdots & & \vdots & \vdots & \vdots & & \vdots \\ 0 & \cdots & 0 & \frac{f_{i,N_{prod}}}{1+\tau_{i,N_{prod}}s} & 0 & \cdots & 0 \end{bmatrix} \tag{3.44}$$

$$\mathbf{G}^{(\mathbf{ij})}_{\mathbf{BHP,i}} = \begin{bmatrix} -\frac{\tau_{i1}J_{i1}s}{1+\tau_{i1}s} & 0 & \cdots & 0 \\ 0 & -\frac{\tau_{i2}J_{i2}s}{1+\tau_{i2}s} & & \vdots \\ \vdots & & \ddots & 0 \\ 0 & \cdots & 0 & -\frac{\tau_{i,N_{prod}}J_{i,N_{prod}}s}{1+\tau_{i,N_{prod}}s} \end{bmatrix} \tag{3.45}$$

In $\mathbf{G}^{(\mathbf{ij})}_{\mathbf{inj,i}}$ only the i-th column have non-zero elements.

Equation 3.43 provides the transfer function if the output is considered to be given by 3.39. However, recalling equation 2.18 the actual output vector can be algebraically constructed from $\mathbf{Y_{ij}}(s)$, as follows:

$$q_j(t) = \sum_{i=1}^{N_{inj}} q_{ij}(t)$$

$$\mathbf{Y}(s) = \left[\begin{array}{c:c:c:c:c} \mathbf{I} & \cdots & \mathbf{I} & \cdots & \mathbf{I} \end{array} \right] \mathbf{Y_{ij}}(s) \tag{3.46}$$

where $\mathbf{I} \in \Re^{N_{prod} \times N_{prod}}$ and is the identity matrix. Therefore, the total transfer functions for the inputs and outputs given by 3.32 is obtained similarly:

$$\mathbf{G}(s) = \left[\begin{array}{c:c:c:c:c} \mathbf{I} & \cdots & \mathbf{I} & \cdots & \mathbf{I} \end{array} \right] \mathbf{G^{(ij)}}(s) \tag{3.47}$$

Once the matrix multiplication above is done, the simplified transfer function structure below is obtained:

$$\mathbf{G}(s) = \left[\begin{array}{c:c} \mathbf{G_{inj}}(s) & \mathbf{G_{BHP}}(s) \end{array} \right] \tag{3.48}$$

$$\mathbf{G_{inj}}(s) = \begin{bmatrix} \frac{f_{11}}{1+\tau_{11}s} & \frac{f_{21}}{1+\tau_{21}s} & \cdots & \frac{f_{N_{inj},1}}{1+\tau_{N_{inj},1}s} \\ \frac{f_{12}}{1+\tau_{12}s} & \frac{f_{22}}{1+\tau_{22}s} & & \frac{f_{N_{inj},2}}{1+\tau_{N_{inj},2}s} \\ \vdots & & \ddots & \vdots \\ \frac{f_{1,N_{prod}}}{1+\tau_{1,N_{prod}}s} & \frac{f_{2,N_{prod}}}{1+\tau_{2,N_{prod}}s} & \cdots & \frac{f_{N_{inj},N_{prod}}}{1+\tau_{N_{inj},N_{prod}}s} \end{bmatrix} \tag{3.49}$$

$$\mathbf{G_{BHP}}(s) = \begin{bmatrix} -\sum_{i=1}^{N_{inj}} \frac{\tau_{i1}J_{i1}s}{1+\tau_{i1}s} & 0 & \cdots & 0 \\ 0 & -\sum_{i=1}^{N_{inj}} \frac{\tau_{i2}J_{i2}s}{1+\tau_{i2}s} & & \vdots \\ \vdots & & \ddots & 0 \\ 0 & \cdots & 0 & -\sum_{i=1}^{N_{inj}} \frac{\tau_{i,N_{prod}}J_{i,N_{prod}}s}{1+\tau_{i,N_{prod}}s} \end{bmatrix} \tag{3.50}$$

3.2.4 CRMIP-Block

In order to explain the derivation of the transfer function for CRMIP-Block, it is necessary to recall equation 2.21 and the assumptions made in section 2.3.4. Taking the Laplace transform from equation 2.21 and assuming zero initial conditions $\left(q_{lij}(0) = p_{wf}^{(lj)}(0) = 0\right)$, one gets:

$$\tau_{lij}\frac{dq_{lij}}{dt} + q_{lij}(t) = f_{lij}i_{lij}(t) - \tau_{lij}J_{lij}\frac{dp_{wf}^{(lj)}}{dt}$$

$$\tau_{lij}sQ_{lij}(s) - \tau_{lij}q_{lij}(0) + Q_{lij}(s) = f_{lij}I_{lij}(s) - \tau_{lij}J_{lij}sP_{wf}^{(lj)}(s) + \tau_{lij}J_{lij}p_{wf}^{(lj)}(0) \tag{3.51}$$

$$(1+\tau_{lij}s)Q_{lij}(s) = f_{lij}I_{lij}(s) - \tau_{lij}J_{lij}sP_{wf}^{(lj)}(s) \tag{3.52}$$

From assumptions given by equations 2.23 and 2.25, the transfer function for the block of the injector is:

$$Q_{1ij}(s) = \frac{f_{ij}}{1+\tau_{1ij}s}I_i(s) \tag{3.53}$$

Now, from assumptions given by equations 2.22 and 2.25, the transfer function for

the blocks that are not the block of the injectors or the block of the producers is given by:

$$Q_{lij}(s) = \frac{1}{1+\tau_{lij}s} Q_{(l-1)ij}(s), \quad l = 2, \ldots, M-1 \tag{3.54}$$

From the assumption given by equation 2.22, the transfer function for the block of the producer is:

$$Q_{Mij}(s) = \frac{1}{1+\tau_{Mij}s} Q_{(M-1)ij}(s) - \frac{\tau_{Mij} J_{Mij} s}{1+\tau_{Mij}s} P_{wf}^{(j)}(s) \tag{3.55}$$

In order to construct the transfer function of the system comprised by the series of blocks between injector i and producer j, it is necessary to consecutively substitute 3.53 in 3.54, and 3.54 in 3.55 to obtain:

$$Q_{ij}(s) = Q_{Mij}(s) = f_{ij} \prod_{l=1}^{M} \left(\frac{1}{1+\tau_{lij}s} \right) I_i(s) - \frac{\tau_{Mij} J_{Mij} s}{1+\tau_{Mij}s} P_{wf}^{(j)}(s) \tag{3.56}$$

Thus, the transfer function for the whole reservoir system considering the same outputs as in equation 3.32 is the block matrix given below:

$$\mathbf{G}(s) = \left[\begin{array}{c:c} \mathbf{G_{inj}}(s) & \mathbf{G_{BHP}}(s) \end{array} \right] \tag{3.57}$$

$$\mathbf{G_{inj}}(s) = \begin{bmatrix} f_{11}\prod_{l=1}^{M}\frac{1}{1+\tau_{l11}s} & f_{21}\prod_{l=1}^{M}\frac{1}{1+\tau_{l21}s} & \cdots & f_{N_{inj},1}\prod_{l=1}^{M}\frac{1}{1+\tau_{l,N_{inj},1}s} \\ f_{12}\prod_{l=1}^{M}\frac{1}{1+\tau_{l12}s} & f_{22}\prod_{l=1}^{M}\frac{1}{1+\tau_{l22}s} & & f_{N_{inj},2}\prod_{l=1}^{M}\frac{1}{1+\tau_{l,N_{inj},2}s} \\ \vdots & & \ddots & \vdots \\ f_{1,N_{prod}}\prod_{l=1}^{M}\frac{1}{1+\tau_{l,1,N_{prod}}s} & f_{2,N_{prod}}\prod_{l=1}^{M}\frac{1}{1+\tau_{l,2,N_{prod}}s} & & f_{N_{inj},N_{prod}}\prod_{l=1}^{M}\frac{1}{1+\tau_{l,N_{inj},N_{prod}}s} \end{bmatrix} \tag{3.58}$$

$$\mathbf{G_{BHP}}(s) = \begin{bmatrix} -\sum_{i=1}^{N_{inj}}\frac{\tau_{Mi1}J_{Mi1}s}{1+\tau_{Mi1}s} & 0 & \cdots & 0 \\ 0 & -\sum_{i=1}^{N_{inj}}\frac{\tau_{Mi2}J_{Mi2}s}{1+\tau_{Mi2}s} & & \vdots \\ \vdots & & \ddots & 0 \\ 0 & \cdots & 0 & -\sum_{i=1}^{N_{inj}}\frac{\tau_{M,i,N_{prod}}J_{M,i,N_{prod}}s}{1+\tau_{M,i,N_{prod}}s} \end{bmatrix} \tag{3.59}$$

In linear control theory, it is known that some higher order systems can have its dynamics approximated by a first order transfer with time delay [22, 9]. In the time domain, if the function $\mathbf{y}(t)$ is equivalent to $\mathbf{g}(t)$ with a time delay θ, it can be written as:

$$\mathbf{y}(t) = \begin{cases} 0 & \text{for } t < \theta \\ \mathbf{g}(t-\theta) & \text{for } t \geq \theta \end{cases} \tag{3.60}$$

The transfer function of the time delay function is given by $e^{-\theta s}$. Therefore, equation

3.58 can be substituted by:

$$\mathbf{G_{inj}}(s) = \begin{bmatrix} \frac{f_{11}e^{-\theta_{11}s}}{1+\tau_{11}s} & \frac{f_{21}e^{-\theta_{21}s}}{1+\tau_{21}s} & \cdots & \frac{f_{N_{inj},1}e^{-\theta_{N_{inj},1}s}}{1+\tau_{N_{inj},1}s} \\ \frac{f_{12}e^{-\theta_{12}s}}{1+\tau_{12}s} & \frac{f_{22}e^{-\theta_{22}s}}{1+\tau_{22}s} & & \frac{f_{N_{inj},2}e^{-\theta_{N_{inj},2}s}}{1+\tau_{N_{inj},2}s} \\ \vdots & & \ddots & \vdots \\ \frac{f_{1,N_{prod}}e^{-\theta_{1,N_{prod}}s}}{1+\tau_{1,N_{prod}}s} & \frac{f_{2,N_{prod}}e^{-\theta_{2,N_{prod}}s}}{1+\tau_{2,N_{prod}}s} & \cdots & \frac{f_{N_{inj},N_{prod}}e^{-\theta_{N_{inj},N_{prod}}s}}{1+\tau_{N_{inj},N_{prod}}s} \end{bmatrix} \tag{3.61}$$

Sayyafzadeh et al. [49] also used a first order transfer function with time delay to model waterflooding reservoirs. The main difference between their method and CRM is that they assumed independent time constants for natural decline (initial conditions) and injection rates, but the results are still very close. Also, the approach proposed here is more general because it includes BHP variation, and representing the transfer function as matrices for multi-input multi-output (MIMO) cases is more convenient, specially for cases with large number of wells.

3.2.5 CRM for Unconventional Reservoirs

The work done by Shahamat et al. [52] was chosen here because of its physical consistency, reliable results, and easy derivation of the differential equation 2.30. In order to obtain the transfer function, equation 2.30 is transformed to the Laplace domain:

$$q = -C\left(R\frac{dq}{dt} + \frac{dp_{wf}}{dt}\right)$$

$$Q(s) = -C\left(RsQ(s) - Rq(0) + sP_{wf}(s) - p_{wf}(0)\right) \tag{3.62}$$

Assuming zero initial conditions ($p_{wf}(0) = 0$ and $q(0) = 0$) and rearranging the previous equation algebraically, the transfer function is obtained for the case of input

$P_{wf}(s)$ and output $Q(s)$:

$$Q(s) = \frac{-Cs}{1+CRs} P_{wf}(s) \tag{3.63}$$

$$\mathbf{G}(s) = \frac{-Cs}{1+CRs} \tag{3.64}$$

As one can see, the transfer function (equation 3.64) is similar to the $\mathbf{G_{BHP}}(s)$ block in the other CRM formulations. Most of the CRM examples in the literature consider constant connectivities and time constants, which results in a linear time-invariant (LTI) system. However, capacitance and resistance are a function of time for unconventional reservoirs, so it is a linear time-variant system [22, 9]. Since the solution is discretized in time, it can also be considered as piecewise LTI system, where capacitance and resistance are constant in each time step. This assumption is also valid for CRM for conventional reservoirs that connectivities [53] and time constants [7] were proved to vary with time, in cases such as transient flow or immature waterfloods, respectively.

3.2.6 Transfer Functions Analysis

Analyzing the transfer functions for CRMT, CRMP, CRMIP and CRMIP-Block, one can realize that these matrices were divided in two blocks:

- A full matrix for injection influence, $\mathbf{G_{inj}}(s)$
- A diagonal matrix for the terms related to the bottom hole pressures, $\mathbf{G_{BHP}}(s)$

$\mathbf{G_{inj}}(s)$ is a full matrix because it is assumed that all of the injectors can affect the production rates at each of the producers; however, if there is an upper limit for interwell distance to be considered, as in [60], it will not be a full matrix. Likewise, $\mathbf{G_{BHP}}(s)$ is a diagonal matrix because of the assumption that the production rate of a specific producer is not affected by the bottom hole pressure of other producers;

this assumption is not always true. Off-diagonal terms can be added in $\mathbf{G_{BHP}}(s)$ to account for neighboring wells competing for the same fluids; however, it will increase the number of parameters in the model and might generate values that are not statistically significant.

Transfer function are suitable to predict the response profile to a certain stimulus. Figures 3.2 and 3.3 depict the production rate response to unit step increase in injection rates and to unit step drop in BHP, respectively. Figure 3.4 shows the production rate response profile for the case of multiple blocks in series, as in the CRM-Block formulation.

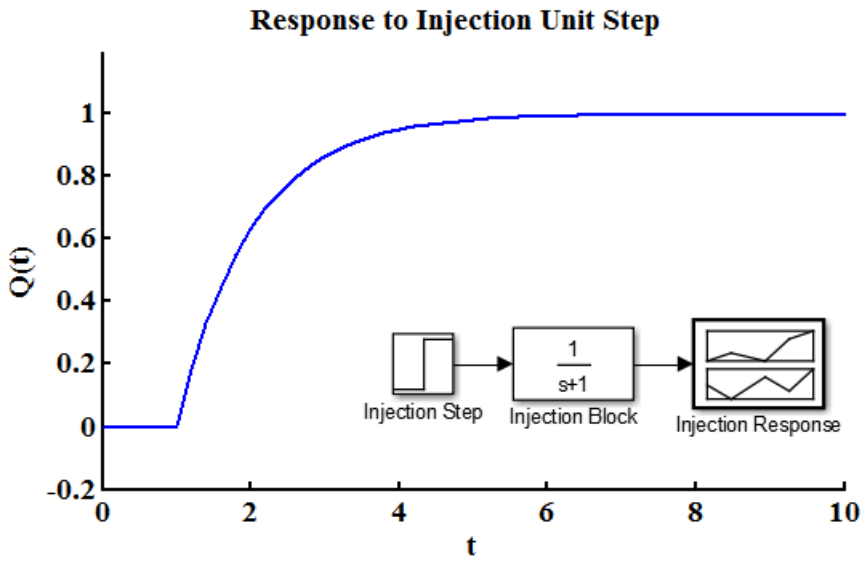

Figure 3.2: Production rate response profile for unit step injection rate increase for CRMT, CRMP and CRMIP.

The relative degree of a transfer function is defined as the degree of the denominator (number of poles) minus the degree of the numerator (number of zeros) [22, 9]. If the relative degree is greater than zero, the transfer function is strictly proper, such

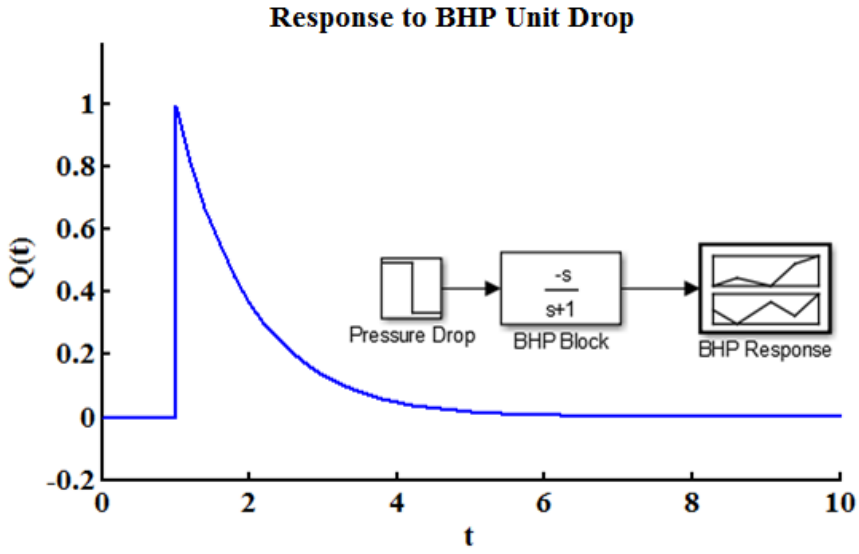

Figure 3.3: Production rate response profile for unit BHP drop for CRMT and CRMP.

as the injection block ($\mathbf{G_{inj}}(s)$). The higher the relative degree (e.g. CRMIP-Block), the longer the system takes to achieve a steady state (figure 3.4). The relative degree of BHP block ($\mathbf{G_{BHP}}(s)$) is zero, which classifies it as a biproper transfer function; thus, the outputs of the system suddenly respond to BHP variations (figure 3.3).

CRM's transfer functions are very useful to compare the different CRM formulations. For example, the difference between CRM and CRMP is basically the number of control volumes. On the other hand, the difference CRMIP and CRMP is that, in CRMIP, for each injector-producer pair a time constant is assigned, and the BHP influence is the summation of the BHP influence in all of the control volumes for a certain producer.

CRMIP-Block has higher order transfer functions in the injection block ($\mathbf{G_{inj}}(s)$). As one can see in figure 3.4, higher order systems can also be approximated as a first order system with time lag, as previously discussed.

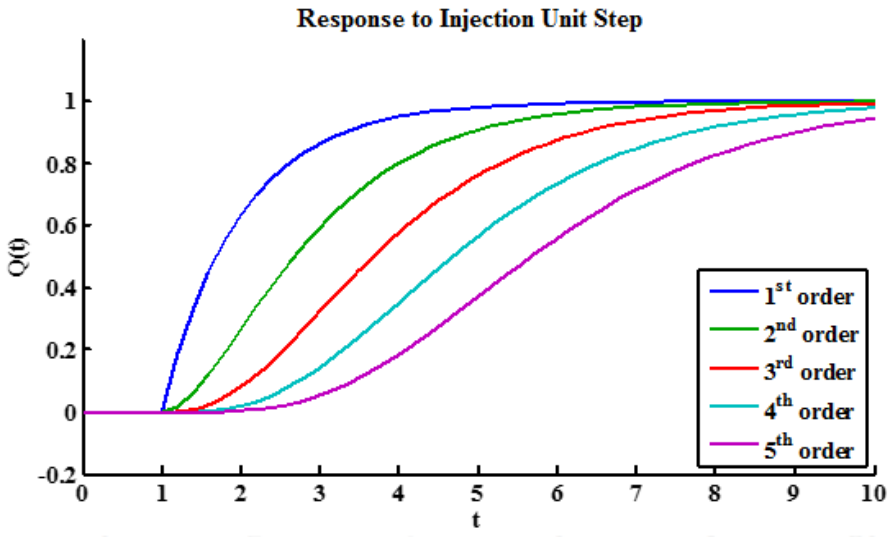

Figure 3.4: Production rate response profile for unit step injection rate increase in the case of blocks in series (CRM-Block).

3.3 Controllability

Controllability is the ability to move the internal states of a given system from any initial state to any final state in a finite time by manipulating the system's external inputs. For linear time-invariant systems in the state space representation, the controllability matrix is defined by:

$$\zeta = \left[\begin{array}{ccccc} \mathbf{B}, & \mathbf{AB}, & \mathbf{A}^2\mathbf{B}, & \ldots, & \mathbf{A}^{n-1}\mathbf{B} \end{array} \right] \tag{3.65}$$

where n is the number of internal states. The system is controllable if the rank of ζ is equal to the number of states (n):

$$\text{rank}(\zeta) = n \tag{3.66}$$

3.4 Observability

Observability is the ability to uniquely determine any unknown initial states of a given system, $\mathbf{x}(0)$, by examining the inputs, $\mathbf{u}(t)$, and outputs, $\mathbf{y}(t)$, over a finite time interval. Controllability and observability are dual properties of linear systems. For linear time-invariant systems in the state space representation, the observability matrix is defined by:

$$\mathbf{\Psi} = \begin{bmatrix} \mathbf{C}^T \\ \mathbf{C}^T\mathbf{A} \\ \mathbf{C}^T\mathbf{A}^2 \\ \vdots \\ \mathbf{C}^T\mathbf{A}^{n-1} \end{bmatrix} \tag{3.67}$$

The system is observable if the rank of $\mathbf{\Psi}$ is equal to the number of states (n):

$$\text{rank}(\mathbf{\Psi}) = n \tag{3.68}$$

3.5 Minimal Realization

In control theory, the realization problem can be stated as follows: given the systems transfer function, $\mathbf{G}(s)$, find $\mathbf{A}$, $\mathbf{B}$, $\mathbf{C}$ and $\mathbf{D}$ that represents the system. In other words, it is the inverse problem of obtaining the transfer function from the state space equation (3.26). As one can realize, the same system can have multiple realizations and for each realization different state vectors, which does not necessarily have a clear physical meaning.

A realization that has the minimum number of states to represent the system is called a minimal realization; it is a controllable and observable representation of the system. Generally, minimal realizations are desirable because they are compu-

tationally more stable and faster, especially for large scale models. Several minimal realization algorithms are available in past works, such as Kalman decomposition [23] and Gilberts realization [16].

4. PARAMETERS ESTIMATION: GREY-BOX SYSTEMS IDENTIFICATION

Unlike the grid-based reservoir simulation framework where many rock and fluid properties are necessary to describe a reservoir and predict its flow behavior, the standard CRM's (and most of the more complex ones) require only three types of parameters, which are connectivities (f_{ij}), time constants (τ_{ij}) and productivity indices (J_{ij}). The quantity of parameters necessary to describe the system is a function of the number of injectors, producers and the CRM formulation chosen, and certainly it is much less than any of the discretized models (using finite differences, finite volumes, etc.). So, instead of starting with a full-physics model, one can determine CRM parameters based solely on production data. This chapter discusses the physical meaning of each type of parameter and how they are estimated.

4.1 Parameters' Physical Meaning

Generally, in order to describe more accurately the reservoir's flow behavior, it is necessary to have more detailed physics models, which requires more properties evaluation. Usually, the data acquisition and analysis that is necessary to evaluate the reservoir's properties is quite expensive and time consuming due to the infrastructure and specialized work force needed. Moreover, many properties, such as permeability and porosity, can only be evaluated locally, requiring the use of many geostatistical techniques to infer their values in other areas of the reservoir, which may lead to parameters that do not represent the reservoir's physics. For all of these reasons, reservoir simulation becomes prohibitively expensive in many practical cases.

As it will be further discussed in this chapter, the CRM's parameters are much easier to estimate, which establishes a much faster and cheaper work flow for practical implementation. Furthermore, all of them can be easily interpreted from an

operational point of view, as it will be explained in the following subsections.

4.1.1 Connectivities

In CRM, the interwell connectivity, f, defines the volume fraction of injected water from a certain injector that flows towards a specified producer. Connectivity can also be thought out as an allocation factor. Frequently, connectivities are also referred to as gains. In terms of control, gains are directly related to the change in the steady state response of the output signal caused by a variation in the input. Figure 4.1 shows the CRMT production rate response to a series of injection rate steps. As one can see, the higher the gain, the higher is the variation in the output.

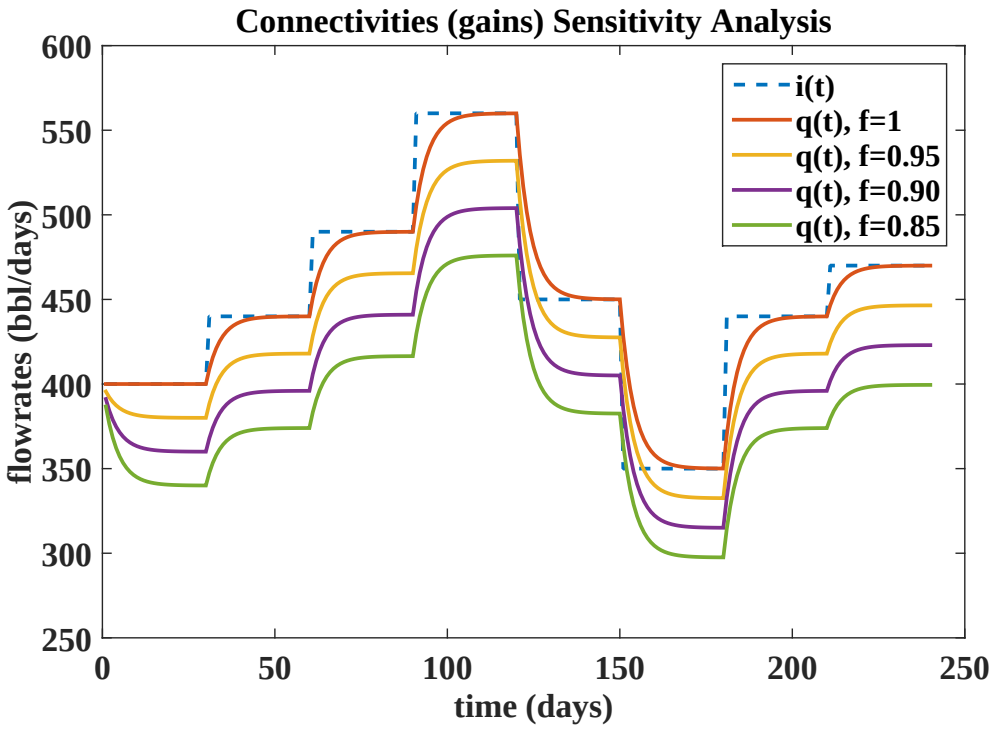

Figure 4.1: Comparison of responses (production rates) for CRMT with different connectivities (gains) for a series of steps input signals (injection rates).

From an operational point of view, by interpreting the connectivities values, an operator in the field can know how much he could expect the production rate of a certain producer to increase due to a variation in the injection rate of a given injector.

In the CRM representation previously presented here, only injector-producer connectivity are taken into account. However, producers that are close to each other will be "competing to produce the same fluid", therefore it is reasonable to consider producer-producer interactions in some cases. Yousef [62] proposed a heuristic equation for handling this situations.

Another approach to describe reservoirs and quantify the interactions between injector-producer, producer-producer and injector-injector is by using the multiwell productivity index (MPI) based method proposed by Kaviani [24, 28, 25]. In the MPI approach, the connectivity indices are not the same as connectivity in CRM. They are used to exclusively describe the role of heterogeneity in rectangular reservoirs by decoupling the effects of well location, skin factor, injection rates and producer's BHP from the connectivity indices' computation.

Gentil [13] shed some light on the physical meaning of regression coefficients for patterned waterfloods, which later on was useful to physically explain connectivities as ratio of the average transmissibility (T_{ij}) between injector (i) and producer (j) to the sum of the transmissibility between injector (i) and all other producers:

$$f_{ij} = \frac{T_{ij}}{\sum_{j=1}^{N_{prod}} T_{ij}} \tag{4.1}$$

Even though this equation is qualitatively useful to analyze connectivity in the presence of high permeability streaks or flow barriers, which are very often presented in the literature, it is not a practical equation, since it is generally unfeasible to exactly define each control volume and compute its transmissibility.

The assumption of constant connectivities has been frequently applied in the literature, however equation 4.1 can be expanded in order to discuss in details the implication of this assumption:

$$f_{ij} = \frac{\left(\frac{k_r k}{\mu L} A\right)_{ij}}{\sum_{j=1}^{N_{prod}} \left(\frac{k_r k}{\mu L} A\right)_{ij}} \quad , \tag{4.2}$$

where k_r is the relative permeability, k is the absolute permeability, A is the effective cross sectional area of flow, μ is the fluid viscosity, L is the average path necessary for fluid to go from injector i to producer j. It is quite reasonable to consider all of these parameters as time varying.

k_r is a function of water saturation. After the water breakthrough, k_r does not change too much in the reservoir control volume. k usually does not change much; changes in k could be due to major events such as fracking. A and L can vary every time that there are significant changes in the flow patterns, such as opening or shutting a well, or even big variations in BHP or injection rates, which would change the streamlines of the system, thus changing the water allocation factor. μ varies due to the variations in the fraction of each component in the reservoir as the waterflooding progresses.

In this context, Jafroodi and Zhang [18] used ensemble Kalman filter to capture the dynamic behavior of the CRM parameters during the history matching stage. As shown in this work, after the water breakthrough these parameters tend to be constant, unless there is a major perturbation to the system. Thiele and Batycky [54] also discussed the dynamic behavior of well allocation factors.

Since connectivities are dynamic parameters, it is important to keep in mind the concept of instantaneous connectivity for future works, which can be defined based

on streamlines. Instantaneous connectivity $f_{ij}(t)$ is the fraction of the total volume injected in injector i at time time t that is carried by the streamtubes defined by the set of streamlines that start in injector i and end in producer j.

4.1.2 Time Constants

The theoretical definition of time constant (τ) was previously shown in equation 2.10:

$$\tau = \frac{c_t V_p}{J}$$

Analyzing this equation, one can see that the time constant is directly related to the time necessary for the pressure wave (caused by a variation in the injection rate) to propagate in the porous media and effectively influence the production signal. If the time constant is higher, it means that the system has a slow response, which could be due to a high compressibility, large pore volume, or low permeability. On the other hand, if the time constant is small, it means that the system responds rapidly to a stimulus, which could be due to a low compressibility, small pore volume, or high permeability. The influence of the time constant for a CRMT production rate response is depicted in figure 4.2, considering a series of injection rate steps.

If a first order system, such as the CRMT, CRMP and CRMIP formulations, is perturbed by a step increase in the input signal, one time constant is the time taken for the system to achieve 63.2% of its final increase (when it achieves steady state) in the output signal [50].

In equation 2.10, c_t is the total compressibility. For a waterflooding reservoir with no free gas, c_t is given by:

$$c_t = c_r + S_w c_w + (1 - S_w) c_o \tag{4.3}$$

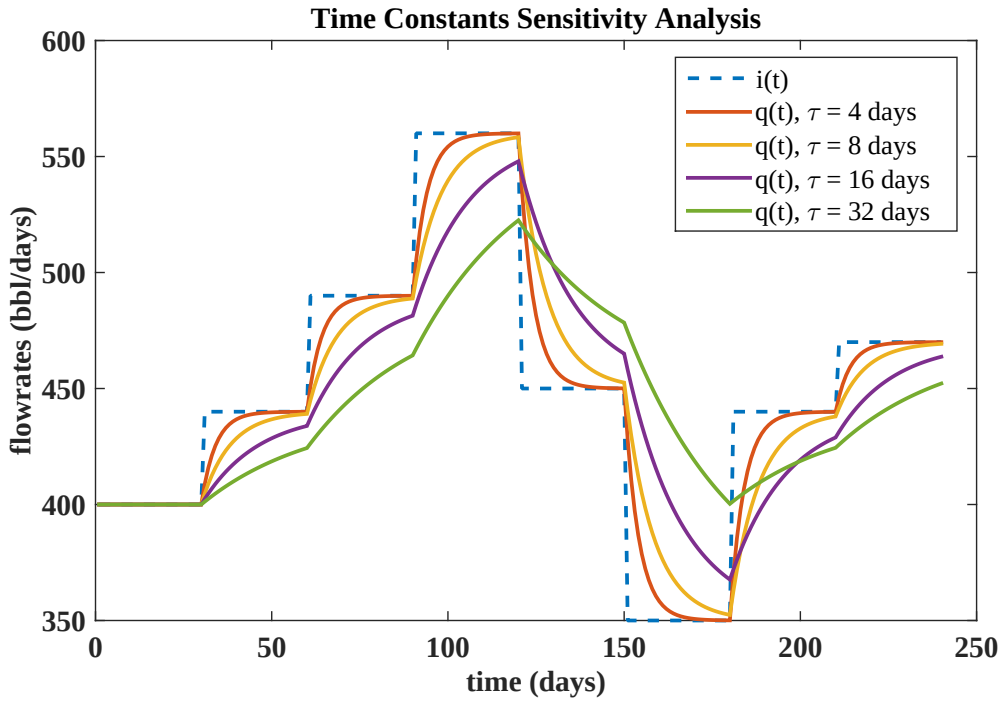

Figure 4.2: Comparison of responses (production rates) for CRMT with different time constants for a series of steps input signals (injection rates).

Where c_r, c_w and c_o are the rock, water and oil compressibility, respectively, and S_w is the water saturation. Therefore, if c_o and c_w are significantly different, c_t will vary a lot as the water front advances. For this reason, most of the CRM applications have been done for mature waterflooding, and in such case the assumption of constant τ is reasonable.

In equation 2.10, V_p is the total pore volume, which also can be time varying. As previously discussed, operational changes such as high injection rates or producers' BHP variation and opening or shutting a well will cause significant changes in the streamlines, changing the flow pattern in the reservoir, which changes the total pore volume (V_p) being drained for a given control volume. For further details in the time-variant behavior of time constants the reader is referred to [6, 7, 18].

4.1.3 Productivity Indices

Productivity indices (J) define the necessary pressure drawdown for a given producer to produce a certain flowrate, as described by the deliverability equation:

$$J = \frac{q}{\Delta p} \tag{4.4}$$

The analytical computation of J depends on rock and fluids properties as well as the well design, for detailed explanation on this topic the reader is referred to [11]. If the reservoir is in steady state flow, the reservoir investigated volume is constant as well as the pressure, which implies constant rock and fluid properties. These assumptions result in a constant productivity index. However, if pseudo-steady state (boundary dominated flow) or transient flow is assumed, J is no longer constant.

CRM assumes boundary dominated flow, therefore J should not be considered constant. However, since water is being injected in the reservoir, keeping its pressure, it is expected that J fluctuates around a certain values as injection rates and producers' BHP vary.

4.2 Systems Identification

Even though the physical meaning of the CRM's parameters is theoretically known, most of the physical properties necessary to determine their values (e.g. V_p, T_{ij}) cannot be directly and accurately measured through lab experiments. Therefore, the most practical approach so far is to directly compute the CRM's parameters (f's, τ's, J's) by analyzing the reservoir's response to excitations in the inputs, which is a system identification technique [35]. The flowchart in figure 4.3 describes this process, which will be explained in details in the following subsections.

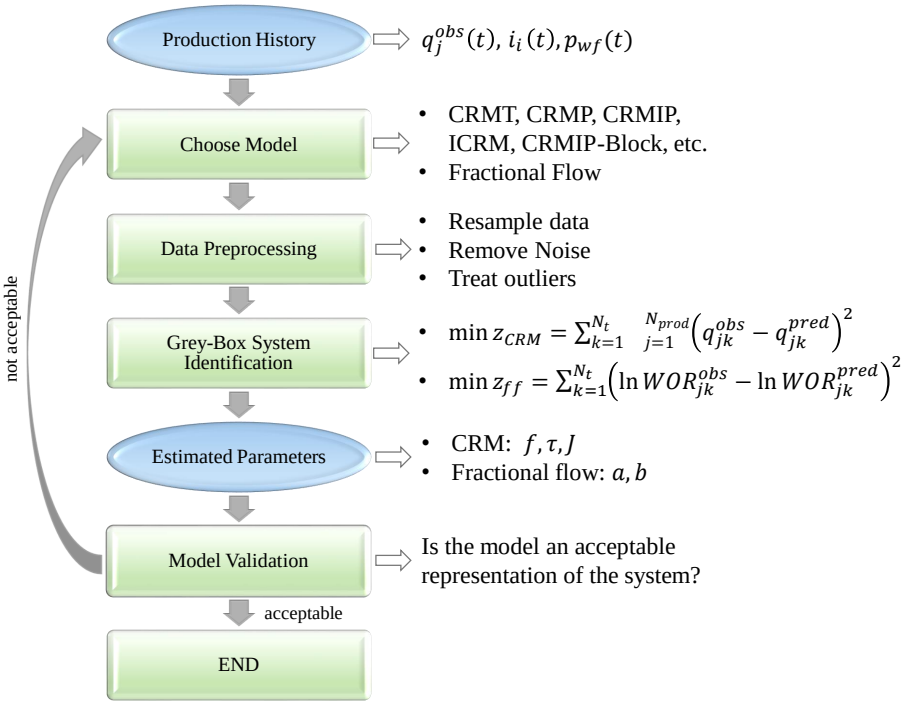

Figure 4.3: System identification flowchart.

4.2.1 Production History Requirements

Unlike most of the commercial reservoir simulators, CRM requires reduced amount of data to history match and predict the reservoir behavior. If only the total production rates are to be computed, then the only information required from the production history is injection rates ($i_i(t)$), producers' BHP ($p_{wf}^{(j)}(t)$) and total production rates ($q_j(t)$). In case oil production rates are to be computed as well, a fractional flow model is required. In this thesis the fractional model developed by Gentil [13] will be applied, in which the only extra data needed to decouple oil and total flowrates is the oil production rates ($qo_j(t)$). Generally, these data required by CRM is abundant and readily available in the field. Furthermore, it is the most reliable data gathered, also known as "hard data".

In practical cases the data required is measured in the field and may be noisy due to the measurement errors or simply oscillations in the field operations. On the other hand, in research experiments, the production history is usually generated by a reservoir simulator, therefore it is a noise free experiment. In this thesis, the production histories for the study cases were generated using the IMEX simulator from the Computer Modelling Group Ltd. (CMG) [36].

In order to obtain a reliable system identification it is necessary that the inputs ($i_i(t)$ and $p_{wf}(t)$) vary within a reasonable range that covers the system's operation. Thus, the simplified model can capture most of the dynamics of the system. For this reason and also due to the lack of real field production history available, the experiments done in this thesis generated the input signals as sequence of steps applying a random uniform distribution, where only the lower and upper limits have to be specified, as shown in figure 4.4.

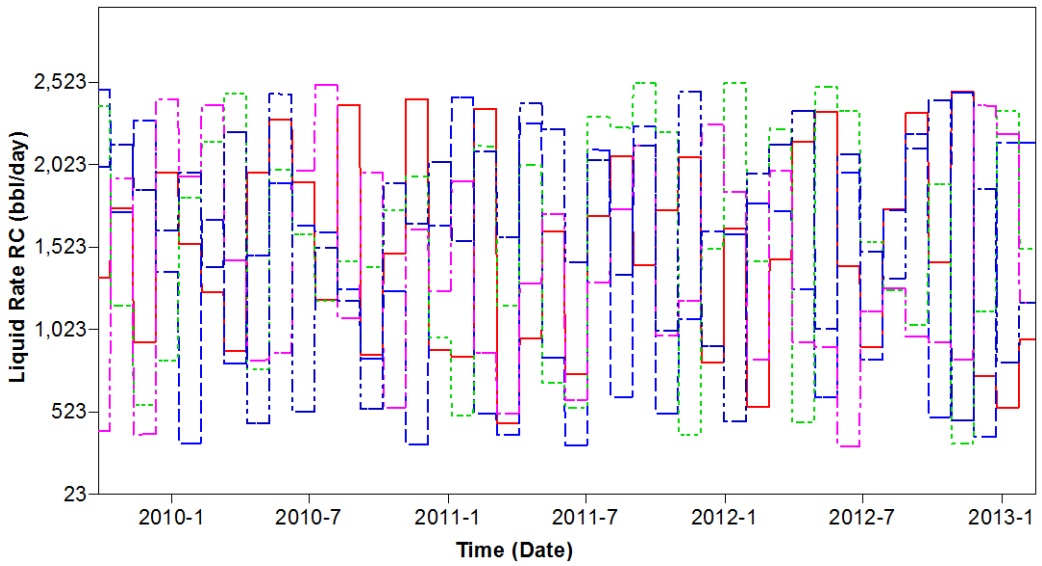

Figure 4.4: Randomly generated steps for injection rates of five wells.

4.2.2 Data Preprocessing

Data acquisition and preprocessing are the most time consuming stages of reservoir modeling and simulation because a group of specialized professionals (engineers, geologists, geophysicists, etc.) have to work together analyzing several sources of data (seismics, well logging, production history, etc.) and reconcile their interpretation to generate realizations that reliably represent the reservoir geology and flow behavior. Due to the fact that CRM requires reduced amount of data, modeling can be accomplished significantly faster, overcoming the time constraints that commonly makes reservoir simulation unfeasible in the industry's routine.

In practical cases it is necessary to treat the noise in the production history, controlling the quality of the data used to model the reservoir. Detailed explanation on this subject is out of the scope of this thesis, and the reader is referred to [5, 59, 27] for further details. In this thesis, the production histories are noise free because they are directly obtained from the IMEX [36] simulation results, therefore there is no requirement for noise treatment.

In systems identification, it is important that the sampled data is evenly spaced in time, so that the dynamic behavior of the system is not biased by a time period with higher sample frequency. Since the reservoir simulators commonly use an adaptive time step, it is necessary to resample the data in order to have a dataset that is evenly spaced in time. As shown in figure 4.4, the input signals ($i_i(t)$ and $p_{wf}^{(t)}(t)$) vary as steps, thus the shape of this signal must be preserved when resampling. On the other hand, the output signal ($q_j(t)$) does not have a predefined shape (figure 4.5) and smoothly varies between consecutive sampled data, therefore linear interpolation is applied to resample them.

If state-space equations are used, $\frac{dp_{wf}^{(j)}}{dt}$ is required. $\frac{dp_{wf}^{(j)}}{dt}$ must be numerically

computed from the resampled production history to assure the same Δt along the experiment, so the effects of pressure variations ($\Delta p_{wf}^{(j)}$) will be always comparable.

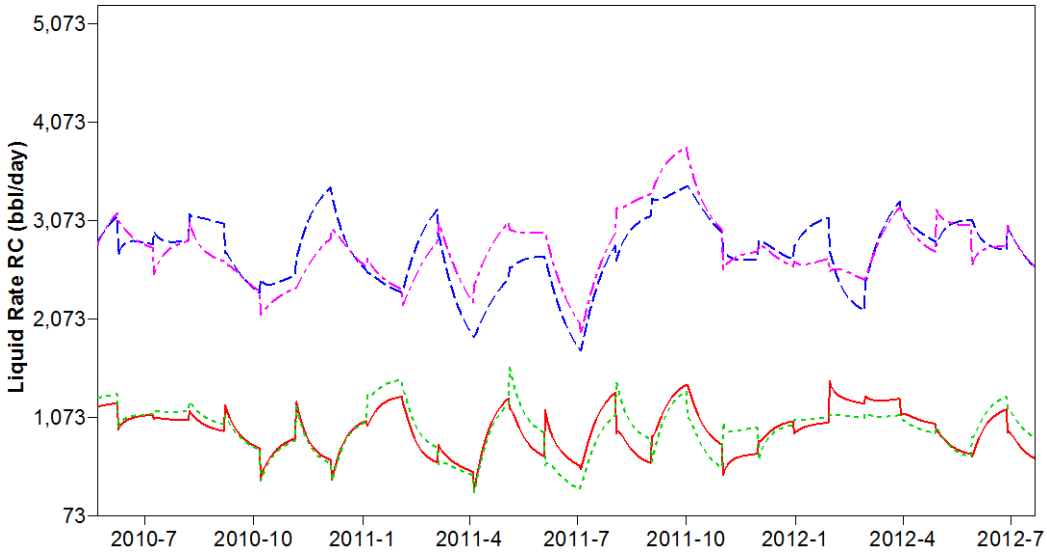

Figure 4.5: Production rates response for four wells for the injection steps shown in figure 4.4 and BHP steps.

4.2.3 Grey-Box System Identification

The classical approach for parameters estimation in CRM is a curve fitting problem, also called history matching. Since the ordinary differential equations governing the system dynamics are known, but the parameters (f_{ij}'s, τ_{ij}'s, J_{ij}'s) are unknown, this is a grey-box system. The parameters are identified using grey box system identification, which is an optimization problem where the sum of squared error between predicted and observed total fluid rates (q_{jk}^{pred} and q_{jk}^{obs}, respectively) is minimized:

$$\min z = \sum_{k=1}^{N_t} \sum_{j=1}^{N_{prod}} \left(q_{jk}^{obs} - q_{jk}^{pred} \right)^2 \tag{4.5}$$

For CRM in a control systems framework, either representing the system through state space equations or transfer functions, q_{jk}^{pred} is computed directly by simulating the system, and thus, there is no need to use the analytical equation previously derived in [62, 46]. In the case studies presented in this thesis, q_{jk}^{obs} is obtained directly from the resampled production history.

Due to this optimization problem's constraints, which will be further discussed here, the most suitable function in MATLAB Optimization Toolbox [37] to solve it is "fmincon". The general optimization problem solved by "fmincon" is given by:

$$\min_{\chi} z(\chi) \text{ such that } \begin{cases} \mathbf{c}(\chi) \leq 0 \\ \mathbf{ceq}(\chi) = 0 \\ \mathbf{a} \cdot \chi \leq \mathbf{b} \\ \mathbf{aeq} \cdot \chi = \mathbf{beq} \\ \mathbf{lb} \leq \chi \leq \mathbf{ub} \end{cases} \tag{4.6}$$

Where χ is the vector to be optimized, $z(\chi)$ is the objective function (scalar) represented by equation 4.5, $\mathbf{c}(\chi)$ is an inequality constraint that could be nonlinear, $\mathbf{ceq}(\chi)$ is an equality constraint that also could be nonlinear, $\mathbf{a}$ and $\mathbf{aeq}$ are matrices, $\mathbf{b}$ and $\mathbf{beq}$ are vectors for inequality and equality linear constraints, respectively, $\mathbf{lb}$ and $\mathbf{ub}$ are lower and upper bounds, respectively. In order to set the optimization problem properly, these matrices and vectors must be defined for each CRM representation, which is done in the following subsections.

4.2.3.1 CRMT

The first step is to define the vector of unknowns:

$$\chi = \begin{bmatrix} f \\ \tau \\ J \end{bmatrix}, \quad \chi \in \Re^{3\times 1} \tag{4.7}$$

As discussed by Weber [59], there are physical constraints related to each of the parameters. However, here a slightly different definitions for these constraints will be assumed:

- In order to be mass conservative, connectivities are not allowed to be higher than one for any representation. If $f > 1$, it means that there is some source of energy other than the injected fluid acting in the reservoir, which should be modeled through another way.

- τ is not allowed to be zero. A zero time constant means incompressible fluid and rock, or zero pore volume, or even infinite productivity index for the given control volume. Furthermore, it causes numerical instability in the state space equations, since $\mathbf{A} = -\frac{1}{\tau}$ and $\mathbf{B} = \begin{bmatrix} \frac{f}{\tau} & -J \end{bmatrix}$. Instead of assuming $\tau \geq 0$, we assume $\tau \geq \tau_{min}$, where $\tau_{min} \approx 0$.

- Since box constraints (upper and lower bounds) are used, it is necessary to define an upper limit for τ and J as well, which are defined as τ_{max} and J_{max}, respectively. This helps the convergence of the algorithm and avoid the time constant to diverge to infinity when a response to a stimulus is not realized, which may be caused by a higher frequency in the input signal than the appropriate one.

Thus, there are only box constraints for CRMT, which are defined as:

$$\mathbf{lb} = \begin{bmatrix} 0 \\ \tau_{min} \\ 0 \end{bmatrix}, \quad \mathbf{ub} = \begin{bmatrix} 1 \\ \tau_{max} \\ J_{max} \end{bmatrix}, \quad \mathbf{lb} \text{ and } \mathbf{ub} \in \Re^{3\times 1} \tag{4.8}$$

4.2.3.2 CRMP

For CRMP the vector of unknowns and box constraints are given by:

$$\chi = \begin{bmatrix} f_{11} \\ f_{12} \\ \vdots \\ f_{N_{inj}N_{prod}} \\ \tau_1 \\ \vdots \\ \tau_{N_{prod}} \\ J_1 \\ \vdots \\ J_{N_{prod}} \end{bmatrix}, \quad \mathbf{lb} = \begin{bmatrix} 0 \\ 0 \\ \vdots \\ 0 \\ \tau_{min} \\ \vdots \\ \tau_{min} \\ 0 \\ \vdots \\ 0 \end{bmatrix}, \quad \mathbf{ub} = \begin{bmatrix} 1 \\ 1 \\ \vdots \\ 1 \\ \tau_{max} \\ \vdots \\ \tau_{max} \\ J_{max} \\ \vdots \\ J_{max} \end{bmatrix},$$

$$\chi, \mathbf{lb} \text{ and } \mathbf{ub} \in \Re^{(N_{inj}+2)N_{prod}\times 1} \tag{4.9}$$

The sum of the connectivities related to a certain injector must be less than or equal to one:

$$\sum_{j=1}^{N_{prod}} f_{ij} \leq 1 \tag{4.10}$$

This is the only linear inequality constraint, it is based on mass conservation. If the

sum of the connectivities is less than one, some of the injected fluid may be leaking to another reservoir region, or there is a significant reduction in the fluid volume due to compressibility. Putting this equation in a matrix format, $\mathbf{a}$ and $\mathbf{b}$ are obtained:

$$\mathbf{a} = \left[\begin{array}{cccc:c} \mathbf{1_{1,N_{prod}}} & \mathbf{0_{1,N_{prod}}} & \cdots & \mathbf{0_{1,N_{prod}}} & \\ \mathbf{0_{1,N_{prod}}} & \mathbf{1_{1,N_{prod}}} & & \vdots & \mathbf{0_{N_{inj},2N_{prod}}} \\ \vdots & & \ddots & \mathbf{0_{1,N_{prod}}} & \\ \mathbf{0_{1,N_{prod}}} & \cdots & \mathbf{0_{1,N_{prod}}} & \mathbf{1_{1,N_{prod}}} & \end{array}\right], \quad \mathbf{a} \in \Re^{N_{inj} \times (N_{inj}+2)N_{prod}} \tag{4.11}$$

$$\mathbf{b} = \mathbf{1_{N_{inj},1}}, \quad \mathbf{b} \in \Re^{N_{inj} \times 1} \tag{4.12}$$

Where $\mathbf{1_{m,n}}$ is a $m \times n$ matrix with all of its elements equal to one, and $\mathbf{0_{m,n}}$ is a $m \times n$ matrix with all of its elements equal to zero. This notation will be further used in this thesis.

4.2.3.3 CRMIP

In order to simulate a system it is necessary to know its initial state. For the CRMT and CRMP representations, the states of the system are expressly known from the production history since they are directly measured physical quantities. However, in the CRMIP representation, the initial states are also unknown because the production rates of each control volume associated with a certain producer are not given in the production history. Therefore, the initial states of the system must be included in the history matching problem and they are constrained by the following equations:

$$0 \leq q_{ij}(0) \leq q_j(0) \tag{4.13}$$

From equation 2.18:

$$\sum_{i=1}^{N_i nj} q_{ij}(0) = q_j(0) \tag{4.14}$$

Thus, the vector of unknowns (χ) and its lower (**lb**) and upper (**ub**) bounds are defined as follows:

$$\chi = \begin{bmatrix} f_{11} \\ f_{12} \\ \vdots \\ f_{N_{inj}N_{prod}} \\ \tau_{11} \\ \tau_{12} \\ \vdots \\ \tau_{N_{inj}N_{prod}} \\ J_{11} \\ J_{12} \\ \vdots \\ J_{N_{inj}N_{prod}} \\ q_{11}(0) \\ q_{12}(0) \\ \vdots \\ q_{N_{inj}N_{prod}}(0) \end{bmatrix}, \quad \mathbf{lb} = \begin{bmatrix} 0 \\ 0 \\ \vdots \\ 0 \\ \tau_{min} \\ \tau_{min} \\ \vdots \\ \tau_{min} \\ 0 \\ 0 \\ \vdots \\ 0 \\ 0 \\ 0 \\ \vdots \\ 0 \end{bmatrix}, \quad \mathbf{ub} = \begin{bmatrix} 1 \\ 1 \\ \vdots \\ 1 \\ \tau_{max} \\ \tau_{max} \\ \vdots \\ \tau_{max} \\ J_{max} \\ J_{max} \\ \vdots \\ J_{max} \\ q_1(0) \\ q_2(0) \\ \vdots \\ q_{N_{prod}}(0) \end{bmatrix},$$

$$\chi, \mathbf{lb} \text{ and } \mathbf{ub} \in \Re^{4N_{inj}N_{prod} \times 1} \tag{4.15}$$

The linear inequality constraint is simply defined by equation 4.10, which in matrix format defines **a** and **b**:

$$\mathbf{a} = \left[\begin{array}{cccc:c} \mathbf{1_{1,N_{prod}}} & \mathbf{0_{1,N_{prod}}} & \cdots & \mathbf{0_{1,N_{prod}}} & \\ \mathbf{0_{1,N_{prod}}} & \mathbf{1_{1,N_{prod}}} & & \vdots & \mathbf{0_{N_{inj},3N_{inj}N_{prod}}} \\ \vdots & & \ddots & \mathbf{0_{1,N_{prod}}} & \\ \mathbf{0_{1,N_{prod}}} & \cdots & \mathbf{0_{1,N_{prod}}} & \mathbf{1_{1,N_{prod}}} & \end{array}\right],$$

$$\mathbf{a} \in \Re^{N_{inj} \times 4N_{inj}N_{prod}} \quad (4.16)$$

$$\mathbf{b} = \mathbf{1_{N_{inj},1}}, \quad \mathbf{b} \in \Re^{N_{inj} \times 1} \quad (4.17)$$

Where $\mathbf{1_{m,n}}$ is a $m \times n$ matrix with all of its elements equal to one, and $\mathbf{0_{m,n}}$ is a $m \times n$ matrix with all of its elements equal to zero.

The only equality constraint is defined by equation 4.14, which is algebraically rearranged to obtain the matrices **aeq** and **beq**:

$$\mathbf{aeq} = \left[\begin{array}{c:cccc} \mathbf{0_{N_{prod},3N_{inj}N_{prod}}} & \mathbf{I} & \mathbf{I} & \cdots & \mathbf{I} \end{array}\right], \quad \mathbf{aeq} \in \Re^{N_{prod} \times 4N_{inj}N_{prod}} \quad (4.18)$$

$$\mathbf{beq} = \begin{bmatrix} q_1(0) \\ q_2(0) \\ \vdots \\ q_{N_{prod}}(0) \end{bmatrix}, \quad \mathbf{beq} \in \Re^{N_{prod} \times 1} \quad (4.19)$$

Where $\mathbf{I}$ is the identity matrix.

4.2.3.4 ICRM

In the work done by Nguyen et al. [43], an ICRM formulation for primary recovery is developed, which estimates dynamic compressible pore volume, productivity index and reservoir pressure. Compared to the traditional buildup test, ICRM has the

advantage that it does not require shutting-in the well, so there is no production loss. For secondary recovery, the parameters estimated are productivity indices, time constants and interwell connectivities. Compared to other CRM formulations, the advantage of ICRM is that it is a linear model. Therefore, there is a unique set of model parameters that minimizes objective function, which is obtained via linear regression. Furthermore, it is much easier to establish confidence intervals, enabling uncertainty assessment in the model. In other words, it is possible to determine if the model parameters are statistically significant by checking how narrow the confidence intervals are.

As previously shown, the ICRM computes the cumulative liquid production at a given time instead of the total liquid production rates. Thus, instead of using equation 4.5 as the objective function, the history matching minimizes the squared error between the cumulative total production from the production history $\left(\left(N_{p,j}^{k}\right)_{obs}\right)$ and the one predicted by model $\left(\left(N_{p,j}^{k}\right)_{pred}\right)$:

$$\min z = \sum_{k=1}^{N_t} \sum_{j=1}^{N_{prod}} \left(\left(N_{p,j}^{k}\right)_{obs} - \left(N_{p,j}^{k}\right)_{pred}\right)^2 \tag{4.20}$$

$\left(N_{p,j}^{k}\right)_{pred}$ is given by equation 2.16, and it is copied here for easy interpretation:

$$N_{p,j}^{k} = (q_{j0} - q_{jk})\tau_j + \sum_{i=1}^{N_{inj}} \left(f_{ij} CWI_i^k\right) + J_j \tau_j (p_{wf,j}^{0} - p_{wf,j}^{k})$$

This is a linear constrained least square problem, the most suitable function in MATLAB Optimization Toolbox [37] to solve it is "lsqlin". The general optimization problem solved by "lsqlin" is given by:

$$\min_{\chi} z(\chi) = \frac{1}{2}\|\mathbf{c}\cdot\chi - \mathbf{d}\|_2^2 \text{ such that } \begin{cases} \mathbf{a}\cdot\chi \leq \mathbf{b} \\ \mathbf{aeq}\cdot\chi = \mathbf{beq} \\ \mathbf{lb} \leq \chi \leq \mathbf{ub} \end{cases} \tag{4.21}$$

Where χ is the vector to be optimized, $\mathbf{c}$ and $\mathbf{d}$ are a matrix and a vector, respectively, that represent the objective function (equation 4.20), $\mathbf{a}$ and $\mathbf{aeq}$ are matrices, $\mathbf{b}$ and $\mathbf{beq}$ are vectors for inequality and equality linear constraints, respectively, $\mathbf{lb}$ and $\mathbf{ub}$ are lower and upper bounds, respectively. In order to set the optimization problem properly, these matrices and vectors must be defined for ICRM.

Even though the control volume is the same as CRMP, the vector of unknowns (χ) is different because the linearity of the objective function must be kept. Thus, instead of determining the productivity indices (J's) directly, $J\tau$ is computed. Thus, the vector of unknowns (χ), lower ($\mathbf{lb}$) and upper ($\mathbf{ub}$) bounds are defined as follows:

$$\chi = \begin{bmatrix} f_{11} \\ f_{21} \\ \vdots \\ f_{N_{inj}N_{prod}} \\ \tau_1 \\ \vdots \\ \tau_{N_{prod}} \\ J_1\tau_1 \\ \vdots \\ J_{N_{prod}}\tau_{N_{prod}} \end{bmatrix}, \quad \mathbf{lb} = \begin{bmatrix} 0 \\ 0 \\ \vdots \\ 0 \\ \tau_{min} \\ \vdots \\ \tau_{min} \\ 0 \\ \vdots \\ 0 \end{bmatrix}, \quad \mathbf{ub} = \begin{bmatrix} 1 \\ 1 \\ \vdots \\ 1 \\ \tau_{max} \\ \vdots \\ \tau_{max} \\ J_{max}\tau_{max} \\ \vdots \\ J_{max}\tau_{max} \end{bmatrix},$$

$$\chi, \mathbf{lb} \text{ and } \mathbf{ub} \in \Re^{(N_{inj}+2)N_{prod}\times 1} \tag{4.22}$$

Since the time constants (τ's) are directly determined, J can be simply computed by dividing $J\tau$ by τ after the optimization problem has been solved. Also, notice the connectivities (f_{ij}'s) are purposely ordered differently than in CRMP, so matrix $\mathbf{c}$ will look simpler.

There is only one linear inequality constraint, which is equation 4.10. Rearranging it in matrix format, $\mathbf{a}$ and $\mathbf{b}$ are obtained:

$$\mathbf{a} = \left[\begin{array}{cccc:c} \mathbf{I} & \mathbf{I} & \cdots & \mathbf{I} & \mathbf{0_{N_{inj},2N_{prod}}} \end{array} \right], \quad \mathbf{a} \in \Re^{N_{inj} \times (N_{inj}+2)N_{prod}} \tag{4.23}$$

$$\mathbf{b} = \mathbf{1_{N_{inj},1}}, \quad \mathbf{b} \in \Re^{N_{inj} \times 1} \tag{4.24}$$

Where $\mathbf{1_{m,n}}$ is a $m \times n$ matrix with all of its elements equal to one, $\mathbf{0_{m,n}}$ is a $m \times n$ matrix with all of its elements equal to zero, and $\mathbf{I}$ is the identity matrix.

For the objective function, the matrix $\mathbf{c}$ and vector $\mathbf{d}$ must be defined. $\mathbf{d}$ expresses the values to be matched, in this case it is defined by the cumulative total production history $\left(\left(N_{p,j}^{k} \right)_{obs} \right)$. Together, the order of elements in $\mathbf{d}$ and χ also define the shape of $\mathbf{c}$. If $\mathbf{d}$ and χ are ordered properly, it can facilitate the assembly of the system of equations. Here, $\mathbf{d}$ is ordered as follows:

$$\mathbf{d} = \left[\begin{array}{c} \mathbf{N_{p,1}} \\ \mathbf{N_{p,2}} \\ \vdots \\ \mathbf{N_{p,N_{prod}}} \end{array} \right], \quad \mathbf{d} \in \Re^{N_{prod}N_t \times 1} \tag{4.25}$$

Where $\mathbf{N_{p,j}}$ is the cumulative production history of the j-th producer:

$$\mathbf{N_{p,j}} = \begin{bmatrix} N_{p,j}^{1} \\ N_{p,j}^{2} \\ \vdots \\ N_{p,j}^{N_t} \end{bmatrix}, \quad \mathbf{N_{p,j}} \in \Re^{N_t \times 1} \tag{4.26}$$

Then, matrix $\mathbf{c}$ can be divided in three blocks:

$$\mathbf{c} = \begin{bmatrix} \mathbf{c_f} & \mathbf{c}_\tau & \mathbf{c_{J\tau}} \end{bmatrix}, \quad \mathbf{c} \in \Re^{N_t N_{prod} \times (N_{inj}+2) N_{prod}} \tag{4.27}$$

$\mathbf{c_f}$, $\mathbf{c}_\tau$ and $\mathbf{c_{J\tau}}$ are blocks that respectively multiply f_{ij}'s, τ_j's and $J_j\tau_j$'s in the objective function. All of them are block diagonal matrices. $\mathbf{c_f}$ represents the influence of the cumulative injection:

$$\mathbf{c_f} = \begin{bmatrix} \mathbf{CWI} & \mathbf{0} & \cdots & \mathbf{0} \\ \mathbf{0} & \mathbf{CWI} & & \vdots \\ \vdots & & \ddots & \mathbf{0} \\ \mathbf{0} & \cdots & \mathbf{0} & \mathbf{CWI} \end{bmatrix}, \quad \mathbf{c_f} \in \Re^{N_t N_{prod} \times N_{inj} N_{prod}} \tag{4.28}$$

Where $\mathbf{CWI}$ is the cumulative injection matrix:

$$\mathbf{CWI} = \begin{bmatrix} CWI_1^1 & CWI_2^1 & \cdots & CWI_{N_{inj}}^1 \\ CWI_1^2 & CWI_2^2 & \cdots & CWI_{N_{inj}}^2 \\ \vdots & \vdots & & \vdots \\ CWI_1^{N_t} & CWI_2^{N_t} & \cdots & CWI_{N_{inj}}^{N_t} \end{bmatrix}, \quad \mathbf{CWI} \in \Re^{N_t \times N_{inj}} \tag{4.29}$$

$\mathbf{c}_\tau$ represents the influence of the production rates:

$$\mathbf{c}_\tau = \begin{bmatrix} \mathbf{q_1} & \mathbf{0} & \cdots & \mathbf{0} \\ \mathbf{0} & \mathbf{q_2} & & \vdots \\ \vdots & & \ddots & \mathbf{0} \\ \mathbf{0} & \cdots & \mathbf{0} & \mathbf{q_{N_{prod}}} \end{bmatrix}, \quad \mathbf{c}_\tau \in \Re^{N_t N_{prod} \times N_{prod}} \tag{4.30}$$

Where $\mathbf{q_j}$ is defined by the production history as follows:

$$\mathbf{q_j} = \begin{bmatrix} q_{j0} - q_{j1} \\ q_{j0} - q_{j2} \\ \vdots \\ q_{j0} - q_{j,N_t} \end{bmatrix}, \quad \mathbf{q_j} \in \Re^{N_t \times 1} \tag{4.31}$$

$\mathbf{c_{J\tau}}$ represents the influence of the producers' BHP:

$$\mathbf{c_{J\tau}} = \begin{bmatrix} \mathbf{p_{wf,1}} & \mathbf{0} & \cdots & \mathbf{0} \\ \mathbf{0} & \mathbf{p_{wf,2}} & & \vdots \\ \vdots & & \ddots & \mathbf{0} \\ \mathbf{0} & \cdots & \mathbf{0} & \mathbf{p_{wf,N_{prod}}} \end{bmatrix}, \quad \mathbf{c_{J\tau}} \in \Re^{N_t N_{prod} \times N_{prod}} \tag{4.32}$$

Where $\mathbf{p_{wf,j}}$ is defined by the producers' BHP from the production history as follows:

$$\mathbf{p_{wf,j}} = \begin{bmatrix} p^0_{wf,j} - p^1_{wf,j} \\ p^0_{wf,j} - p^2_{wf,j} \\ \vdots \\ p^0_{wf,j} - p^{N_t}_{wf,j} \end{bmatrix}, \quad \mathbf{p_{wf,j}} \in \Re^{N_t \times 1} \tag{4.33}$$

Once all these matrices and vectors have been defined, the optimization problem

(equation 4.21) can be solved to estimate f_{ij}'s, τ_j's and J_j's, which can applied to the CRMP's state space equation to simulate the future behavior of the system. In the next section, the optimization algorithm selection and the computation of the gradient and hessian will be explained.

4.2.4 Choice of Optimization Algorithm

The choice of optimization algorithm must be based on the properties of the model, such as the behavior of the objective function, type of variables, type of constraints, dimension of the problem, etc.. The objective function of the CRM formulations presented here (equation 4.5), except ICRM, is a nonlinear least-square problem, and it is a smooth function with continuous variables (χ). The derivatives of the objective function are possible to be computed, however it is a daunting task due to its size and complexity. As previously discussed, there are three types of constraints in the CRM problems:

- Box constraints: $\chi_{\mathbf{min}} \leq \chi \leq \chi_{\mathbf{max}}$, applies to CRMT, CRMP and CRMIP;
- Linear inequality constraint: $\mathbf{a} \cdot \chi \leq \mathbf{b}$, applies to CRMP and CRMIP;
- Linear equality constraint: $\mathbf{aeq} \cdot \chi \leq \mathbf{beq}$, applies only to CRMIP.

The derivatives of these type of constraints are really simple to compute. The dimension of the problem depends on the number of wells as shown in table 4.1.

Table 4.1: Number of parameters to be estimated for each model.

Model	Number of parameters
CRMT	3
CRMP	$(N_{inj} + 2)\, N_{prod}$
CRMIP	$4N_{inj}N_{prod}$
ICRM	$(N_{inj} + 2)\, N_{prod}$

Based on this analysis of the problem, the sequential quadratic programming (SQP) algorithm was chosen to estimate the parameters. The gradient is numerically computed and an approximation of the hessian matrix is computed using the Broyden-Fletcher-Goldfarb-Shanno (BFGS) algorithm. For details on the SQP or BFGS algorithms the reader is referred to [44].

In order to understand how accurate the estimated parameters are, it is also important to understand how the objective function varies with them, in order words, how sensitive the objective function is to each type of parameter. This subject is addressed in the next subsection.

4.2.5 Sensitivity Analysis

Connectivities (gains, f) define how much production rates vary due to a step variation in injection rates when a steady state is achieved. Therefore, changing the connectivities of the system is equivalent to shifting the response up or down (figure 4.1). Time constants are related to the time required to achieve the steady state, a faster system has lower τ, while a slower system has higher τ. Thus, if only the time constant is changed, the system still tends to the same stationary point (figure 4.2).

The homogeneous five-spot depicted at figure 4.6 was simulated to show the impact of f and τ in the objective function (equation 4.5). In order to have a two-dimensional problem so that the behavior of equation 4.5 can be plotted and analyzed, the CRMT formulation was chosen and the bottomhole pressures were kept constant, thus J is not estimated.

As one can see in figure 4.7, the objective function is much more sensitive to connectivity than to time constant because changing connectivities shifts the whole response curve up or down, generating a big error, changing the order of magnitude of the objective function, which does not happen when changing time constants.

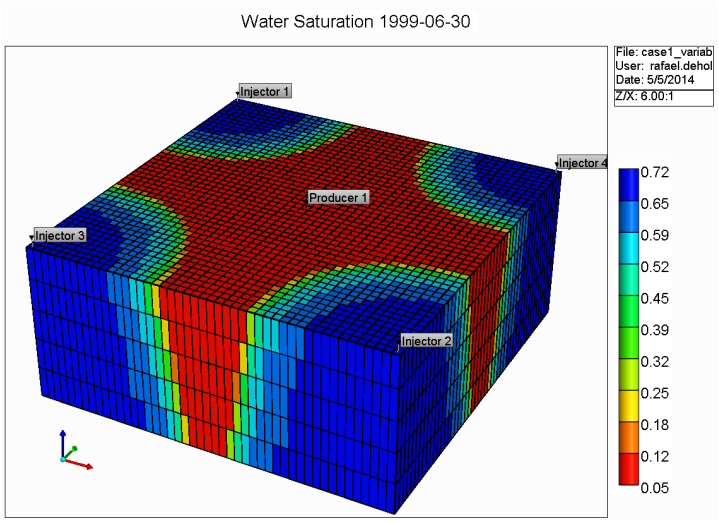

Figure 4.6: Water saturation of homogeneous five spot pattern used for the sensitivity analysis.

The active-set SQP method was used for this optimization problem [44]. As shown in figure 4.8, starting with different initial guesses, the problem will quickly converge to the right value of connectivity; however, the time constants estimation is still inaccurate. This example is trivial, but enough to realize that parameters estimation can be very complicated when applying to systems with several control volumes.

Jafroodi and Zhang [18] used ensemble Kalman filter to estimate dynamic f and τ for history matching using 100 ensemble realizations. After the history matching, the dynamic connectivities fit within a narrow band while the dynamic time constants fit within a broad band. This results also corroborate that the objective function is significantly more sensitive to connectivities than time constants.

4.3 Fractional Flow Model

Once the f's τ's and J's were estimated it is easy to forecast the total liquid production. However, in field operations, it is usually necessary to predict oil rates

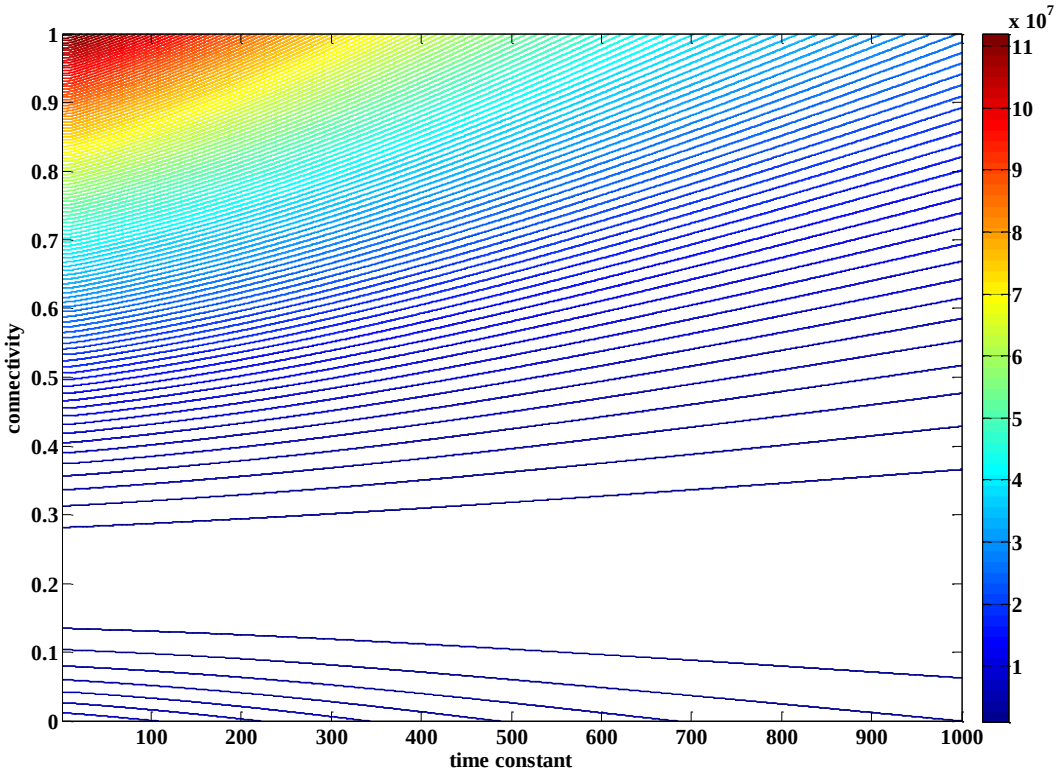

Figure 4.7: Objective function behavior for the CRMT applied to the five spot pattern.

as well. Thus, a fractional flow must be used for this sake. Among many options available in the literature, the empirical power law developed by Gentil [13] was chosen because of its simplicity. Also, the only data required for this model is total injection (i_{ik}) and production rates (q_{jk}), which also was a requirement for CRM, and oil production rates (qo_{jk}). The limitation of this model is that it must be used only for mature waterflooding, specifically when the water cut is greater than 0.5. The model is defined by the following equation:

$$qo_{jk} = \frac{1}{1 + a_j CWI_{eff,jk}^{b_j}} q_{jk} \tag{4.34}$$

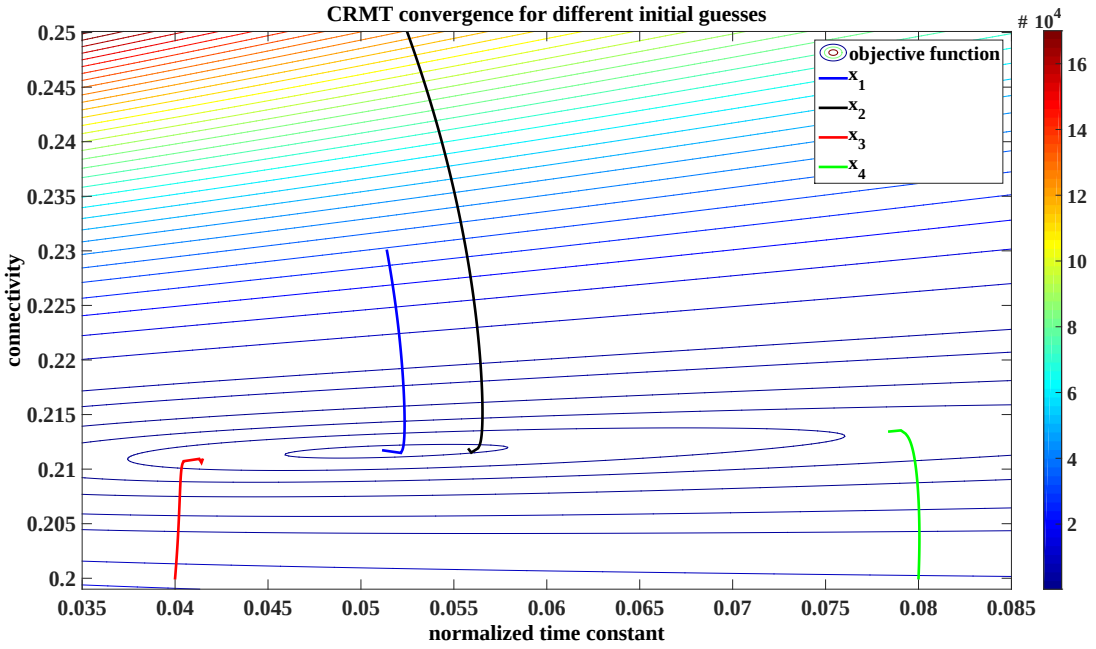

Figure 4.8: Contours of the objective function and convergence of the active set SQP method for CRMT.

Where a_j and b_j are the parameters that define the model for producer j, and $CWI_{eff,jk}$ is the cumulative water injected that effectively influences the production rates in producer j at the k-th time step. $CWI_{eff,jk}$ is defined by:

$$CWI_{eff,jk} = \sum_{\kappa=1}^{k} \sum_{i=1}^{N_t} f_{ij} I_{i\kappa} \tag{4.35}$$

The advantage of this power law fractional flow model is that it can be converted to a straight line equation, as follows:

$$\ln\left(\frac{q_{jk}}{qo_{jk}} - 1\right) = \ln\left(\frac{qw_{jk}}{qo_{jk}}\right) = \ln\left(WOR_{jk}\right) = \ln\left(a_j\right) + b_j \ln\left(CWI_{eff,jk}\right) \tag{4.36}$$

Where qw_{jk} is the water production rate and WOR_{jk} is the water oil ratio of producer j at the k-th time step.

Once the problem was linearized, a linear regression is applied to estimate the coefficients a_j and b_j, which has the following objective function:

$$\min z = \sum_{k=k_{oil}}^{N_t} \left(\ln \left(WOR_{jk}^{obs} \right) - \ln \left(WOR_{jk}^{pred} \right) \right)^2 \tag{4.37}$$

Where WOR_{jk}^{obs} is the water oil ratio computed or directly obtained from the production history and $\ln \left(WOR_{jk}^{pred} \right)$ is computed by equation 4.36. k_{oil} is the time when the fractional flow parameters estimation window starts, which may be different from the CRM history matching window, since the water cut must be higher than 0.5 for this fractional flow model. This problem can be solved independently for each producer.

The only constraint imposed to equation 4.37 is:

$$b_j \geq 0 \tag{4.38}$$

To assure that the water oil ratio will increase as more water is injected.

Once all the CRM and fractional flow model parameters have been estimated, it is necessary to judge if the model really represent the dynamics of the system with the desired degree of accuracy. If it does, then the model is validated and can be used for certain managerial decisions. If it does not, then it is necessary to choose another model that is more likely to capture the physics of the reservoir and go through the same steps again. The model validation step will be exemplified in the next chapter.

5. CASE STUDIES

In this chapter, three case studies are presented to exemplify the use of the state space equations developed in chapter 3 with the grey-box system identification algorithm explained in chapter 4. Analyzing the time response, the models (ICRM, CRMP, or CRMIP) will be validated based on the production data. The three reservoirs were purposely chosen to demonstrate the CRM's applicability in different levels of heterogeneity:

- Case 1 – 5×4 (5 injectors and 4 producers) homogeneous with flow barriers;
- Case 2 – 8×7 channelized;
- Case 3 – 8×7 shoreface environment.

5.1 Case 1: Homogeneous Reservoir with Flow Barriers

In order to validate the concepts developed in the previous chapters, the method is applied to the simple reservoir with a predictable flow behavior depicted in figure 5.1. This 5 injectors $\times$ 4 producers homogeneous reservoir with flow barriers is based on the on the one presented in [7]. The reservoir properties are listed in table 5.1.

The production history data is presented in appendix A. The values of injection rates were generated by an uniform distribution with minimum of 300 bbl/day and maximum of 2525 bbl/day varying monthly (figure A.1). Analogously, the producers' BHP were generated by an uniform distribution with minimum of 120 psi and maximum of 180 psi varying monthly (figure A.2). The observed production rates were computed using IMEX [36] and are shown in figure A.3. Due to the symmetry

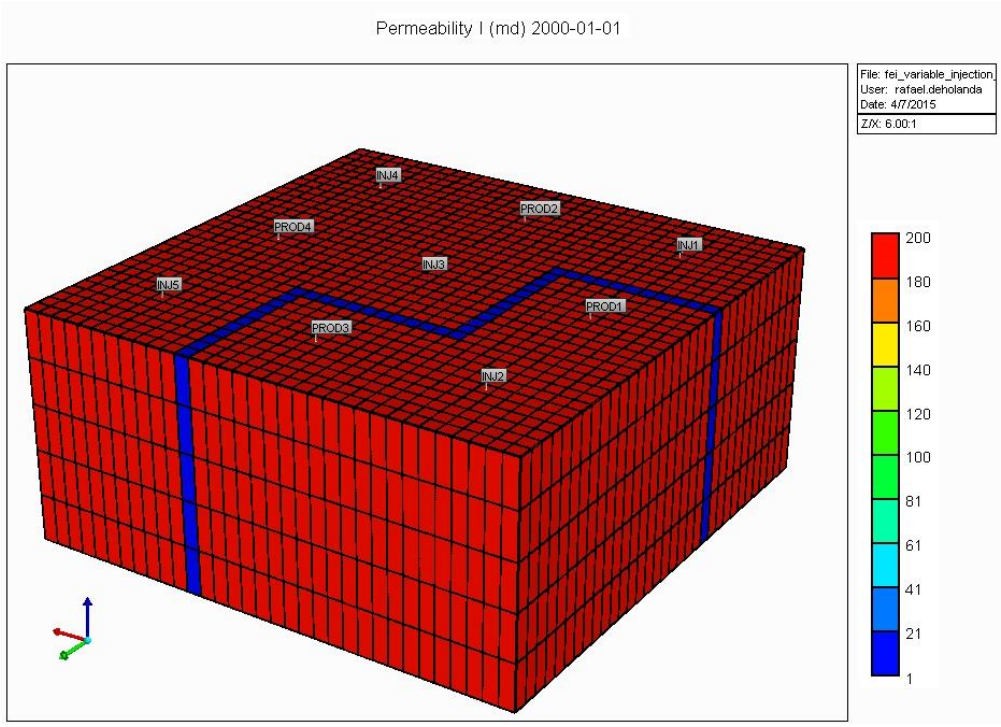

Figure 5.1: Horizontal permeability for case 1.

of this problem and inputs uniformly varying in the same range, it is easy to realize a similar production behavior for wells "PROD1" and "PROD3", as well as for "PROD2" and "PROD4".

The time window selected for history matching is from 3200 days ($\approx$ 9 years) to 5000 days ($\approx$ 14 years), such that the water breakthrough already happened in all of the producers, reducing the effects of nonlinearities in the CRM parameters. The model validation window is from 5000 days ($\approx$ 14 years) to 7200 days ($\approx$ 20 years).

Once the production history has been obtained and the appropriate time windows have been selected, the CRM's are generated by history matching the production data as described in chapter 4. Three models had their capability to represent the system tested: ICRM, CRMP and CRMIP. The liquid production rates for the

Table 5.1: Reservoir properties for case 1 (adapted from [7]).

Parameters	Value
Number of Grid Blocks	$33 \times 33 \times 5$
Grid Block Size (ft)	$77.5 \times 77.5 \times 38.75$
Producer-Injector Well Spacing (ft)	852.5
Porosity	0.2
Horizontal Permeability (k_h, md)	200
Horizontal Permeability in the barrier (k_h, md)	1
Vertical Permeability (k_v, md)	$k_v = \frac{k_h}{10}$
Oil Compressibility (psi^{-1})	3×10^{-5}
Water Compressibility (psi^{-1})	1×10^{-6}
Water Compressibility (psi^{-1})	1×10^{-6}
Initial Reservoir Pressure (psi)	1250
End-Point Water Relative Permeability	0.3
End-Point Oil Relative Permeability	1

history matching and validation windows from the production data and the CRM's are compared in figure A.4.

Figure A.4 suggests that all CRM's capture the dynamic behavior of this reservoir with a reasonable accuracy. Even though the ICRM response follows all the trends in the observed flowrates, it does not overlap the production history as well as the CRMP and CRMIP responses. Analyzing more carefully, there are notable overshoots in the wells "PROD1" and "PROD3", which is caused by productivity indices being estimated by values that are higher than the real ones. This is confirmed in table A.1, where the ICRM productivity indices can be compared to the ones obtained from CRMP and CRMIP, which are better representations of the system. Still in table A.1, ICRM estimates $J_2 = 0.00$, which is not physically meaningful. Furthermore, due to symmetry and inputs varying within the same range, the relationship $J_2 \approx J_4$ should apply to be physically consistent, for CRMP it does, for ICRM it does not.

Analyzing the time constant estimates in table A.2, the values for the ICRM time constants are significantly different from the ones for CRMP, which is based on the same control volumes. The cause of this is that ICRM does a history matching for the cumulative liquid production, so the information in the flowrates is smoothed out, losing accuracy in estimating the parameters that represent the dynamics of the reservoir. As shown in figure A.5, ICRM, CRMP and CRMIP perform a good history matching for the cumulative liquid production. However, CRMP and CRMIP still are better than ICRM in forecasting the cumulative liquid production, this is evident for well "PROD3".

Comparing the CRMP to the CRMIP liquid production rates in figure A.4, the CRMIP fits better the production history at the expense of estimating more parameters. However, the differences between the CRMP and CRMIP responses are small. Therefore, CRMP is a representative model of the dynamics of the reservoir. The homogeneity of this reservoir enables the use of CRMP by making the assumption of one single time constant for all injector-producer pairs plausible. Indeed, CRMIP is a more robust model for the fact that different injector-producer pairs may have different time constants. For instance, "PROD3" should respond faster to injection rates variations in "INJ2" than in the other injectors due to the flow barrier, it reflects in a lower time constant between "INJ2" and "PROD3" than for "PROD3" and the other injectors, as one can see in table A.2.

Figure 5.2 shows the connectivity maps for the CRM realizations. Indeed, the connectivities are capable to infer the transmissibility trends in the reservoir, as described in [13], identifying the presence of the low permeability barrier separating "PROD1", "PROD3" and "INJ2" from the other wells. Also, the symmetry in the permeability is preserved in all models, specially for the larger connectivity values. The connectivities estimates for all the models are consistent with the features of

the reservoir, which corroborates the sensitivity analysis in section 4.2.5. Since the history matching objective function is more sensitive to connectivities, they are most likely to be good estimates than other parameters, having a narrower confidence interval.

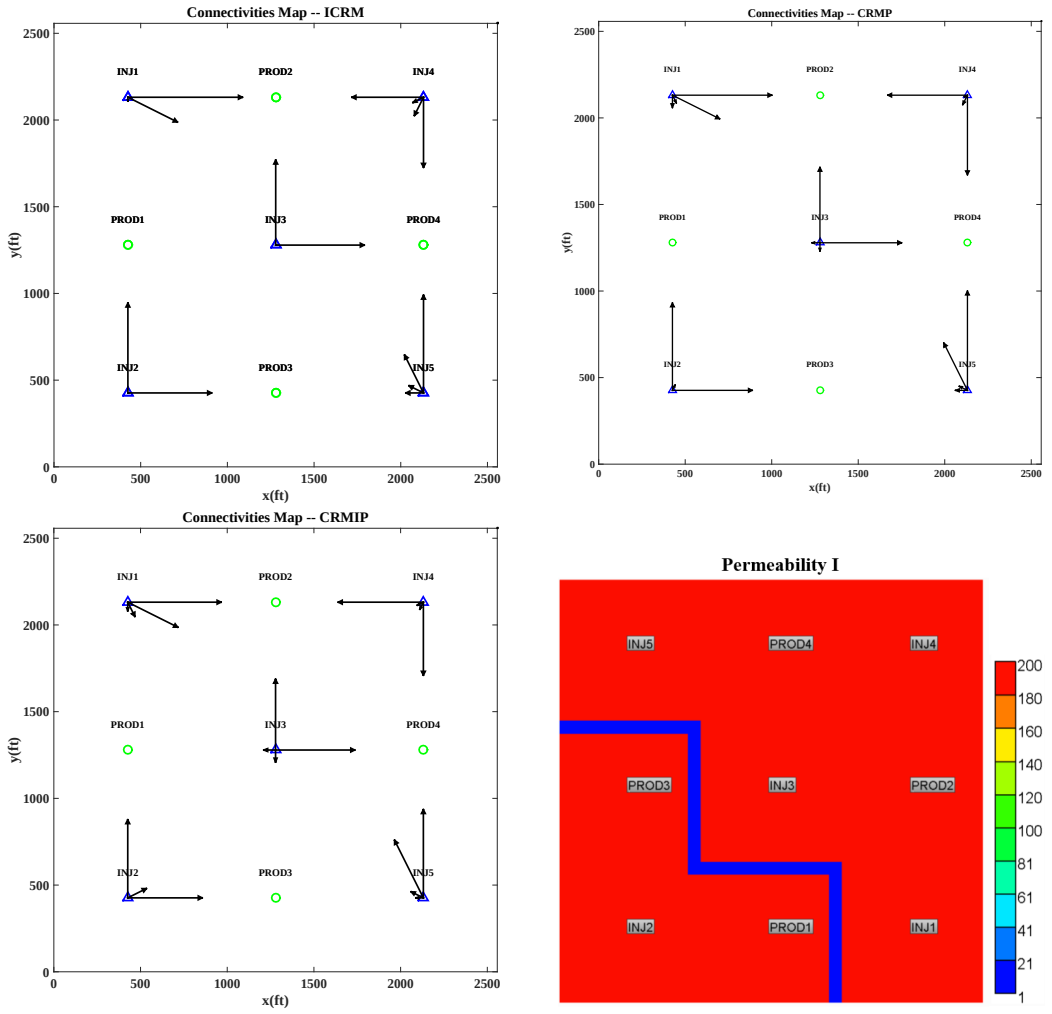

Figure 5.2: Connectivity maps for ICRM, CRMP and CRMIP compared to the horizontal permeability (case 1).

The CRMP and CRMIP estimates are more consistent than the ICRM ones also

for connectivities. For example, “INJ3” is also connected to “PROD1” and “PROD3” because the flow barrier is not completely sealing, thus such connectivity must be low, but not zero as in the ICRM (figure 5.2). The connectivity estimated values are also shown in table A.3. The sum of connectivities related to a certain injector is one, indicating that the injected fluid is not leaking. On the other hand, the sum of connectivities related to a certain producer can be used to indicate the producers that receive more pressure support from the injectors, which are “PROD2” and “PROD4”, since the pressure support for “PROD1” and ”PROD3” is almost reduced to “INJ2”. It is also important to highlight that connectivities were filtered, assigning zero to any of them that was less than 10^{-3} in order to simplify the production rates computation. The connectivities estimates are in agreement with the ones obtained in [7].

Figure A.6 shows the water cut computed using the fractional flow model proposed in [13]. This model fits well in the history matching window, specially after 3500 days. However, the water cut is overestimated in the prediction window for wells “PROD2” and “PROD4”, which leads to pessimistic oil rates predictions for those wells at late time, as one can see in figure A.7. Even though the fractional flow model depends on the connectivities estimates, no significant difference was realized in the water cut (figure A.6) when comparing ICRM, CRMP and CRMIP. Also, since production is happening at high water cut, the differences in liquid production rates between CRM’s (figure A.4) are reduced when comparing oil rates (figure A.7).

The results previously discussed can be summarized in figure 5.3, where the mean square error (MSE) is plotted for each CRM and each well taking into account history matching and model validation windows. The total production rates MSE, suggest that CRMIP is the most reliable representation. However, CRMP is almost as accurate as CRMIP. These differences are more expressive in the cumulative production.

Indeed, ICRM is not the best even to predict cumulative production. The fractional flow prediction are not much affected by the CRM chosen, even though it relies on the connectivity estimates. In a mature waterflood, the oil production rates are less sensitive to the choice of model than the total production rates. Another statistical parameter also used as a measurement of the goodness of fitting is the normalized root mean square error (NRMSE), which is shown in figure A.8 and can be used for comparison between different wells, since it is normalized. The closer the NRMSE is to one, the better is the fit to the data.

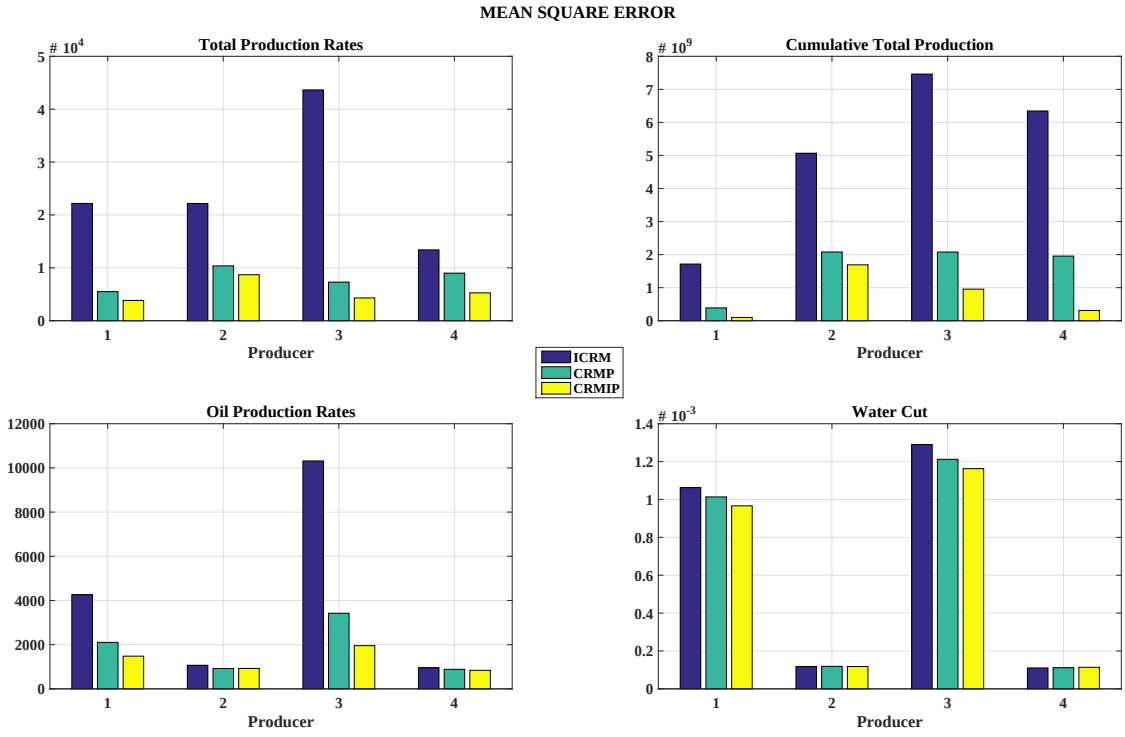

Figure 5.3: Mean square error for ICRM, CRMP and CRMIP (case 1).

Figure 5.4 depicts the productivity indices and time constant maps obtained using the CRMIP representation. Theoretically, each injector-producer pair is assigned one

productivity index (J_{ij}), one time constant (τ_{ij}) and one connectivity (f_{ij}). However, figure 5.4 shows that a maximum of two J_{ij}'s per producer is enough to capture the response to the producers' BHP variations, and the rest of J_{ij}'s are zero (table A.1). In this case, a zero productivity indices for a given injector-producer control volume does not mean that there is no response to the producer's BHP variation, instead it means that the BHP response must be analyzed for the producer as a whole, not separately for its control volumes.

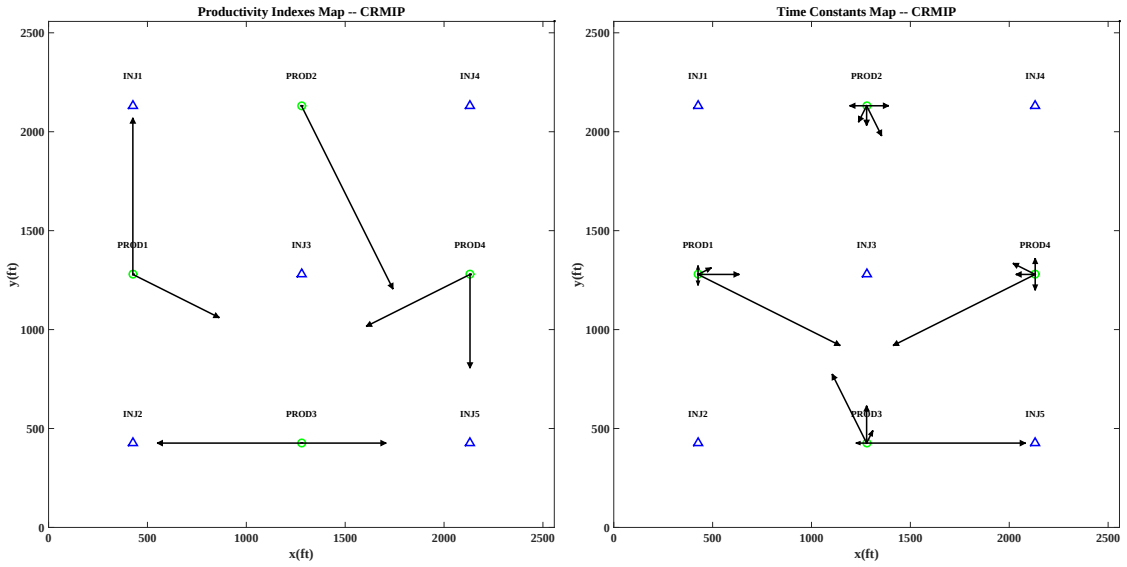

Figure 5.4: Productivity indices and time constants maps for the CRMIP representation (case 1).

Analyzing the CRMIP transfer function (equations 3.48, 3.49 and 3.50), one can see that the BHP response is given by the summation of biproper terms linked to the same input ($P_{wf}^{(j)}$), which in the time domain is the summation of exponential terms. Moreover, the BHP and injection responses are only linked by the time constants (τ_{ij}'s). Therefore, assigning few productivity indices to a producer, and computing

the time constants related to them separately, can significantly reduce the size of the history matching problem, specially for reservoirs with large number of wells.

The BHP response is mostly controlled by the reservoir properties in the near wellbore region. For this reason, it can be decoupled from the injector-producer control volumes. The same does not apply to the injection response because the signal needs to travel all the way to the producer, therefore connectivities really are interwell properties. These observation and the results obtained here indicate that the CRMIP representation can be simplified and a model with the same degree of accuracy can be obtained.

As previously discussed in chapter 3, a linear system representation may not be controllable or observable, which means that it is not a minimal realization. In other words, it is possible to represent the same system with less states than the actual realization. As shown in table 5.2, the CRMIP is observable and controllable, therefore, it is indeed a minimal realization for case 1.

Table 5.2: Results after controllability and observability analysis and model reduction for CRMIP (case 1).

	Number of States
CRMIP	20
Uncontrollable (CRMIP)	0
Unobservable (CRMIP)	0
Minimal Realization	20
Model Reduction (99% preserved)	7

Even in a minimal realization, it is possible to reduce even further the order of the model by removing states that give negligible contribution to the dynamics of

the system. This leads to the notion of model reduction of large scale dynamical systems [2]. Since, the model reduction is not the focus of this thesis, we will only describe the process in terms of the Hankel singular values of the dynamical system [9, 2]. In this case, one can perform what is called balancing the system, whereby one determines the controllable and observable description of the system. Model reduction follows by removing simultaneously the states that are uncontrollable (or weakly controllable) and unobservable (or weakly observable). Model reduction has been recently applied in reservoir simulation [14, 15]. The reader can refer to the above cited references for more details.

The Hankel singular values (HSV) can be used to estimate the amount of states that can be removed from the system penalizing its dynamics within a given tolerance. A state with higher HSV means that it has a more significant contribution to the physics of the system while very low HSV means negligible contribution. Thus, the normalized cumulative sum of the HSV's in decreasing order indicates the fraction (or percentage) of the system dynamics preserved when the rest of the states are neglected. Figure 5.5 shows the HSV's for the CRMIP representation, indicating that it is possible to keep 99% of the CRMIP dynamics with only 7 states, instead of the original 20.

Figure A.9 compares the liquid production rates of the reduced order model with the CRMIP and CRMP. Indeed, the reduced model accurately represents the CRMIP dynamics, consequently the reservoir dynamics. The reduced model only have three states more than the CRMP representation, so it is comparable in complexity, however it decribes the dynamics of the system more accurately than CRMP for wells "PROD1", "PROD3" and "PROD4", but not for "PROD2", which can be fixed if a reduced model with more states is obtained.

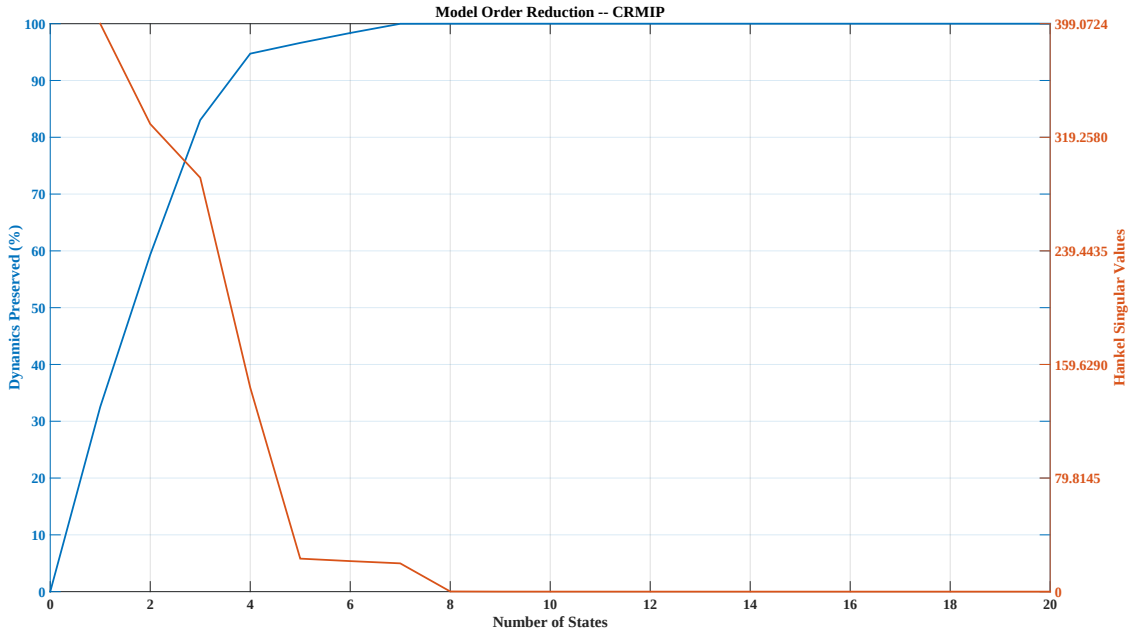

Figure 5.5: Hankel singular values decomposition and system's dynamics preserved after model reduction for CRMIP (case 1).

5.2 Case 2: Channelized Reservoir

It was straightforward to predict the flow behavior in case 1. Even though case 1 is a valid proof of concept, it is too idealistic. In practice, a real reservoir can be very heterogeneous depending on the geological history of the formation. Thus, it can be quite complicate to predict the subsurface flow behavior just by looking at the permeability maps, as it was previously done. Building reliable models for very heterogeneous reservoirs is also a daunting and time consuming task. Generally, an interdisciplinary group (geophysicists, geologists, reservoir engineers, etc.) acquire and analyze data to develop a model based on well-known concepts. Since reservoirs are data poor environments, where the uncertainty is high, many realizations may be necessary.

The objective of case 2 and 3, to be discussed next, is to test the state space

equations CRM's applicability in more realistic scenarios. Case 2 and 3 are based on the SPE-10 model, which was originally proposed to compare upscaling methods. For further information regarding the SPE-10 model, the reader is referred to [10].

Case 2 is based on layers 80 to 85 of the SPE-10 model. The horizontal permeability map for each of these layers is shown in figure 5.6. It is a fluvial environment, where a strong contrast is noticed (figure 5.6), high permeability channels are shown in reddish colors while poor facies are depicted by the blueish colors. The wells are placed as a five-spot pattern with 8 injectors and 7 producers. The main modifications made to the original SPE-10 model are shown in table 5.3.

Table 5.3: SPE-10 model modifications for cases 2 and 3.

Parameters	Value
Number of Grid Blocks	$60 \times 220 \times 6$
Grid Block Size (ft)	$50 \times 25 \times 5$
Transmissibility Multipliers	0.1

Appendix B presents the production history data and results obtained using CRM's for case 2. Injection rates for all the injector vary monthly between 100 bbl/day and 300 bbl/day (figure B.1). Producers' BHP vary every 6 months between 3400 psi and 3600 psi (figure B.2). The observed production rates obtained using IMEX [36] are shown in figure B.3. The history matching window is from 2000 days ($\approx$ 5.5 years) to 4745 days (13 years), starting after water breakthrough for all producers. The model validation window is from 4745 days (13 years) to 7300 days (20 years).

Figures B.4 and figure B.5 show the liquid production rates for the history matching and validation windows from the production data, ICRM, CRMP and CRMIP.

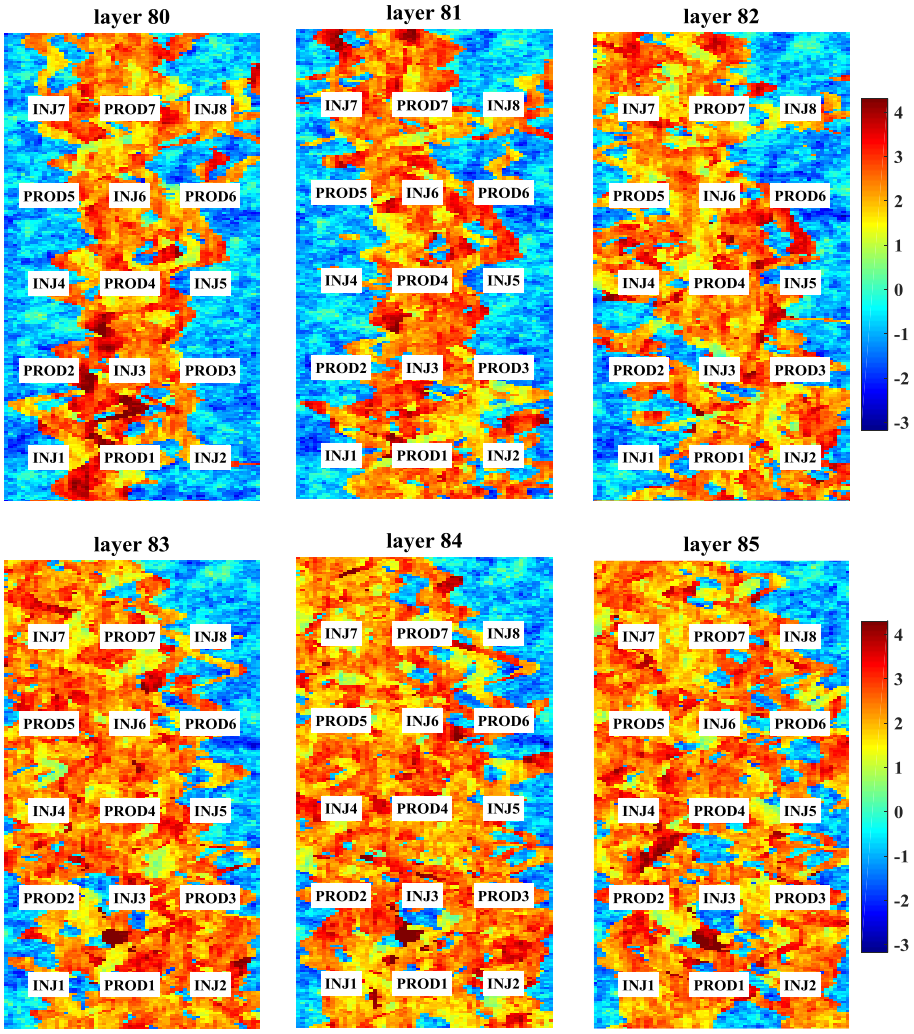

Figure 5.6: Logarithm of horizontal permeability (md) for layers 80 to 85 of the SPE-10 model.

Differently from case 1, the differences between models and production history are notable, they do not overlap as well as in the first case. This suggests that the choice of model becomes more important as reservoir complexity increases.

Starting from the simplest model, ICRM is problematic in wells "PROD1", "PROD2" and "PROD5", overshooting their responses when there are changes in the BHP. Due to this problem, there are negative production rates for "PROD5", which

is unacceptable. As previously discussed, this is caused by an overestimation of the productivity indices, as one can compare with CRMP (table B.1), which does not present these overshoots and considers the same control volumes. The productivity indices estimates for wells "PROD3", "PROD4" and "PROD7" are zero, which is also unreasonable.

The ICRM time constant estimates are not acceptable as well. For example, analyzing "PROD4" liquid production rates in figure B.4, one can see that the ICRM production curve looks like a series of steps, this caused by underestimating the time constant as shown in table B.2, thus the model provides a faster response to a stimulus than the actual reservoir's production rate response. Therefore, the ICRM productivity indices and time constant estimates do not represent the reservoir dynamics.

Comparing CRMP and CRMIP to the production history, the CRMIP representation captures the reservoir dynamics much better than CRMP. Even when CRMIP does not match the production history, it still follows all the trends of the system dynamics, for example, "PROD3" flowrates after 6700 days (figure B.4). On the other hand, CRMP tends to provide a smoother response than the production history and does not capture all of the trends as CRMIP, because only one time constant is assigned for each producer. This CRMP behavior is clearer in wells "PROD3" and "PROD6", which are partially drilled in the poor facies (layers 80 to 82) and partially in the channels (layers 83 to 86). Comparing case 2 to 1, it is evident that in very heterogeneous reservoirs the price of estimating more parameters when using CRMIP becomes justifiable since the CRMIP performance can be remarkably better than CRMP.

In control theory, a state observer is capable to estimate the system states by examining its inputs and outputs. Thus, we expect to improve CRMIP short-term

predictability in future works by coupling it with a state observer to remove the offset, for example, in "PROD3" after 6700 days (figure B.4).

Comparing ICRM, CRMP and CRMIP connectivity maps shown in figures 5.7 and 5.8, the ICRM connectivity estimates are not in agreement with CRMP and CRMIP, and based on the previous discussion, are not representative of the reservoir properties. The CRMP connectivity estimates are close to the CRMIP ones, as one can analyze more carefully in table B.3. This result is in agreement with the sensitivity analysis in section 4.2.5. Since the CRMIP provides better results, its connectivities are the ones taken as reference.

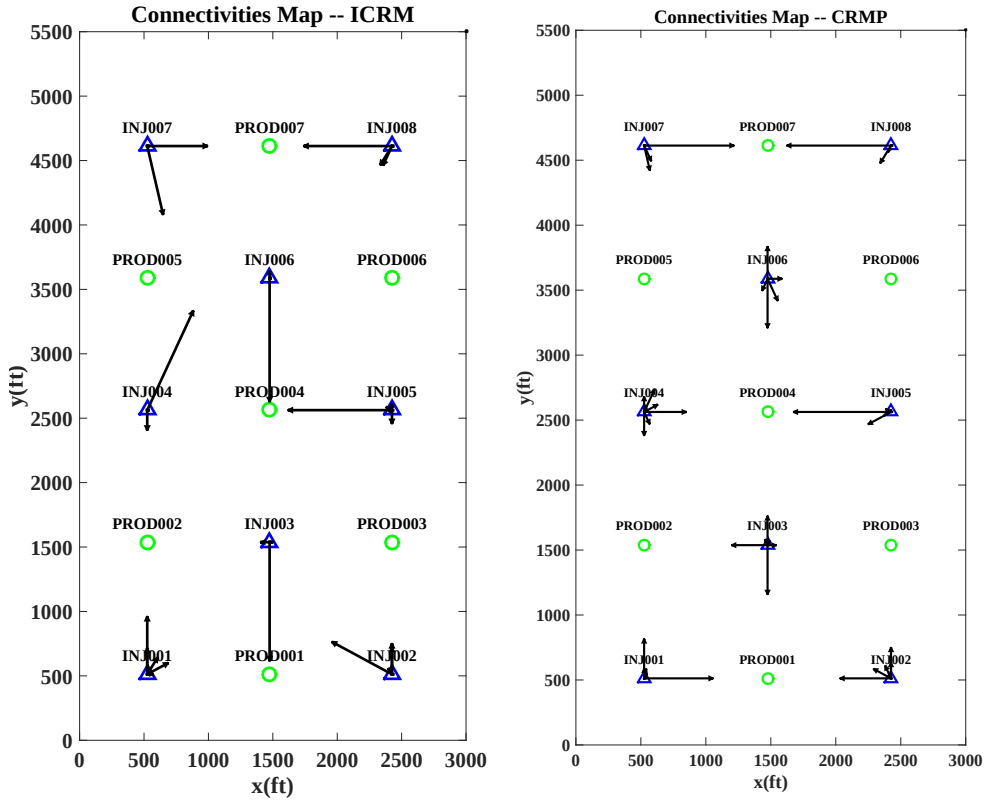

Figure 5.7: ICRM and CRMP connectivity maps (case 2).

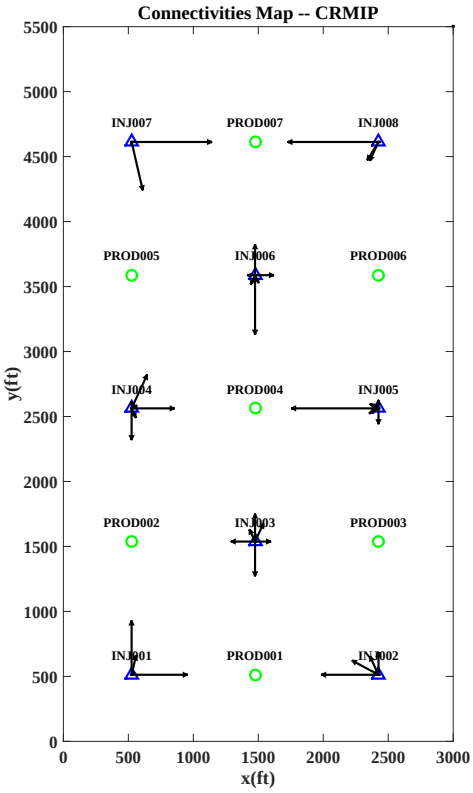

Figure 5.8: CRMIP connectivity map (case 2).

Analyzing figure 5.8, "PROD3", "PROD5" and "PROD6" are not very connected to the injectors, since they are in the poor facies in the upper layers (figure 5.6). On the other hand, "PROD1", "PROD4" and "PROD7" are in the middle of the channels in all the layers, having a high connectivity with injectors. Also, it is important to notice that in channelized reservoirs high connectivity in distant injector-producer pairs is more likely to happen, an example is "INJ7" and "PROD1": $f_{71} = 0.373$ (table A.3).

Cumulative production is shown in figures B.6 and B.7. All CRM's provide a good history matching for cumulative production. Analyzing the prediction window, it is not conclusive which one is the best model. For example, ICRM performs better

than CRMIP and CRMP for "PROD3" and "PROD6", on the other hand, CRMIP is the most accurate for "PROD1" and "PROD2".

Figures B.8 and B.9 show the water cut computed using the fractional flow model [13]. This model fits well in the history matching window, except when the water cut is less than 0.5, as in "PROD3" and "PROD5". The results obtained corroborate what has been observed in case 1, even though this empirical fractional flow model depends on the connectivities estimates, the differences between the ICRM, CRMP and CRMIP's capability to predict water cut are negligible. However, the fractional flow parameters a_j and b_j can be different (table B.4). In the prediction window, "PROD3", "PROD4", "PROD5" and "PROD6" have their water cut slightly over-estimated.

Oil production rates are presented in figures B.10 and B.11. The same observations done for the liquid production rates (figures B.4 and B.5) applies here, however the differences between the CRM's are reduced because of production in higher water cut. Therefore, CRMIP is also significantly better than the others.

Figure 5.9 summarizes the results previously discussed by showing the mean square error for each method in each producer. It is clear the CRMIP outperforms CRMP, which is better than ICRM, when predicting liquid rates and oil rates. On the other hand, there is no general rule regarding the best cumulative production model, where ICRM could outperform the other CRM models in some wells. The water cut predictions are equivalent for all the models. Analogously, the normalized root mean square is shown in figure B.12.

The productivity indices and time constants maps for the CRMIP representation are shown in figure 5.10. The higher productivity index values are for wells "PROD1" and "PROD7", which are fully drilled in the high permeability channels. The high productivity indices are associated with low time constants, as one can confirm in

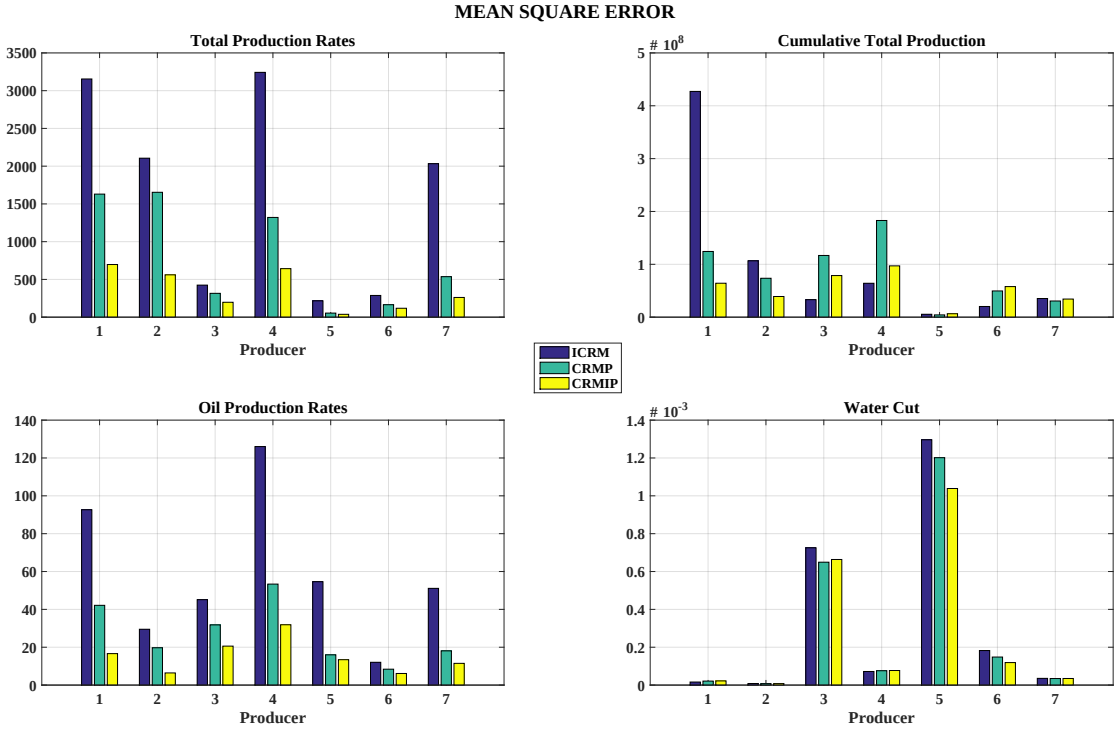

Figure 5.9: Mean square error for ICRM, CRMP and CRMIP (case 2).

tables B.1 and B.2, which means a fast response to producers' BHP changes, and is in agreement with the expected dynamics in high permeability channels. Again, the CRMIP representation generated several zero productivity indices for control volumes, a maximum of three nonzero J_{ij}'s was enough per producer. As discussed in case 1, this suggests that the CRMIP representation can be simplified and provide similar results with less parameters, confirming that productivity indices are a localized property being more dependent on the near wellbore region characteristics, instead of being an interwell property, such as connectivity.

Computing the controllability and observability matrices and their ranks, the CRMIP realization had 55 uncontrollable and 55 unobservable states, which means that CRMIP is not a minimal realization. Therefore, it is possible to reduce the

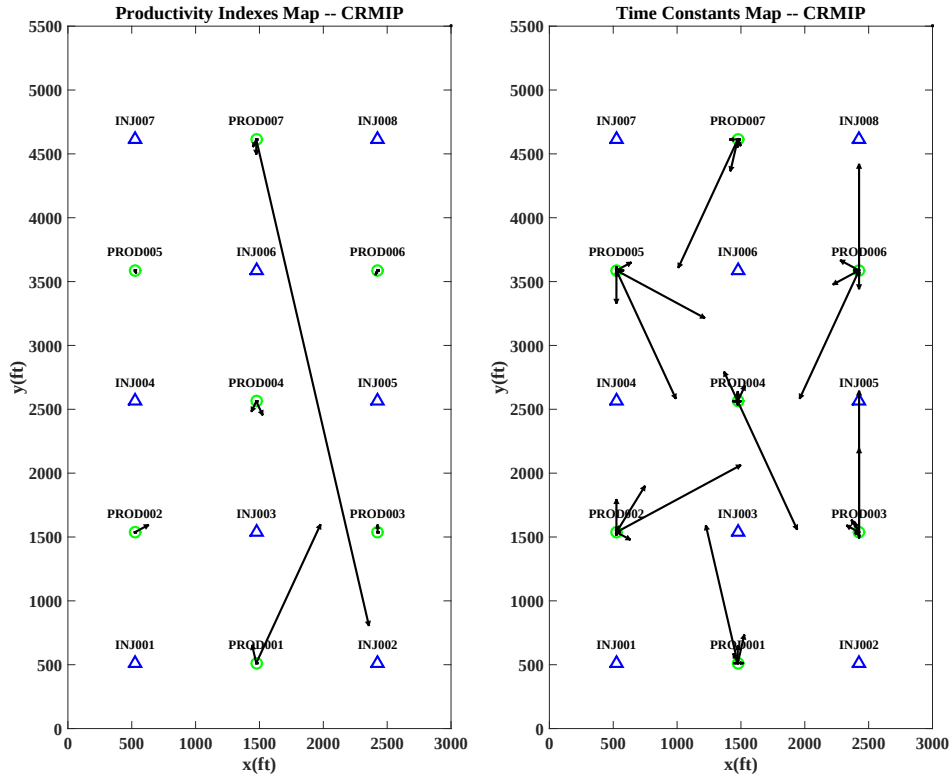

Figure 5.10: Productivity indices and time constants maps for the CRMIP representation (case 2).

number of states in CRMIP without penalizing its dynamics. The CRMIP minimal realization obtained has 45 states, reducing 11 states from the original formulation (table 5.4) and is more stable for control purposes.

The number of states of the system can still be further reduced from the minimal realization, however its dynamics will be penalized. Analyzing the Hankel singular values for the minimal realization (figure 5.11), 99% of the CRMIP dynamics can be preserved with only one state more than the CRMP representation. Thus, a model as good as CRMIP can be obtained almost with the same order as CRMP.

Figures B.13 and B.14 compare the liquid production rates of the reduced order model with the CRMIP and CRMP. Indeed, the reduced model accurately represents

Table 5.4: Results after controllability and observability analysis and model reduction for CRMIP (case 2).

	Number of States
CRMIP	56
Uncontrollable (CRMIP)	55
Unobservable (CRMIP)	55
Minimal Realization	45
Model Reduction (99% preserved)	8

the CRMIP dynamics, consequently the reservoir dynamics. The reduced model only have one state more than the CRMP representation, therefore it is also much simpler than CRMIP. However, it does not give a smooth response as CRMP, and is capable to predict the same oscillations as in CRMIP, for instance, this observation is evident in wells "PROD3", "PROD5" and "PROD6".

5.3 Case 3: Shoreface Environment Reservoir

Case 3 is based on the six top layers of the SPE-10 model [10], which represents a shoreface depositional environment. The horizontal permeability maps are shown in figure 5.12. In case 2 there was a vertical continuity in the channels pattern with high areal contrast in permeability when moving from the poor to the rich facies, and vice-versa. Case 3 is comprised by thin bedding planes, the areal transitions are much smoother, however there is not much vertical continuity, so the patterns significantly change when comparing consecutive layers.

As shown in figure 5.12, there are seven producers and eight injectors located exactly in the same place as in case 2. The modifications in the SPE-10 model listed in table 5.3 also apply to case 3. Production history data is presented in Appendix C. Injection rates for all the injector vary monthly between 100 bbl/day and 300

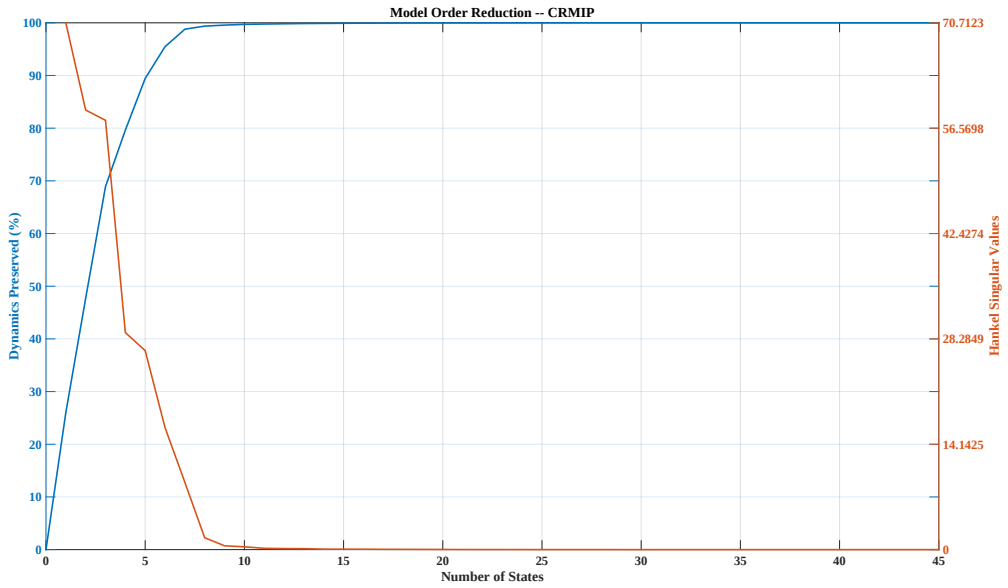

Figure 5.11: Hankel singular values decomposition and system's dynamics preserved after model reduction for CRMIP's minimal realization (case 2).

bbl/day (figure C.1). Producers' BHP vary every 6 months between 3150 psi and 3850 psi (figure C.2). The observed production rates obtained using IMEX [36] are shown in figure C.3. The history matching window is from 2000 days ($\approx$ 5.5 years) to 4745 days (13 years), starting after water breakthrough for all producers. The model validation window is from 4745 days (13 years) to 7300 days (20 years).

Figures C.4 and C.5 show the production rates obtained with the CRM's compared to the ones from the production history. The ICRM present the same problems previously discussed. ICRM computes negative production rates for "PROD1" and "PROD5", which is caused by an overestimation of the productivity indices, as one can see in table C.1. Also, the ICRM estimates zero productivity indices for "PROD2", "PROD4" and "PROD7", which is physically inconsistent. Moreover, the ICRM time constant estimates are not realiable as well. For example, the ICRM production rate response for "PROD4" looks like steps, which is the result from a

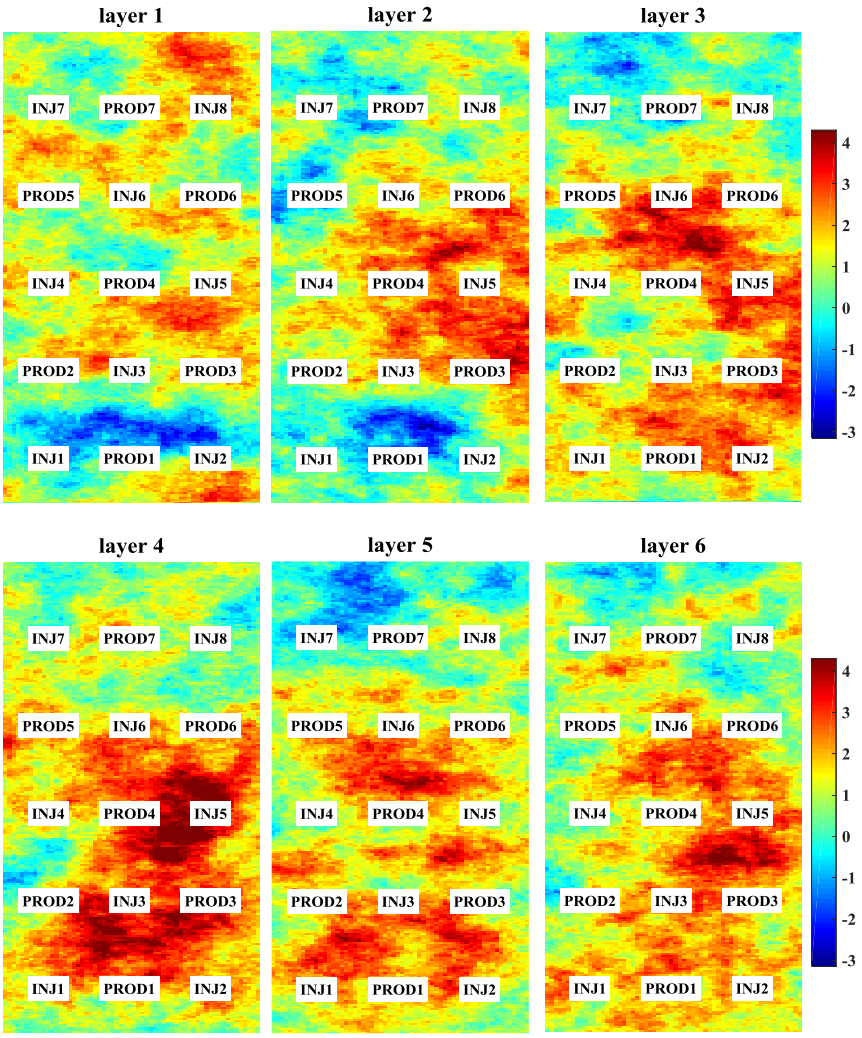

Figure 5.12: Logarithm of horizontal permeability (md) for layers 1 to 6 of the SPE-10 model.

very low time estimate, as one can see in table C.2, and is not consistent with the one observed in the production history, the same happens to "PROD5".

Comparing CRMP and CRMIP production responses, they are almost overlapping in "PROD1". In other wells they are also quite similar. Generally, the CRMIP captures reservoir the dynamics better than CRMP, following most of the trends noted in the production history. CRMP gives a smoother response, since only one

time constant is considered for all types stimulus acting in a producer. The big changes in production rates in "PROD2" and "PROD6" in the prediction window are caused by BHP variations, and none CRMP or CRMIP are capable to predict them accurately, in fact, these exemplify a case where the CRM parameters are time varying. The existing offset in "PROD2" and "PROD6" production response can be reduced using an observer to estimate the actual states of the reservoir in real-time, improving CRM's predictability.

The cumulative liquid production is depicted in figures C.6 and C.7. Since ICRM does the history matching for the cumulative production, maybe it could provide more reliable predictions than CRMP and CRMIP. Indeed, ICRM outperforms CRMP and CRMIP when predicting cumulative liquid production for "PROD2", "PROD4", "PROD6" and "PROD7", but not for the others. Therefore, it is not conclusive which is the best model for cumulative production rates. Since CRMIP provides represents the system dynamics reliably, it seems to be a safer choice. Generally, the CRMP and CRMIP cumulative production predictions are in good agreement in all the case studies.

The water cut computed using the fractional flow model proposed in [13] are shown in figures C.8 and C.9. The fractional flow parameters are shown in table C.3. "PRO3", "PROD4", "PROD5" and "PROD6" have their water cut slightly overestimated in the prediction window. Generally, the history matching is good, major differences are observed at low water cut in "PROD3" and "PROD5", because this fractional flow is recommended for higher water cuts. There is not any remarkable difference in the water cut computed with ICRM, CRMP, or CRMIP. Using this fractional flow model, the oil rates were computed, results are shown in figures C.10 and C.11. As one can see, the CRMP and CRMIP provides good predictions, the differences seen in figures C.4 and C.5 are reduced due to production in higher water

cuts.

The results previously discussed for case 3 are summarized by comparing the mean square error in figure 5.13, and the normalized mean square error in figure C.12. CRMIP is the best model to predict liquid and oil production rates, however s CRMP has a similar performance in some well (ex: "PROD6"). Sometimes, ICRM performs better than CRMP and CRMIP predicting cumulative production rates, however it does not represent the reservoir dynamics well, so its use must be avoided. The fractional flow model used can adjust well to all CRM's to accurately predict each well's water.

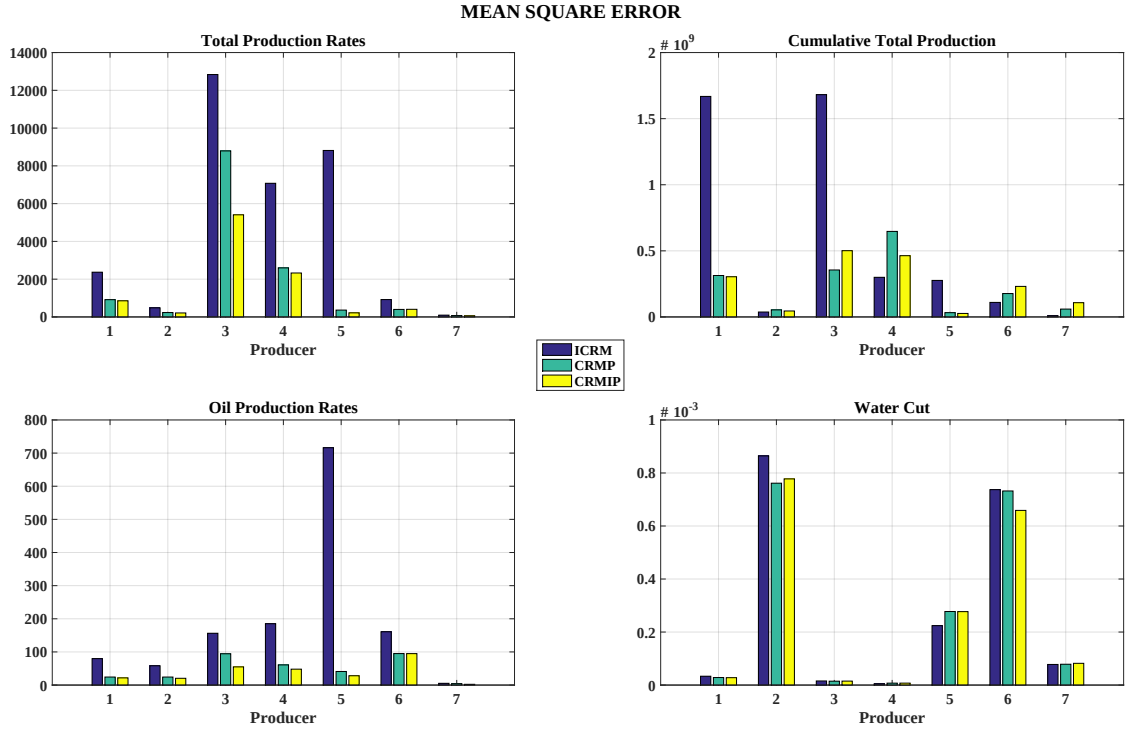

Figure 5.13: Mean square error for ICRM, CRMP and CRMIP (case 3).

The connectivity maps are shown in figures 5.14 and 5.15, numerical values are provided in table . Comparing the ICRM, CRMP and CRMIP connectivity estimates and the CRMIP results as reference, one can see that ICRM captures some trends in the water allocation (ex: “INJ1”, “INJ7”), however the differences are quite significant (ex: “INJ5”, “INJ6” and “INJ8”). Therefore, ICRM does not provide reliable connectivity estimates as well. The CRMP and CRMIP maps are in agreement, the major differences can noted in “INJ2”, “INJ4” and “INJ5”.

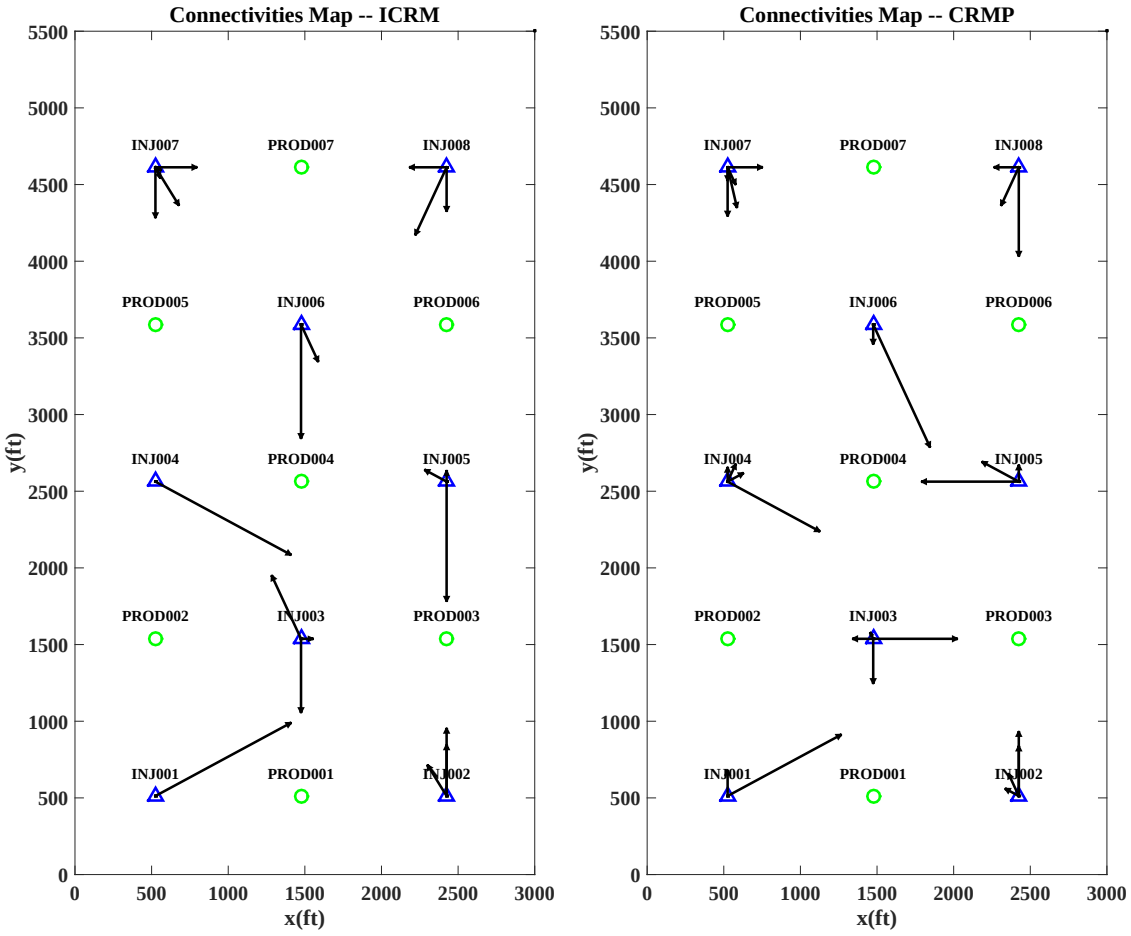

Figure 5.14: ICRM and CRMP connectivity maps (case 3).

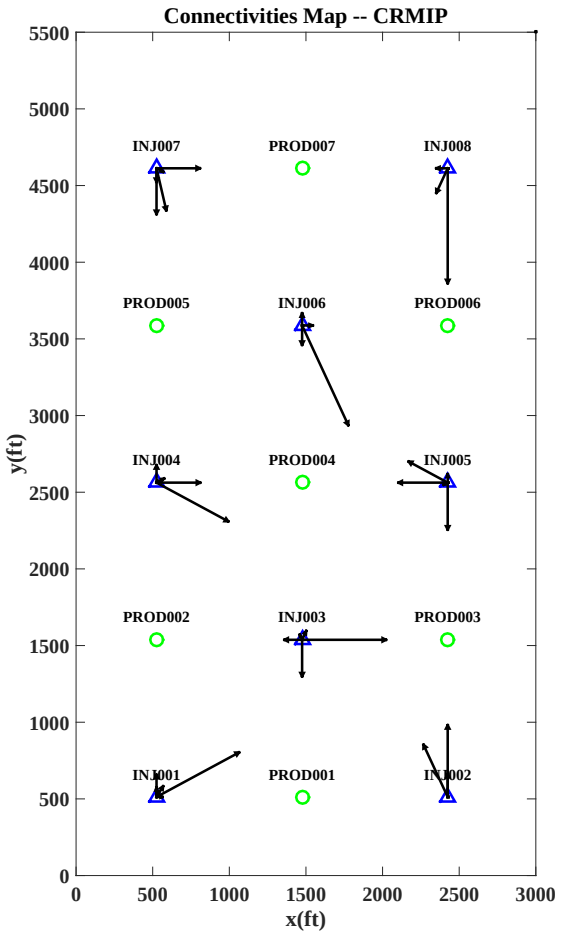

Figure 5.15: CRMIP connectivity map (case 3).

It is not straightforward to correlate the connectivity maps with the permeability maps in figure 5.12 as it was in case 2, where the highest connectivities were pointing to wells in the channels. Looking at the permeability maps it is possible to have an idea how flow evolves horizontally, however the vertical continuity of the high permeability regions also must be taken into account, since they are thin bedding planes with high vertical contrast. For example, "PROD3" is located in high permeability regions in all of the layers, this creates good flow paths between "PROD3" and the injectors, resulting in high values of connectivities. The opposite happens to

"PROD2" and "PROD7", which are mostly drilled in the low and moderate permeability zones. Since the flow path can be very tortuous, in a shoreface environment reservoir it is also possible to have high permeability in distant injector-producer pairs, an example is: $f_{83} = 0.749$.

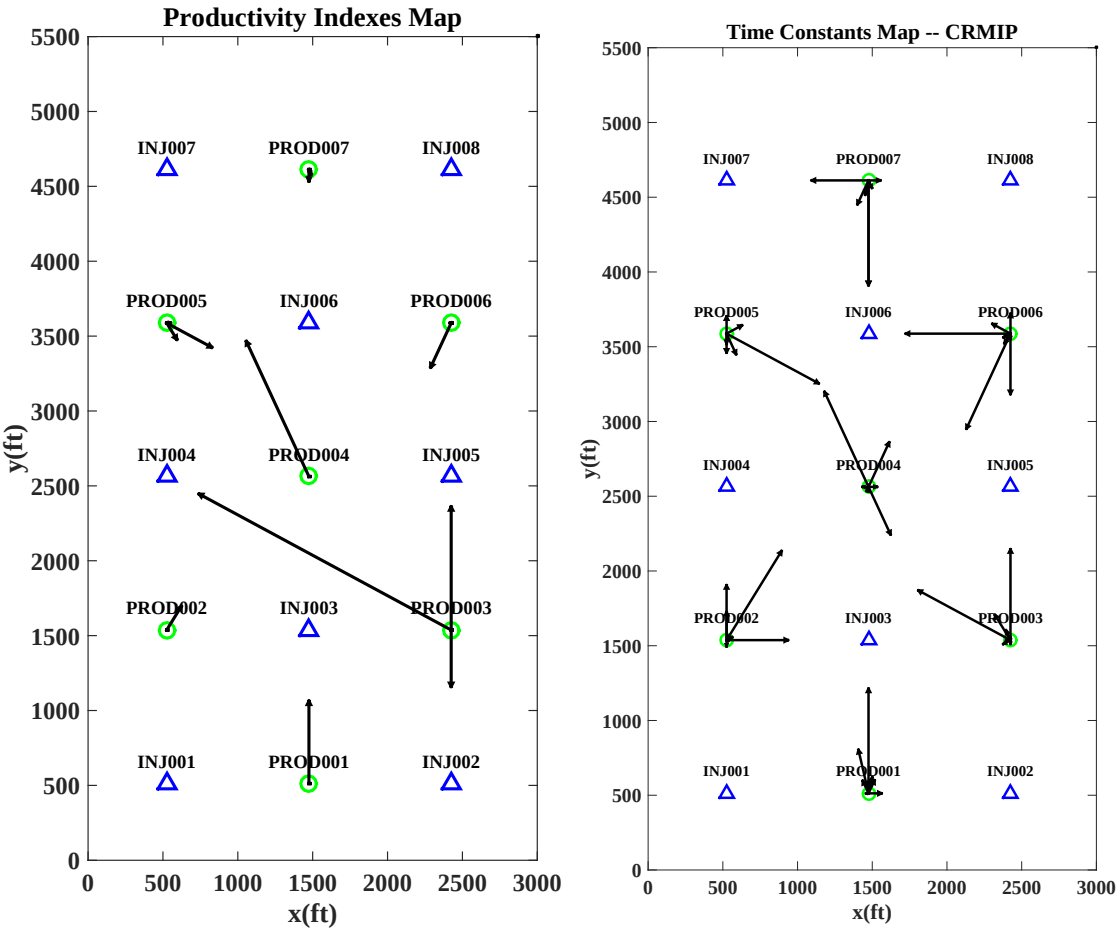

Figure 5.16: Productivity indices and time constants maps for the CRMIP representation (case 3).

Figure 5.16 presents the productivity indices and time constants maps for the CRMIP representation. Similarly to the results obtained in cases 1 and 2, it is pos-

sible to significantly reduce the number of parameters estimated, since only nonzero 3 productivity indices per producer are enough to describe the response to its BHP variation. It is easy to see what are the time constant associated with each productivity index. As previously discussed, "PROD3" is in the high permeability zone, this is confirmed by examining its high productivity indices, on other hand, 'PROD2" and "PROD7" are mostly in low to moderate permeability zones this is reflected in their low productivity indices.

Analyzing the controllability and observability of the CRMIP representation, after filtering the connectivity values by assigning zero to all the connectivities that were less than 10^{-3}, there was 15 uncontrollable states and 17 unobservable states, as shown in table 5.5, therefore the system was uncontrollable and unobservable. A minimal realization was obtained with 43 states, which means a reduction of 13 states from the original CRMIP realization.

Table 5.5: Results after controllability and observability analysis and model reduction for CRMIP (case 3).

	Number of States
CRMIP	56
Uncontrollable (CRMIP)	15
Unobservable (CRMIP)	17
Minimal Realization	43
Model Reduction (99% preserved)	8

Analyzing the Hankel singular values shown in figure 5.17, 99% of the CRMIP dynamics can be preserved using a realization with 8 states obtained from model order reduction, which is comparable in size to the CRMP representation (7 states)

and in quality with CRMIP.

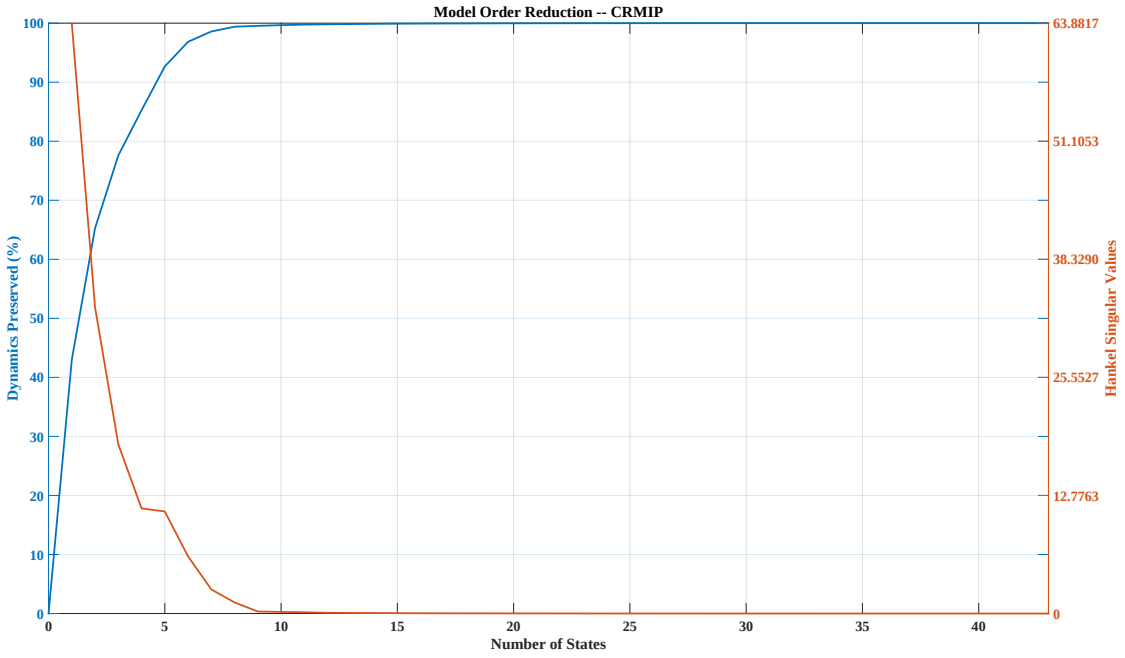

Figure 5.17: Hankel singular values decomposition and system's dynamics preserved after model reduction for CRMIP's minimal realization (case 3).

Figures C.13 and C.14 compare the liquid production rates of the reduced order model with the CRMIP and CRMP. Indeed, the reduced model accurately represents the CRMIP dynamics, consequently the reservoir dynamics, except for "PROD7", where the reduced model overshoots the production response when there are changes in BHP, such problem must be overcome by generating reduced realizations with more states. As for case 2, the reduced model only have one state more than the CRMP representation. However, it does not provide a smooth response as CRMP, and, in general, is capable to predict the same oscillations as in CRMIP, for instance, this observation is evident in wells "PROD2", "PROD3", "PROD4" and "PROD6".

6. CONCLUSIONS AND RECOMMENDATIONS FOR FUTURE WORK

6.1 Concluding Remarks

1. Representing CRM with state space equations opens the venues for implementation of linear control theory algorithms, which can improve CRM's predictability and tracking performance, it also facilitates real-time reservoir optimization.

2. The CRM transfer functions clarify the input-output relationships defined in each CRM representation, facilitating the choice of model.

3. Defining the constraints and objective functions of the history matching problem as matrices, enables the straightforward use of optimization algorithms, speeding up the reservoir modeling stage.

4. A sensitivity analysis in the history matching objective function coupled with the CRM parameters' physical understanding indicates that connectivity estimates are usually more accurate than time constant estimates.

5. Generally, ICRM provides bad productivity index and time constant estimates. In simple cases, such as case 1, ICRM is useful for connectivity estimates and production rates prediction. ICRM is not a reliable representation for complex reservoir, as cases 2 and 3, for history matching and predicting production rates.

6. The CRMP representation captures the reservoir dynamics better when there is more homogeneity around the producers because it assumes only one time constant for all injector-producer pairs. The CRMP connectivity estimates are

usually consistent with the CRMIP ones.

7. The CRMIP representation performs better predicting production rates, in the expense of estimating more parameters, and frequently generating physically meaningless parameters, such as several zero productivity index per producer.

8. Many times the CRMIP representation is not a minimal realization, thus it is possible to obtain a lower order and more stable to control realization without penalizing the system dynamics.

9. Analyzing the Hankel singular values, the results have shown that, penalyzing less than 1 % of the system dynamics, it is possible to obtain reduced order models from the CRMIP that have only few states more the CRMP.

6.2 Future Works

6.2.1 CRM for Closed-Loop Reservoir Management

Analogously to Jansen et al. [20], the flowchart for CRM in a systems framework with closed-loop reservoir management is shown in figure 6.1. The production history of the reservoir, i. e. inputs and outputs of the real system, is detected by sensors in the field. The processed production history will be used in the observer to estimate the states of the system and history matching using CRM in a control systems framework. The CRM model is necessary to maximize oil production or net present value in a given time horizon; therefore, using optimization algorithms the optimal input values of the system must be defined and applied in the field to control the real system.

Using CRM with closed-loop reservoir management is expected to outperform the open-loop strategy because the feedback controller keeps track of the system response, adjusting the inputs to achieve the desirable setpoint for the outputs in

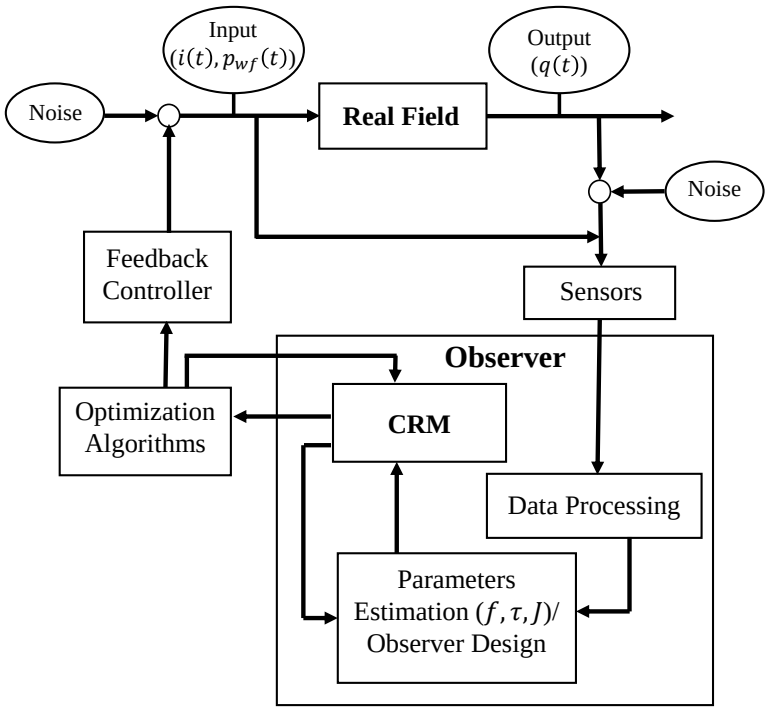

Figure 6.1: CRM for closed-loop reservoir management.

a stable and timely manner. As discussed in chapter 4, the models parameters may be time-variant in many situations. In such cases, CRM would be reliable only for short-term prediction. Therefore, another advantage of closed-loop reservoir management is that the systems parameters are constantly updated, which reduces the uncertainties, providing more reliable predictions.

6.2.2 Dynamic Parameters

As discussed in section 4.1, rigorously, the CRM parameters are time-varying. Big operational changes, such as shutting wells, drilling a new well, or even high variations in the inputs, can cause considerable changes in the streamlines, therefore the assumption of constant connectivities, time constants and productivity indices does not hold. Also, before the water breakthrough this problem is expressively

nonlinear.

Few works in the literature have considered CRM parameters as time-varying [18, 6]. Usually, even in these works, the parameters are considered constant when predicting production rates. Indeed, it is necessary to improve the predictability of this time-varying behavior, improving CRM robustness, but keeping it simple.

6.2.3 Decline Curves and BHP Response

As discussed in chapter 2, CRM is based on the superposition in time and space of the natural reservoir's production decline, and the responses to injection rates and producers' BHP variations. However, the actual formulation only consider these factors as exponential (CRMT, CRMP), or a series of exponential (CRMIP) terms, which may not be the most appropriate representation sometimes. Thus, coupling CRM with different types of decline curve other than exponential could improve its performance for some reservoirs. Also, taking advantage of superposition in time and space, the BHP response term can be changed from the original models to explain better the depletion in the nearwell region.

6.2.4 CRM for Unconventional Reservoirs

Traditionally, CRM has been mostly applied to flooding processes. Even though unconventional reservoirs have been developed by primary depletion, some previous works have indicated that secondary and tertiary recovery are attractive solutions to significantly enhance oil recovery in some reservoirs [42, 58]. Moreover, some unconventional oil plays can have some areas with richer permeability, not in the micro to nano-Darcy scale, where flooding processes are feasible. An example is the pilot waterflooding plant operating in Bakken since 2006 [61]. Since there is a very high number of well in such reservoirs, CRM might be a good model to approach them due to its simplicity. The low permeability reservoirs' transient flow behavior

also results in a linear time-variant system because connectivities and time constants are time dependent [53]. Furthermore, the literature review shows that the porous media suffers significant changes over time, changing the connectivities not only due to the transient flow behavior, but also due to structural transformations in the fracture system [12], which may require several history matching windows to fit the model taking into account such effects.

Because unconventional reservoirs are slow systems, the signals may take too long to reach the producer, or be dissipated on their way; parameters such as permeability and interwell distance are crucial to analyze this. Therefore, closed-loop reservoir management has limited applicability, but real time history matching is still encouraged, since parameters such as capacity and resistivity can be inferred from the transient response.

In the literature, the CRM formulations for unconventional reservoirs have been tested only for synthetic examples with a single well. Since the principles have been established, it would be important to apply them at a field scale now. Besides the transient flow nature, the effects of changes in the porous media characteristics with time should be considered as well since it can affect the production significantly.

REFERENCES

[1] Alejandro Albertoni and Larry W. Lake. Inferring interwell connectivity only from well-rate fluctuations in waterfloods. *SPE Reservoir Evaluation & Engineering*, 6(1):6–16, February 2003.

[2] Athanasios C. Antoulas. *Approximation of Large-Scale Dynamical Systems (Advances in Design and Control)*. Society for Industrial and Applied Mathematics, Philadelphia, Pennsylvania, USA, 2005.

[3] W. A. Bruce. An electrical device for analyzing oil-reservoir behavior. *Petroleum Technology*, 151(1):112–124, December 1943.

[4] B. Can and C. S. Kabir. Containing data noise in unconventional-reservoir-performance forecasting. *Journal of Natural Gas Science and Engineering*, 18(0):13–22, May 2014.

[5] Fei Cao. A New Method of Data Quality Control in Production Data Using the Capacitance-Resistance Model. Masters thesis, University of Texas, Austin, Texas, USA, 2011.

[6] Fei Cao. *Development of a Two-Phase Flow Coupled Capacitance Resistance Model*. Phd dissertation, University of Texas, Austin, Texas, USA, 2014.

[7] Fei Cao, Haishan Luo, and Larry W. Lake. Development of a fully coupled two-phase flow based capacitance resistance model (CRM). In *SPE Improved Oil Recovery Symposium*. Society of Petroleum Engineers, April 2014.

[8] Fei Cao, Haishan Luo, and Larry W. Lake. Oil rate forecast by inferring fractional flow models from field data. In *SPE Reservoir Simulation Symposium*. Society of Petroleum Engineers, February 2015.

[9] Chi-Tsong Chen. *Linear System Theory and Design*. Oxford series in electrical and computer engineering. Oxford University Press, New York, New York, USA, 3rd edition, 1999.

[10] M.A. Christie and M.J. Blunt. Tenth spe comparative solution project: A comparison of upscaling techniques. In *SPE Reservoir Simulation Symposium*. Society of Petroleum Engineers, February 2001.

[11] M.J. Economides, A.D. Hill, C. Ehlig-Economides, and D. Zhu. *Petroleum Production Systems*. Prentice Hall, Upper Saddle River, New Jersey, USA, 2nd edition, 2013.

[12] Perapon Fakcharoenphol, Sarinya Charoenwongsa, Hossein Kazemi, and Yu-Shu Wu. The effect of water induced stress to enhance hydrocarbon recovery in shale reservoirs. In *SPE Annual Technical Conference and Exhibition*. Society of Petroleum Engineers, October 2012.

[13] P. H. Gentil. The Use of Multilinear Regression Models in Patterned Waterfloods: Physical Meaning of the Regression Coefficients. Masters thesis, University of Texas, Austin, Texas, USA, 2005.

[14] Mohammadreza Ghasemi, Ashraf Ibrahim, and Eduardo Gildin. Reduced order modeling in reservoir simulation using the bilinear approximation techniques. In *SPE Latin America and Caribbean Petroleum Engineering Conference*. Society of Petroleum Engineers, May 2014.

[15] Mohammadreza Ghasemi, Yanfang Yang, Eduardo Gildin, Yalchin Efendiev, and Victor Calo. Fast multiscale reservoir simulations using POD-DEIM model reduction. In *SPE Reservoir Simulation Symposium*. Society of Petroleum Engineers, February 2015.

[16] E. G. Gilbert. Controllability and observability in multivariable control systems. *Journal for the Society for Industrial and Applied Mathematics*, 2:128–151, 1963.

[17] Dilhan Ilk and Thomas Alwin Blasingame. Decline curve analysis for unconventional reservoir systems – variable pressure drop case. In *SPE Unconventional Resources Conference*. Society of Petroleum Engineers, November 2013.

[18] Nelia Jafroodi and Dongxiao Zhang. New method for reservoir characterization and optimization using CRM-EnOpt approach. *Journal of Petroleum Science and Engineering*, 77(2):155–171, May 2011.

[19] Jan Dirk Jansen. *A Systems Description of Flow Through Porous Media*. SpringerBriefs in Earth Sciences. Springer International Publishing, Cham, Zug, Switzerland, 2013.

[20] Jan Dirk Jansen, Roald Brouwer, and Sippe G. Douma. Closed loop reservoir management. In *SPE Reservoir Simulation Symposium*. Society of Petroleum Engineers, February 2009.

[21] C. Shah Kabir and Larry Wayne Lake. A semianalytical approach to estimating EUR in unconventional reservoirs. In *North American Unconventional Gas Conference and Exhibition*. Society of Petroleum Engineers, June 2011.

[22] Thomas Kailath. *Linear Systems*. Prentice Hall information and system sciences series. Prentice-Hall, Englewood Cliffs, New Jersey, USA, 1980.

[23] R. E. Kalman. Mathematical description of linear dynamical systems. *Journal of the Society for Industrial and Applied Mathematics (Series A: Control)*, 1(2):152–192, 1963.

[24] Danial Kaviani. *Interwell Connectivity Evaluation from Wellrate Fluctuations: A Waterflooding Management Tool*. Phd dissertation, Texas A&M University,

College Station, Texas, USA, 2009.

[25] Danial Kaviani and Jerry L. Jensen. Reliable connectivity evaluation in conventional and heavy oil reservoirs: A case study from Senlac heavy oil pool, western Saskatchewan. In *Canadian Unconventional Resources and International Petroleum Conference*. Society of Petroleum Engineers, October 2010.

[26] Danial Kaviani, Jerry L. Jensen, and Larry W. Lake. Estimation of interwell connectivity in the case of unmeasured fluctuating bottomhole pressures. *Journal of Petroleum Science and Engineering*, 90–91(0):79–95, July 2012.

[27] Danial Kaviani, Mohammad Soroush, and Jerry L. Jensen. How accurate are capacitance model connectivity estimates? *Journal of Petroleum Science and Engineering*, 122(0):439–452, October 2014.

[28] Danial Kaviani and Peter P. Valko. Inferring interwell connectivity using multiwell productivity index (MPI). *Journal of Petroleum Science and Engineering*, 73(1–2):48–58, August 2010.

[29] Jong S. Kim, Larry W. Lake, and Thomas F. Edgar. Integrated capacitance-resistance model for characterizing waterflooded reservoirs. In *IFAC Workshop on Automatic Control in Offshore Oil and Gas Production*. International Federation of Automatic Control, June 2012.

[30] Basak Kurtoglu and Hossein Kazemi. Evaluation of Bakken performance using coreflooding, well testing, and reservoir simulation. In *SPE Annual Technical Conference and Exhibition*. Society of Petroleum Engineers, October 2012.

[31] Basak Kurtoglu, James A. Sorensen, Jason Braunberger, Steven Smith, and Hossein Kazemi. Geologic characterization of a Bakken reservoir for potential

CO2 EOR. In *Unconventional Resources Technology Conference*. Society of Petroleum Engineers, August 2013.

[32] Pongsathorn Lerlertpakdee, Behnam Jafarpour, and Eduardo Gildin. Efficient production optimization with flow-network models. *SPE Journal*, 19(6):1083–1095, December 2014.

[33] Ximing Liang, Larry W. Lake, Thomas F. Edgar, Ali Al-Yousef, Morteza Sayarpour, and Daniel Weber. Optimization of oil production based on a capacitance model of production and injection rates. In *Hydrocarbon Economics and Evaluation Symposium*. Society of Petroleum Engineers, April 2007.

[34] G. Liu, J. A. Sorensen, J. R. Braunberger, R. Klenner, J. Ge, C. D. Gorecki, E. N. Steadman, and J. A. Harju. CO2-based enhanced oil recovery from unconventional reservoirs: A case study of the Bakken formation. In *SPE Unconventional Resources Conference*. Society of Petroleum Engineers, April 2014.

[35] Lennart Ljung. *System Identification : Theory for the User*. Prentice Hall information and system sciences series. Prentice Hall PTR, Upper Saddle River, New Jersey, USA, 2nd edition, 1999. Autre tirage: 2006.

[36] Computer Modeling Group Ltd. *Version 2013*. Computer Modeling Group Ltd., Calgary, Alberta, Canada, 2013.

[37] MATLAB. *Version 8.3.0 (R2014a)*. The MathWorks Inc., Natick, Massachusetts, USA, 2014.

[38] Shahab D. Mohaghegh. Reservoir modeling of shale formations. *Journal of Natural Gas Science and Engineering*, 12(0):22–33, May 2013.

[39] Gustavo A. Moreno. Multilayer capacitance-resistance model with dynamic connectivities. *Journal of Petroleum Science and Engineering*, 109(0):298–307,

September 2013.

[40] Samiha Morsy, J. J. Sheng, and Roland O. Ezewu. Potential of waterflooding in shale formations. In *SPE Nigeria Annual International Conference and Exhibition*. Society of Petroleum Engineers, August 2013.

[41] Samiha Morsy, J. J. Sheng, Ahmed Mohamed Gomaa, and M. Y. Soliman. Potential of improved waterflooding in acid-hydraulically- fractured shale formations. In *SPE Annual Technical Conference and Exhibition*. Society of Petroleum Engineers, October 2013.

[42] Samiha Morsy, J. J. Sheng, and M. Y. Soliman. Waterflooding in the Eagle Ford shale formation: Experimental and simulation study. In *SPE Unconventional Resources Conference and Exhibition-Asia Pacific*. Society of Petroleum Engineers, November 2013.

[43] Anh Phuong Nguyen, Jong Suk Kim, Larry Wayne Lake, Thomas F. Edgar, and Byron Haynes. Integrated capacitance resistive model for reservoir characterization in primary and secondary recovery. In *SPE Annual Technical Conference and Exhibition*. Society of Petroleum Engineers, October 2011.

[44] Jorge Nocedal and Stephen J. Wright. *Numerical Optimization*. Springer series in operations research and financial engineering. Springer, New York, New York, USA, 2nd edition, 2006.

[45] M. Salazar, H. Gonzalez, S. Matringe, and D. Castieira. Combining decline-curve analysis and capacitance-resistance models to understand and predict the behavior of a mature naturally fractured carbonate reservoir under gas injection. In *SPE Latin America and Caribbean Petroleum Engineering Conference*. Society of Petroleum Engineers, April 2012.

[46] Morteza Sayarpour. *Development and Application of Capacitance-Resistive Models to Water/CO2 Floods*. Phd dissertation, University of Texas, Austin, Texas, USA, 2008.

[47] Morteza Sayarpour, C. Shah Kabir, and Larry Wayne Lake. Field applications of capacitance resistive models in waterfloods. In *SPE Annual Technical Conference and Exhibition*. Society of Petroleum Engineers, September 2008.

[48] Morteza Sayarpour, E. Zuluaga, C. Shah Kabir, and Larry Wayne Lake. The use of capacitance-resistance models for rapid estimation of waterflood performance and optimization. *Journal of Petroleum Science and Engineering*, 69(34):227–238, December 2009.

[49] Mohammad Sayyafzadeh, Peyman Pourafshary, Manouchehr Haghighi, and Fariborz Rashidi. Application of transfer functions to model water injection in hydrocarbon reservoir. *Journal of Petroleum Science and Engineering*, 78(1):139–148, July 2011.

[50] Dale E. Seborg, Duncan A. Mellichamp, Thomas F. Edgar, and Francis J. Doyle III. *Process Dynamics and Control*. John Wiley & Sons, Hoboken, New Jersey, USA, 3rd edition, 2011.

[51] Mohammad Sadeq Shahamat and Roberto Aguilera. A new method for production decline analysis of tight gas formations. In *Canadian Unconventional Resources and International Petroleum Conference*. Society of Petroleum Engineers, October 2010.

[52] Mohammad Sadeq Shahamat, L. Mattar, and Roberto Aguilera. A physics-based method for production data analysis of tight and shale petroleum reservoirs using succession of pseudo-steady states. In *SPE/EAGE European Uncon-*

ventional Resources Conference and Exhibition. Society of Petroleum Engineers, February 2014.

[53] Mohammad Soroush. *Interwell Connectivity Evaluation Using Injection and Production Fluctuation Data*. Phd dissertation, University of Calgary, Calgary, Alberta, Canada, 2013.

[54] Marco R. Thiele and Roderick P. Batycky. Using streamline-derived injection efficiencies for improved waterflood management. *SPE Reservoir Evaluation & Engineering*, 9(2):187–196, April 2006.

[55] Peter P. Valko. Assigning value to stimulation in the Barnett shale: a simultaneous analysis of 7000 plus production hystories and well completion records. In *SPE Hydraulic Fracturing Technology Conference*. Society of Petroleum Engineers, February 2009.

[56] Peter P. Valko, L. E. Doublet, and T. A. Blasingame. Development and application of the multiwell productivity index (MPI). *SPE Journal*, 5(1):21–31, March 2000.

[57] WL Wahl, LD Mullins, RH Barham, and WR Bartlett. Matching the performance of saudi arabian oil fields with an electrical model. *Journal of Petroleum Technology*, 14(11):1275–1282, November 1962.

[58] Xiaoqi Wang, Peng Luo, Vahapcan Er, and Shen-Shong Sam Huang. Assessment of CO2 flooding potential for Bakken formation, Saskatchewan. In *Canadian Unconventional Resources and International Petroleum Conference*. Society of Petroleum Engineers, October 2010.

[59] Daniel Weber. *The Use of Capacitance-Resistance Models to Optimize Injection Allocation and Well Location in Water Floods*. Phd dissertation, University of

Texas, Austin, Texas, USA, 2009.

[60] Daniel Weber, Thomas F. Edgar, Larry Wayne Lake, Leon S. Lasdon, Sami Kawas, and Morteza Sayarpour. Improvements in capacitance-resistive modeling and optimization of large scale reservoirs. In *SPE Western Regional Meeting*. Society of Petroleum Engineers, March 2009.

[61] Travis Wood and Bryan Milne. Waterflood potential could unlock billions of barrels. Report, Crescent Point Energy, 2011.

[62] Ali A. Yousef. *Investigating Statistical Techniques to Infer Interwell Connectivity from Production and Injection Rate Fluctuations*. Phd dissertation, University of Texas, Austin, Texas, USA, 2006.

[63] Ali A. Yousef, Pablo Hugo Gentil, Jerry L. Jensen, and Larry Wayne Lake. A capacitance model to infer interwell connectivity from production and injection rate fluctuations. In *SPE Annual Technical Conference and Exhibition*. Society of Petroleum Engineers, October 2005.

[64] Hui Zhao, Zhijiang Kang, Xiansong Zhang, Haitao Sun, Lin Cao, and Albert C. Reynolds. Insim: A data-driven model for history matching and prediction for waterflooding monitoring and management with a field application. In *SPE Reservoir Simulation Symposium*. Society of Petroleum Engineers, February 2015.

APPENDIX A

DATA AND RESULTS FOR CASE 1

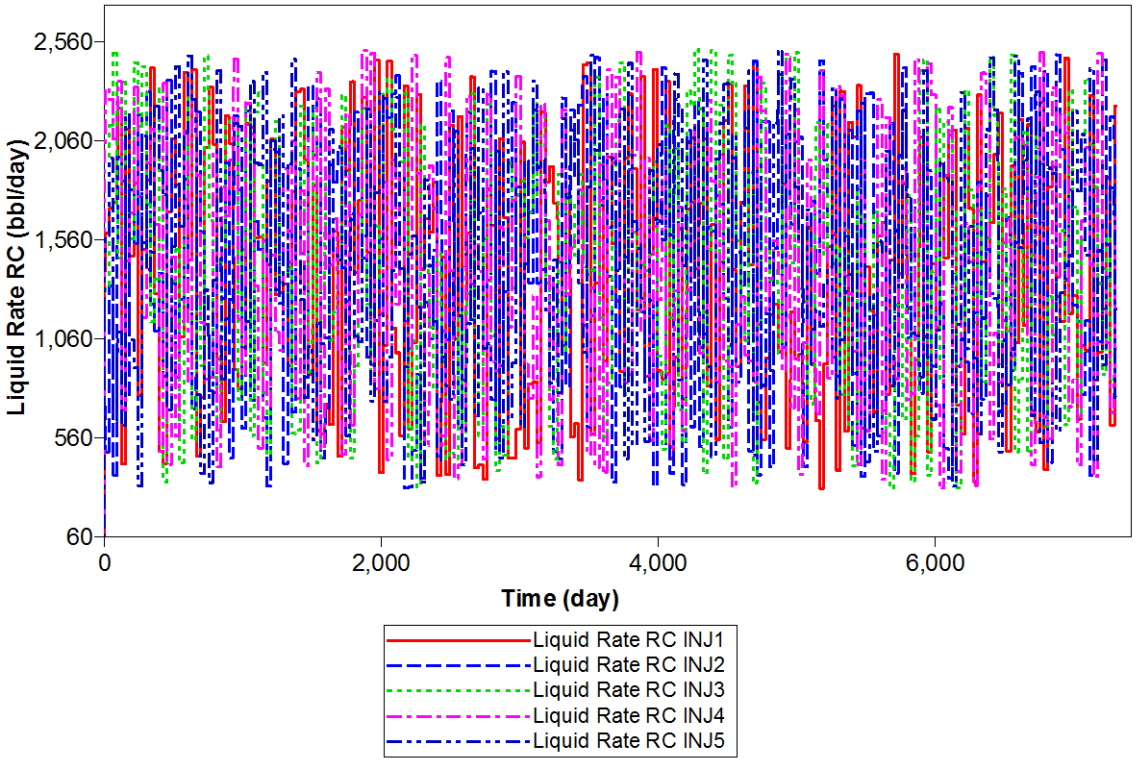

Figure A.1: Injection rates (bbl/day) for the five injectors during simulation time (days) in case 1.

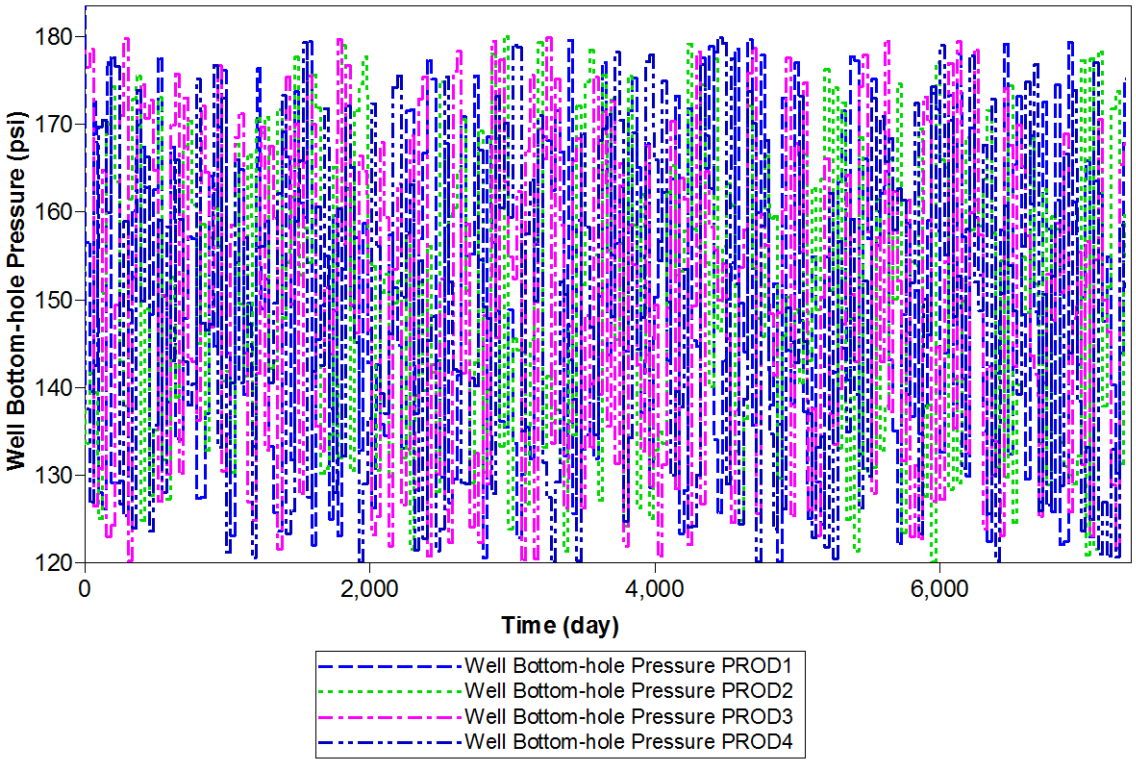

Figure A.2: Bottom hole pressures (psi) for the four producers during simulation time (days) in case 1.

Table A.1: Productivity indices estimates (case 1).

	CRMIP					CRMP	ICRM
i / j	1	2	3	4	5		
1	5.25	0.00	0.00	0.00	3.23	8.31	12.71
2	0.00	0.00	0.00	0.00	6.88	6.74	0.00
3	0.00	4.84	0.00	0.00	2.83	7.42	16.29
4	0.00	3.89	0.00	0.00	3.13	6.95	9.55

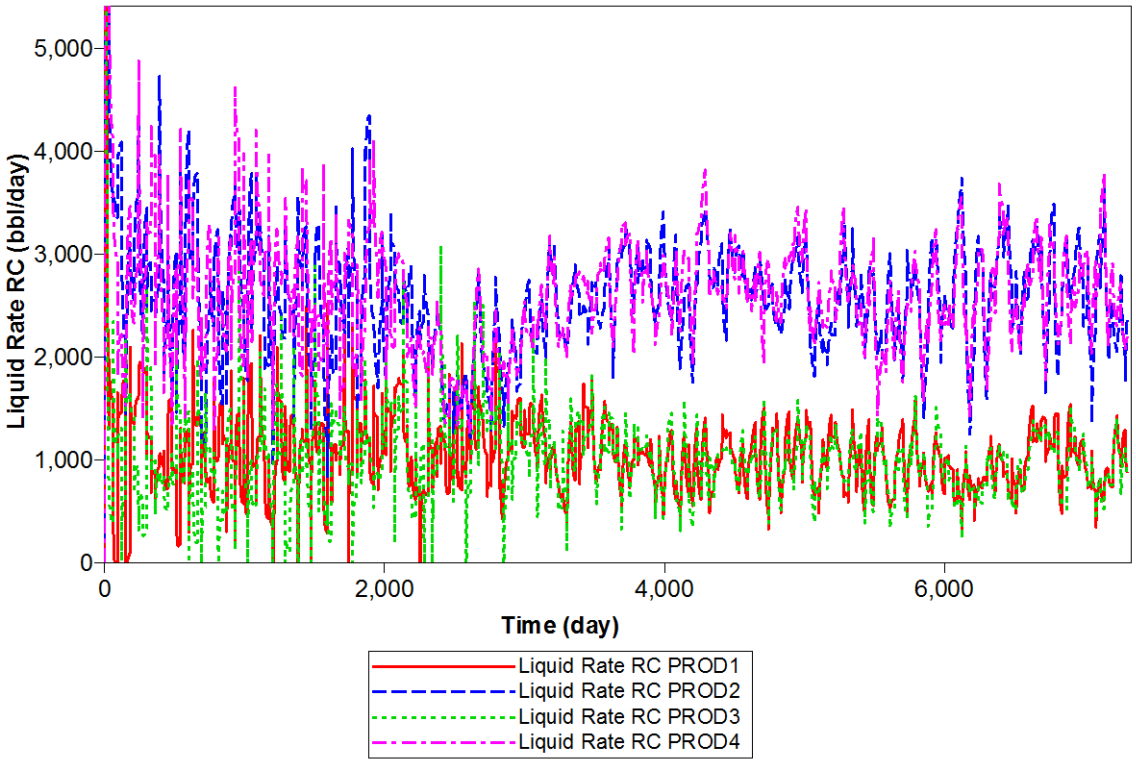

Figure A.3: Production rates (bbl/day) for the four producers from production history (IMEX [36]) in case 1.

Table A.2: Time constant estimates (case 1).

	CRMIP					CRMP	ICRM
i / j	1	2	3	4	5		
1	10.18	12.83	51.24	17.99	200.00	15.07	29.63
2	20.56	22.22	24.00	26.98	41.68	25.12	20.63
3	96.60	12.68	46.29	16.87	200.00	14.82	35.96
4	30.52	200.00	23.55	19.56	19.09	23.45	17.01

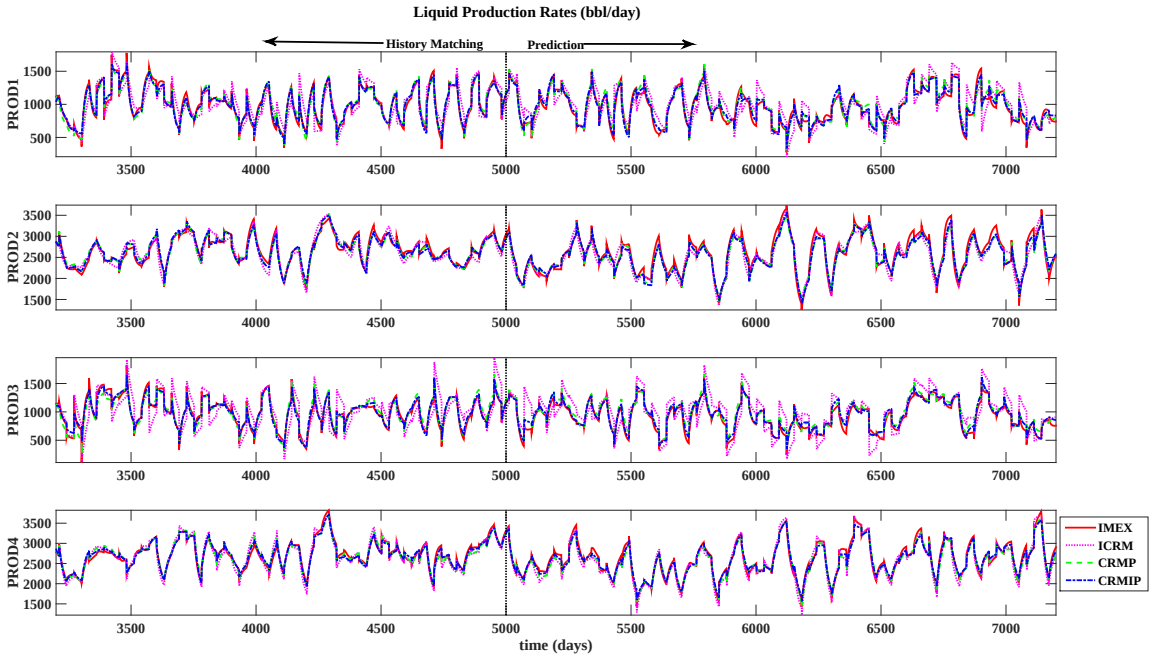

Figure A.4: Liquid production rates (bbl/days) for ICRM, CRMP and CRMIP compared to the production history (case 1).

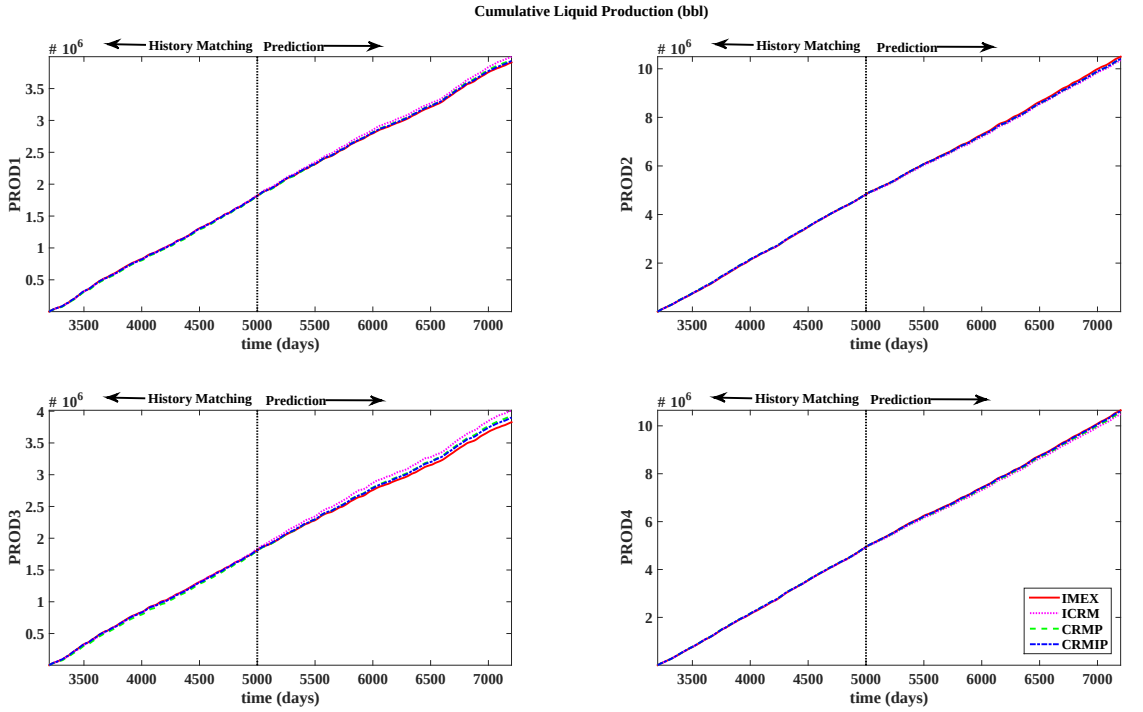

Figure A.5: Cumulative liquid production (bbl) for ICRM, CRMP and CRMIP compared to the production history (case 1).

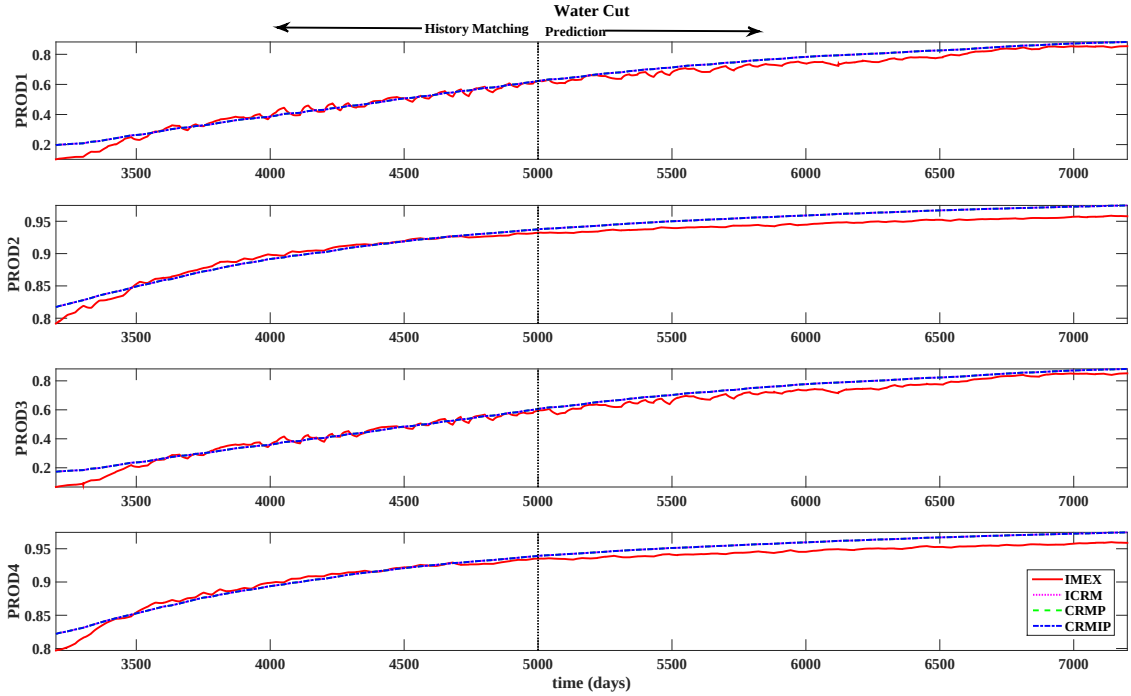

Figure A.6: Water cut for ICRM, CRMP and CRMIP compared to the production history (case 1).

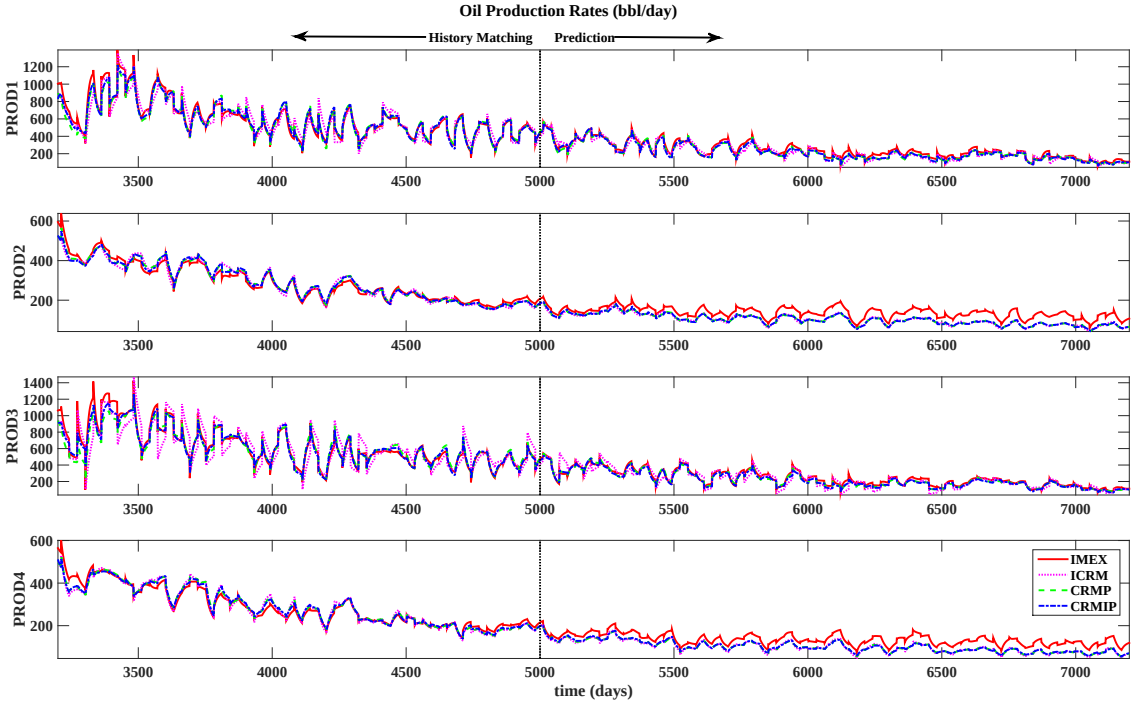

Figure A.7: Oil production rates (bbl/days) for ICRM, CRMP and CRMIP compared to the production history (case 1).

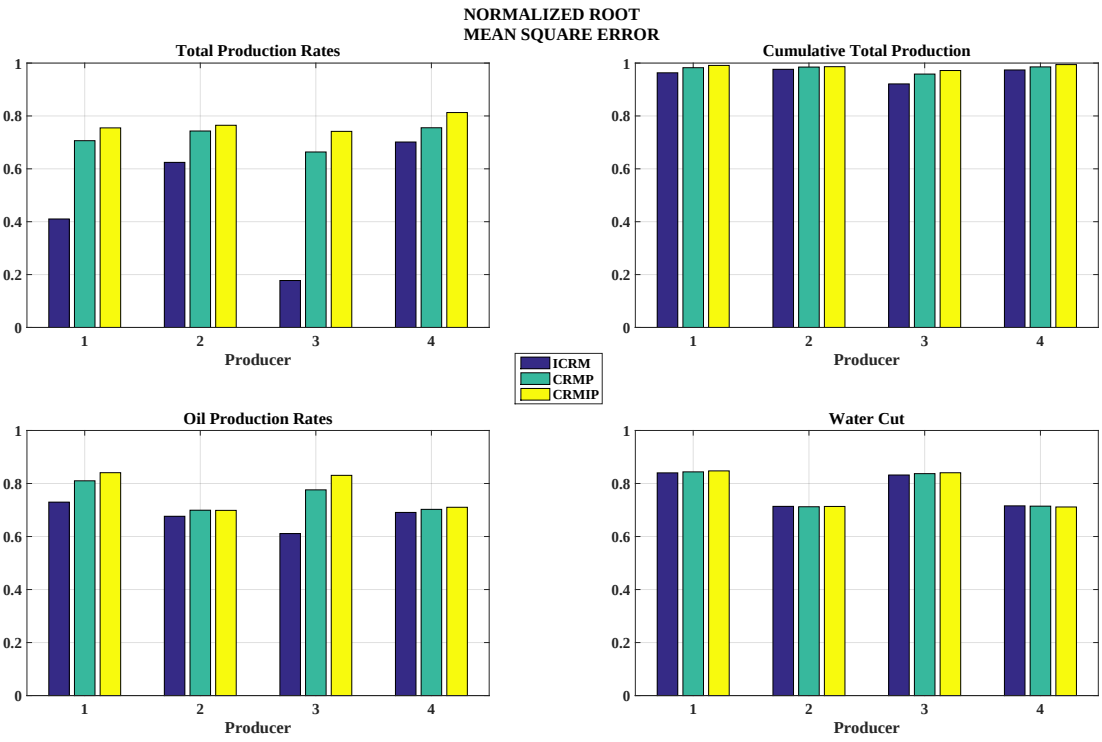

Figure A.8: Normalized root mean square for ICRM, CRMP and CRMIP (case 1).

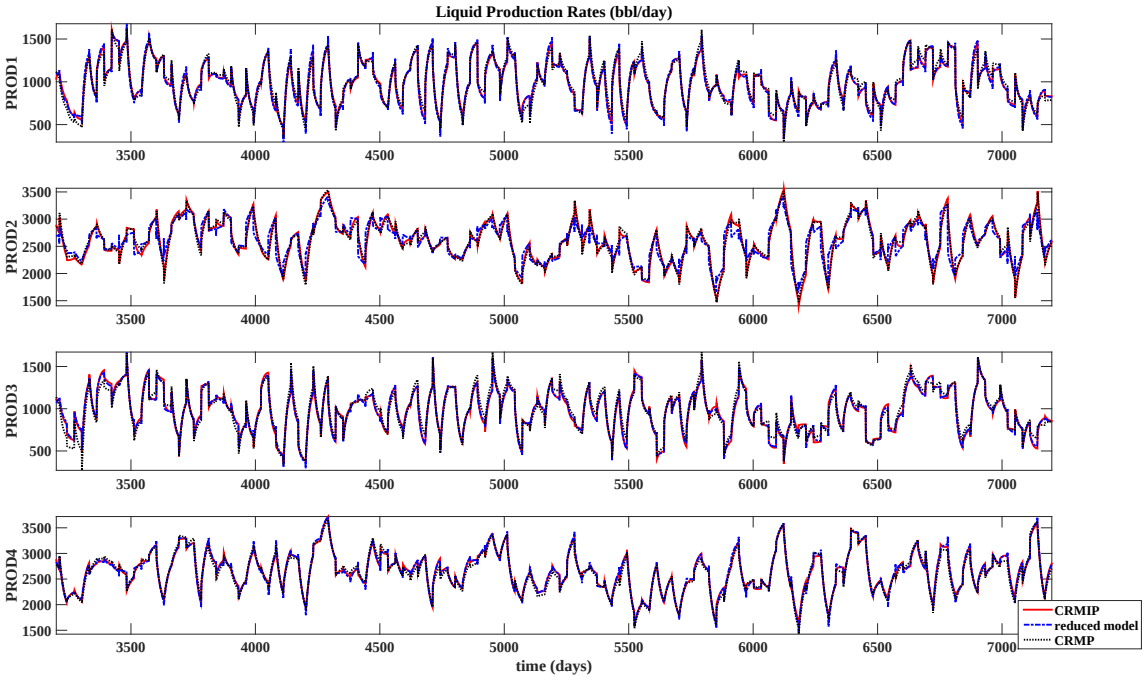

Figure A.9: Comparison between CRMP, CRMIP and reduced order model liquid production rates (bbl/days) for case 1.

Table A.3: Connectivity estimates (case 1).

	i / j	1	2	3	4	5	sum
ICRM	1	0.021	0.518	0.000	0.068	0.092	0.699
	2	0.660	0.000	0.490	0.412	0.244	1.806
	3	0.000	0.482	0.000	0.117	0.101	0.700
	4	0.319	0.000	0.510	0.403	0.563	1.795
	sum	1.000	1.000	1.000	1.000	1.000	
CRMP	1	0.071	0.504	0.046	0.020	0.053	0.694
	2	0.574	0.034	0.435	0.460	0.305	1.808
	3	0.050	0.461	0.047	0.061	0.069	0.688
	4	0.305	0.000	0.472	0.459	0.573	1.809
	sum	1.000	0.999	1.000	1.000	1.000	
CRMIP	1	0.049	0.450	0.068	0.038	0.078	0.683
	2	0.538	0.002	0.407	0.490	0.371	1.808
	3	0.091	0.429	0.069	0.045	0.043	0.677
	4	0.322	0.119	0.456	0.421	0.508	1.826
	sum	1.000	1.000	1.000	0.994	1.000	

Table A.4: Fractional flow parameters for ICRM, CRMP and CRMIP (case 1).

Producer		1	2	3	4
ICRM	a	7.46E-29	2.06E-18	3.05E-30	6.04E-18
	b	4.2299	2.6504	4.4319	2.5856
CRMP	a	1.05E-28	1.98E-18	5.29E-30	5.36E-18
	b	4.2100	2.6525	4.4006	2.5919
CRMIP	a	1.83E-28	2.22E-18	7.13E-30	4.12E-18
	b	4.1770	2.6455	4.3862	2.6067

APPENDIX B

DATA AND RESULTS FOR CASE 2

Table B.1: Productivity indices estimates (case 2).

	CRMIP								CRMP	ICRM
i / j	1	2	3	4	5	6	7	8		
1	0.0000	0.0000	0.0000	0.0000	6.1033	0.0000	0.7071	0.0000	0.84	1.69
2	0.0000	0.0000	0.0000	0.0000	0.5900	0.0000	0.0000	0.0000	0.61	1.21
3	0.0000	0.0000	0.0000	0.0000	0.2671	0.0000	0.0000	0.0000	0.34	0.00
4	0.4246	0.5761	0.0000	0.0000	0.0000	0.0000	0.0000	0.0000	1.05	0.00
5	0.0000	0.0000	0.0903	0.0000	0.0000	0.0000	0.0000	0.0000	0.09	0.80
6	0.0078	0.0000	0.1638	0.0000	0.0000	0.0000	0.0000	0.0000	0.22	0.39
7	0.0000	20.0076	0.5637	0.2892	0.0000	0.0000	0.0000	0.0000	0.91	0.00

Table B.2: Time constant estimates (case 2).

	CRMIP								CRMP	ICRM
i / j	1	2	3	4	5	6	7	8		
1	4.99	6.98	5.58	13.85	0.02	23.73	200.00	40.24	7.90	40.55
2	3.49	21.32	4.57	5.76	200.00	8.20	45.61	76.12	7.94	7.23
3	5.06	7.30	4.63	19.20	200.00	14.34	19.45	117.87	200.00	5.76
4	1.56	200.00	4.39	6.03	3.87	12.97	45.15	23.28	6.67	1.00
5	45.89	3.68	200.00	7.32	141.81	9.50	4.58	22.80	49.43	8.62
6	5.69	25.25	200.00	40.97	5.87	6.74	29.25	150.16	86.44	31.03
7	44.94	0.00	6.21	200.00	8.85	9.85	10.61	2.94	8.41	5.52

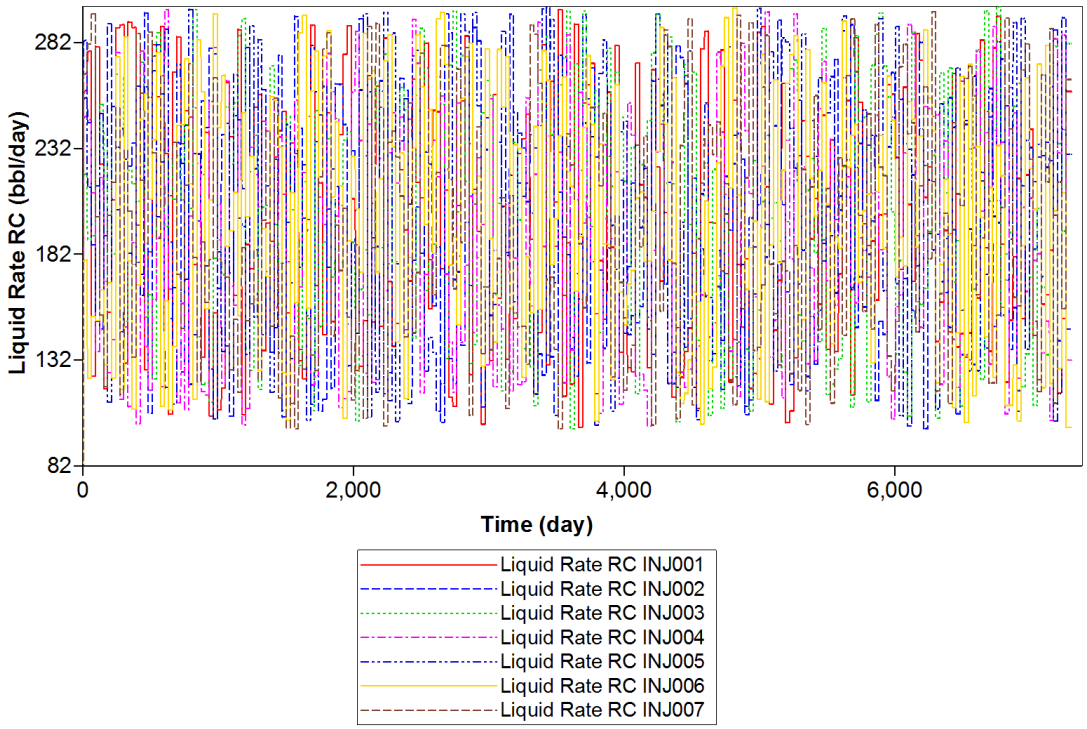

Figure B.1: Injection rates (bbl/day) for the eight injectors during simulation time (days) in case 2.

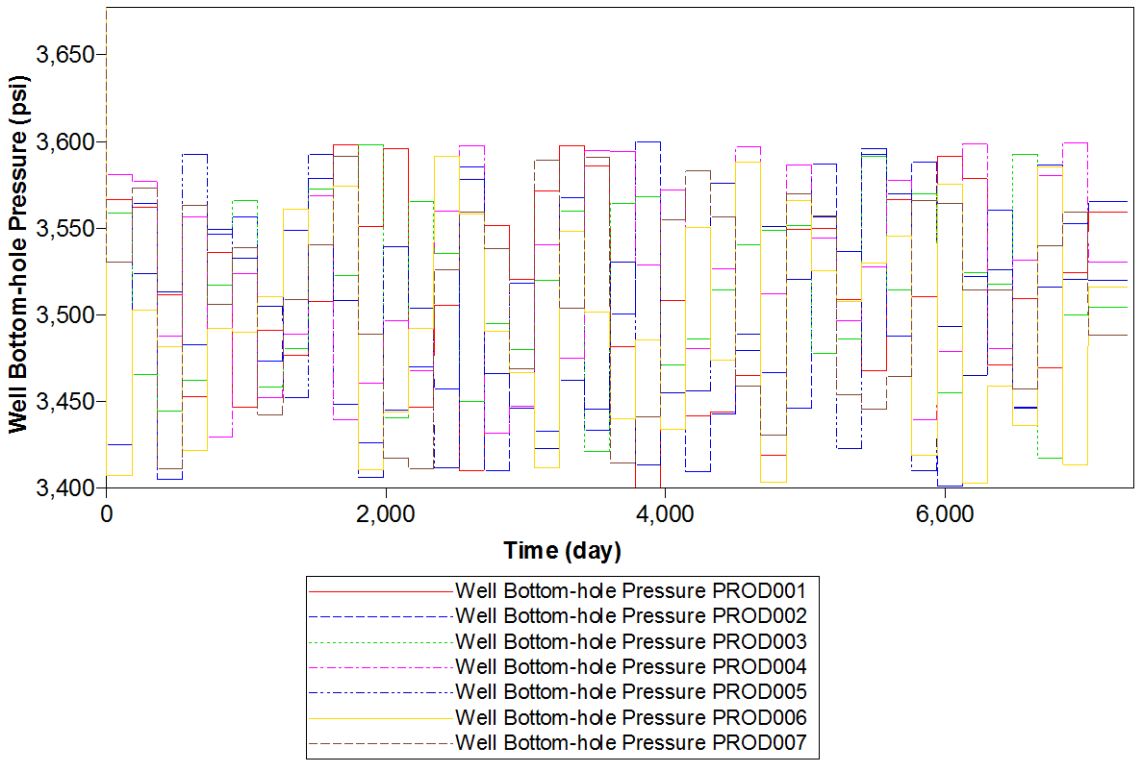

Figure B.2: Bottom hole pressures (psi) for the seven producers during simulation time (days) in case 2.

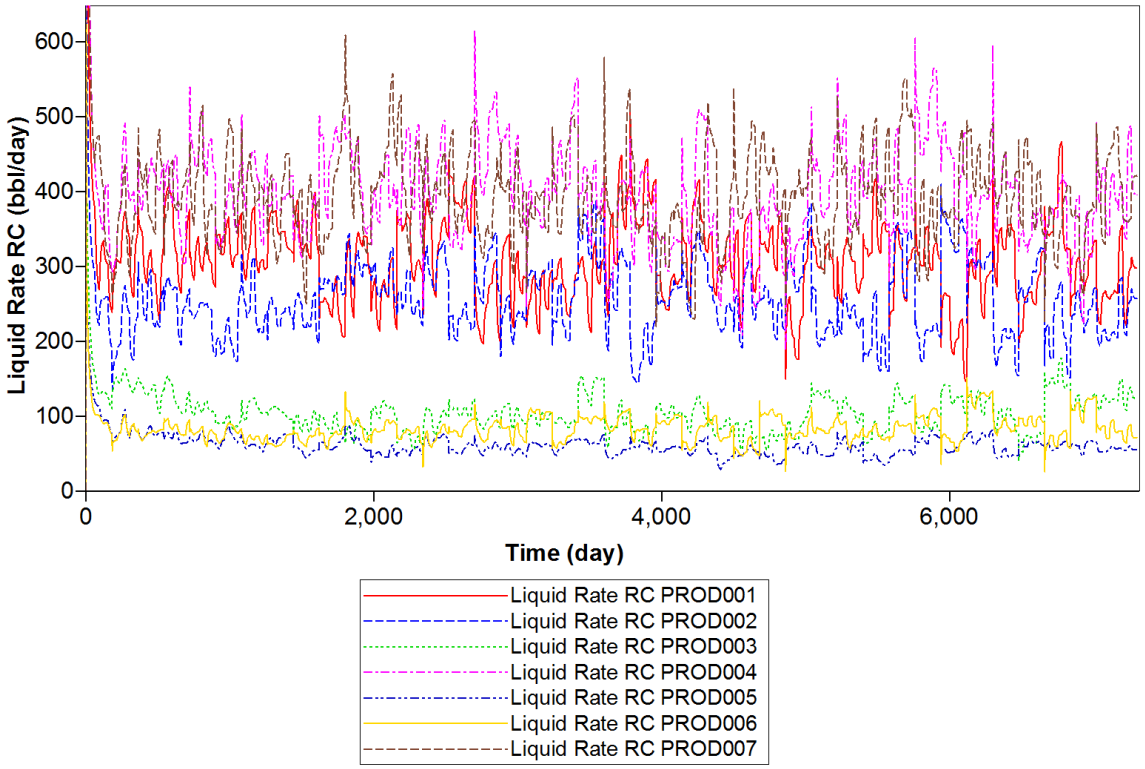

Figure B.3: Production rates (bbl/day) for the seven producers from production history (IMEX [36]) in case 2.

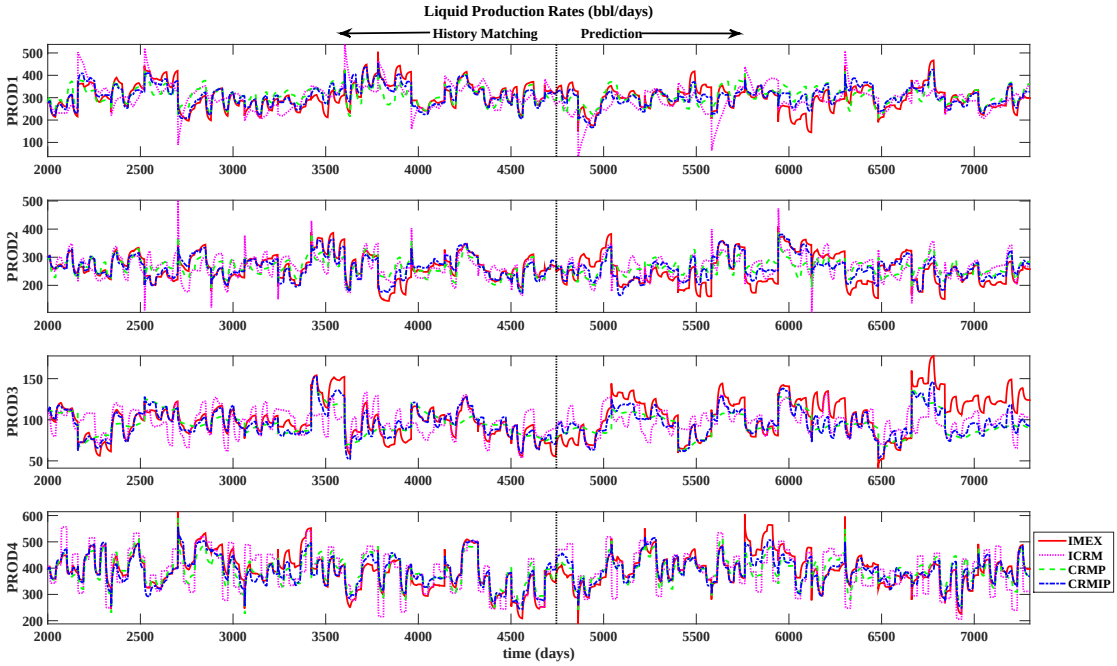

Figure B.4: Liquid production rates (bbl/days) for ICRM, CRMP and CRMIP compared to the production history for producers 1 to 4 (case 2).

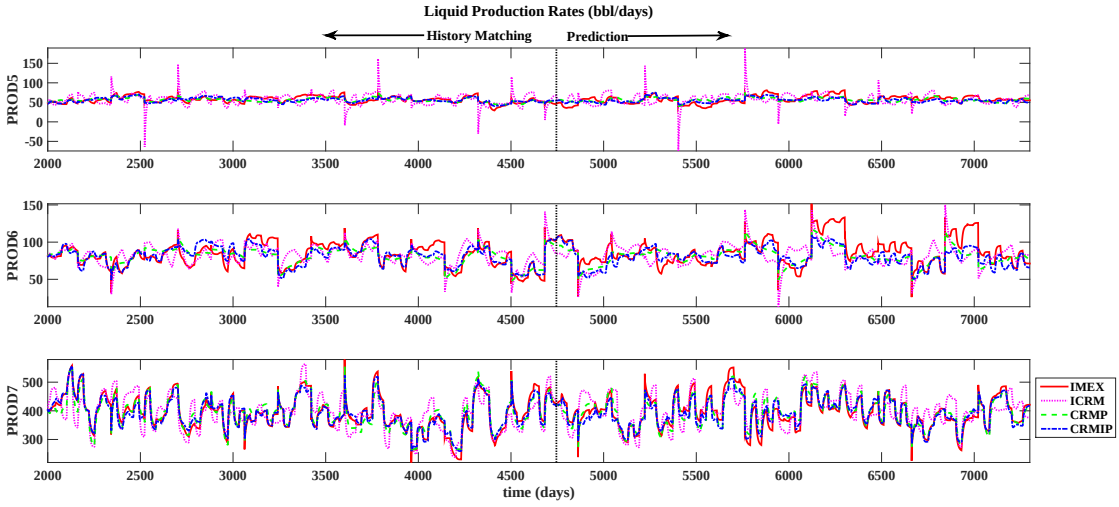

Figure B.5: Liquid production rates (bbl/days) for ICRM, CRMP and CRMIP compared to the production history for producers 5 to 7 (case 2).

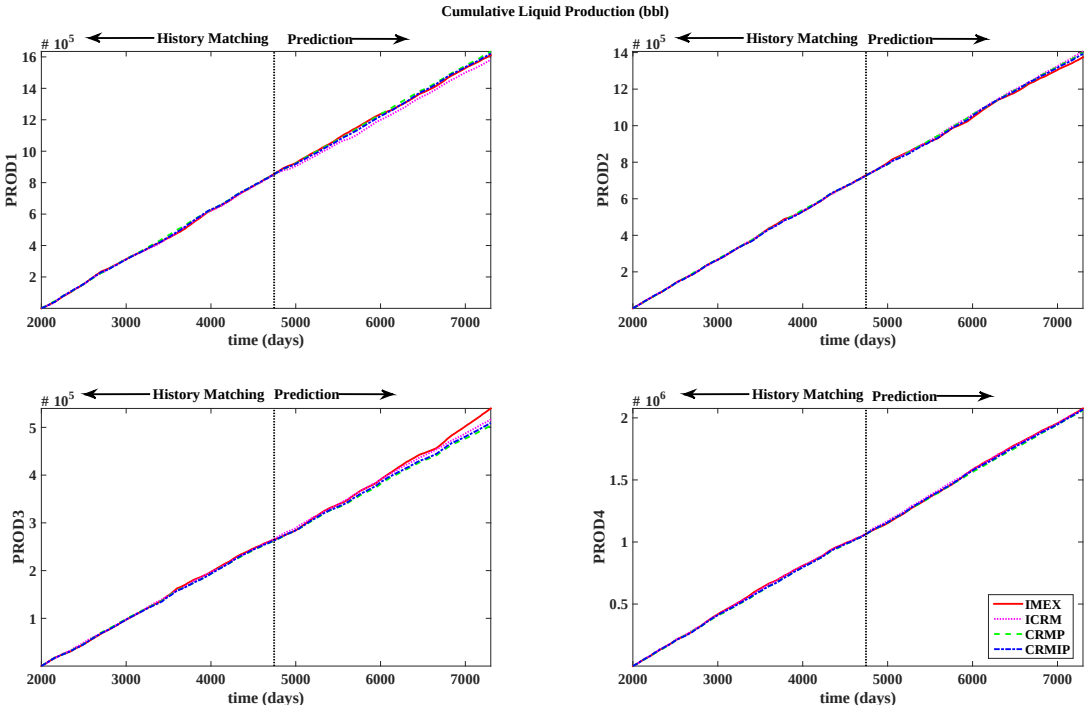

Figure B.6: Cumulative liquid production (bbl) for ICRM, CRMP and CRMIP compared to the production history for producers 1 to 4 (case 2).

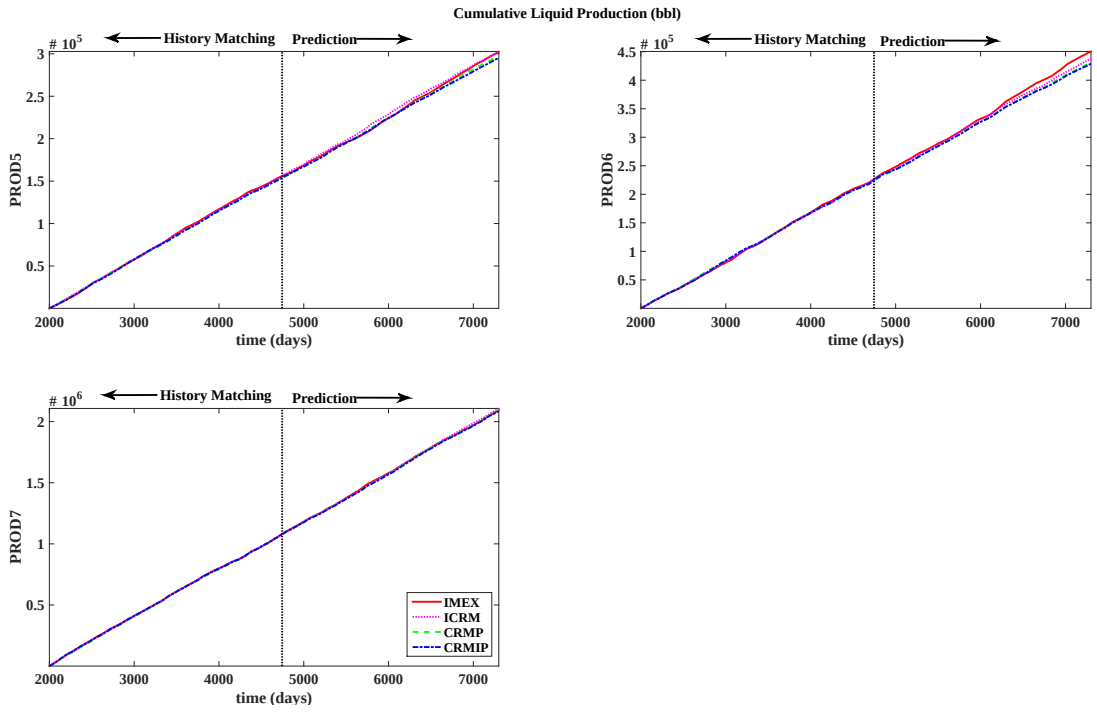

Figure B.7: Cumulative liquid production (bbl) for ICRM, CRMP and CRMIP compared to the production history for producers 5 to 7 (case 2).

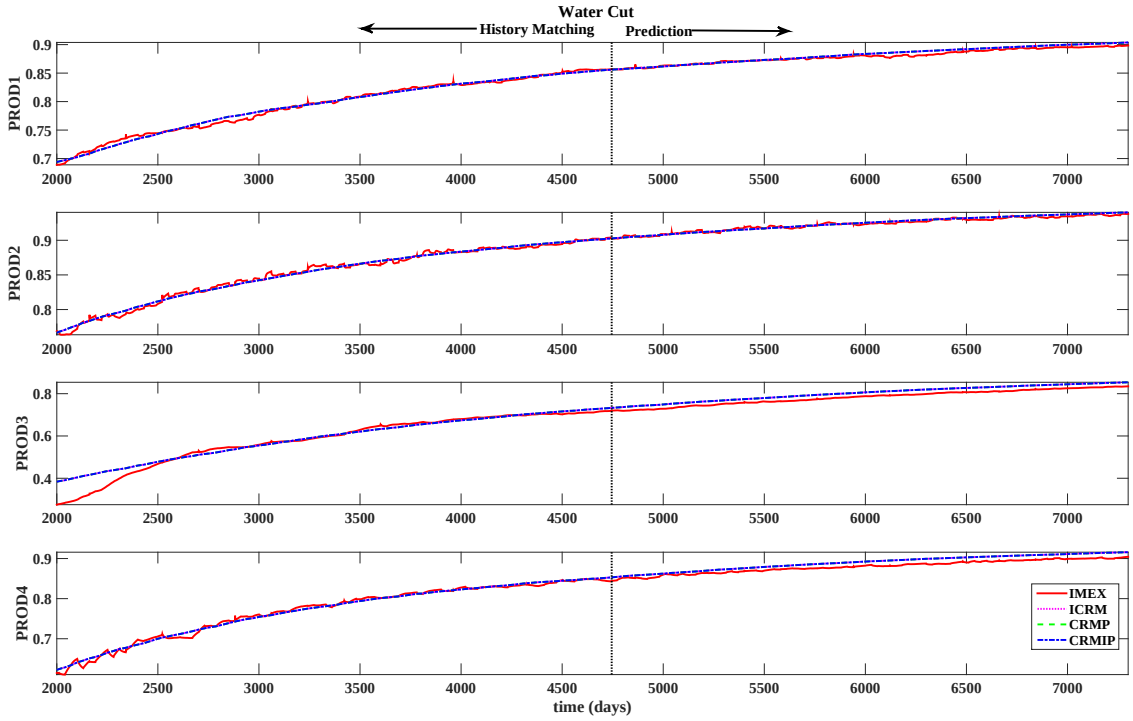

Figure B.8: Water cut for ICRM, CRMP and CRMIP compared to the production history for producers 1 to 4 (case 2).

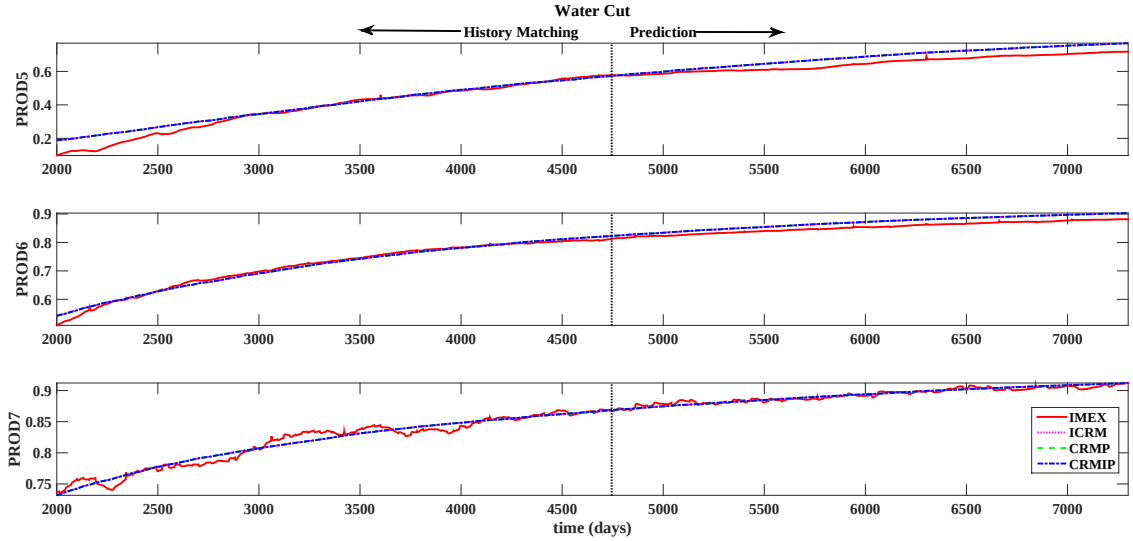

Figure B.9: Water cut for ICRM, CRMP and CRMIP compared to the production history for producers 5 to 7 (case 2).

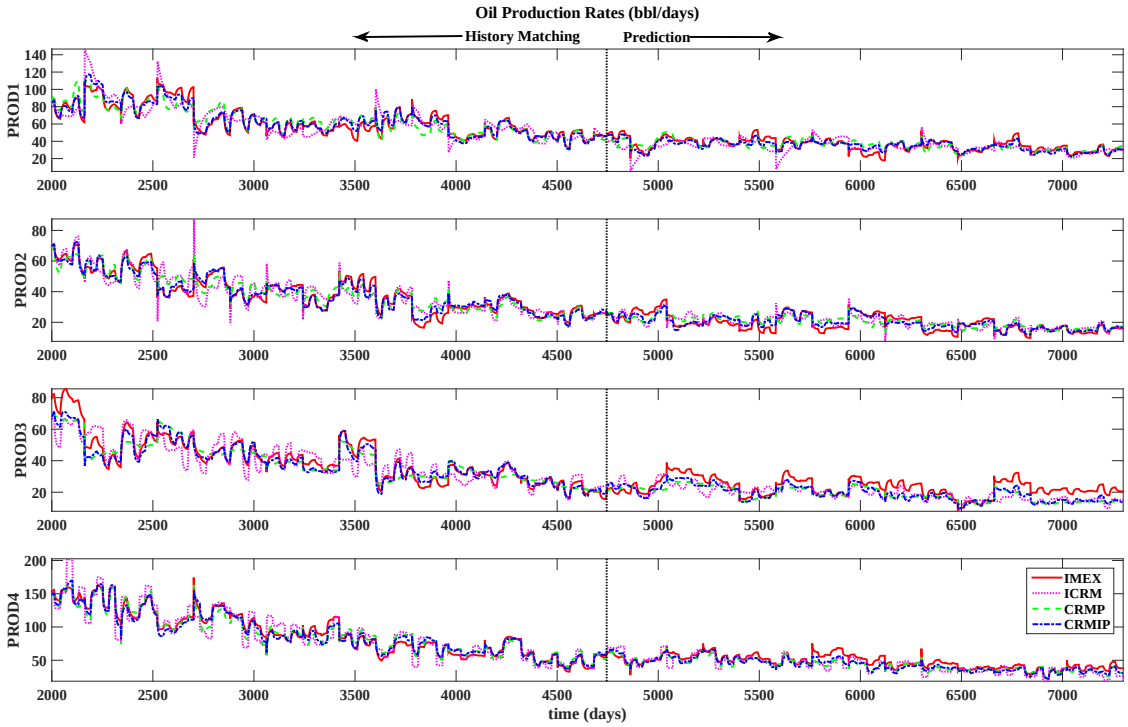

Figure B.10: Oil production rates (bbl/days) for ICRM, CRMP and CRMIP compared to the production history for producers 1 to 4 (case 2).

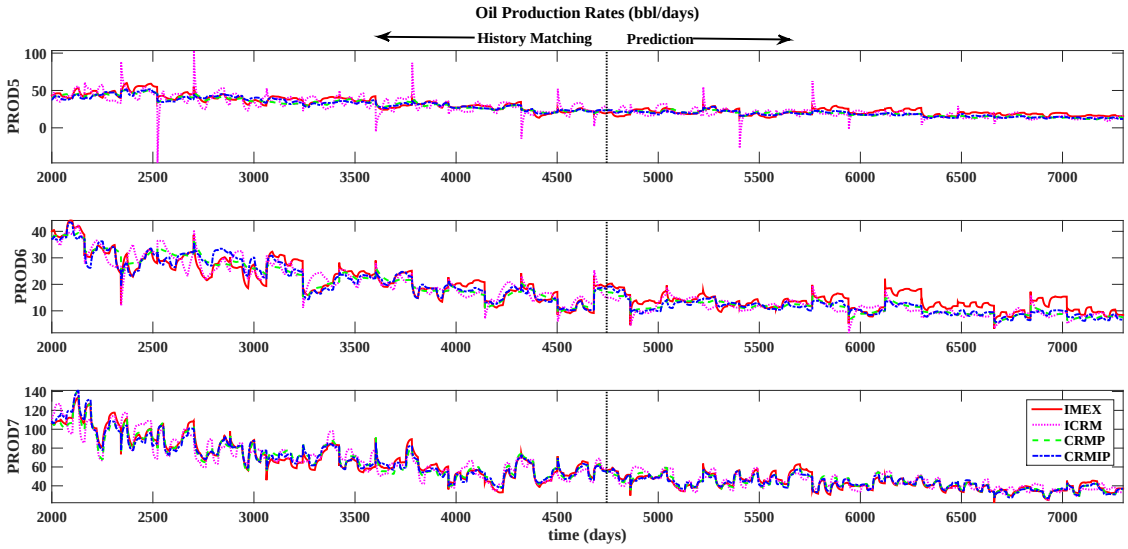

Figure B.11: Oil production rates (bbl/days) for ICRM, CRMP and CRMIP compared to the production history for producers 5 to 7 (case 2).

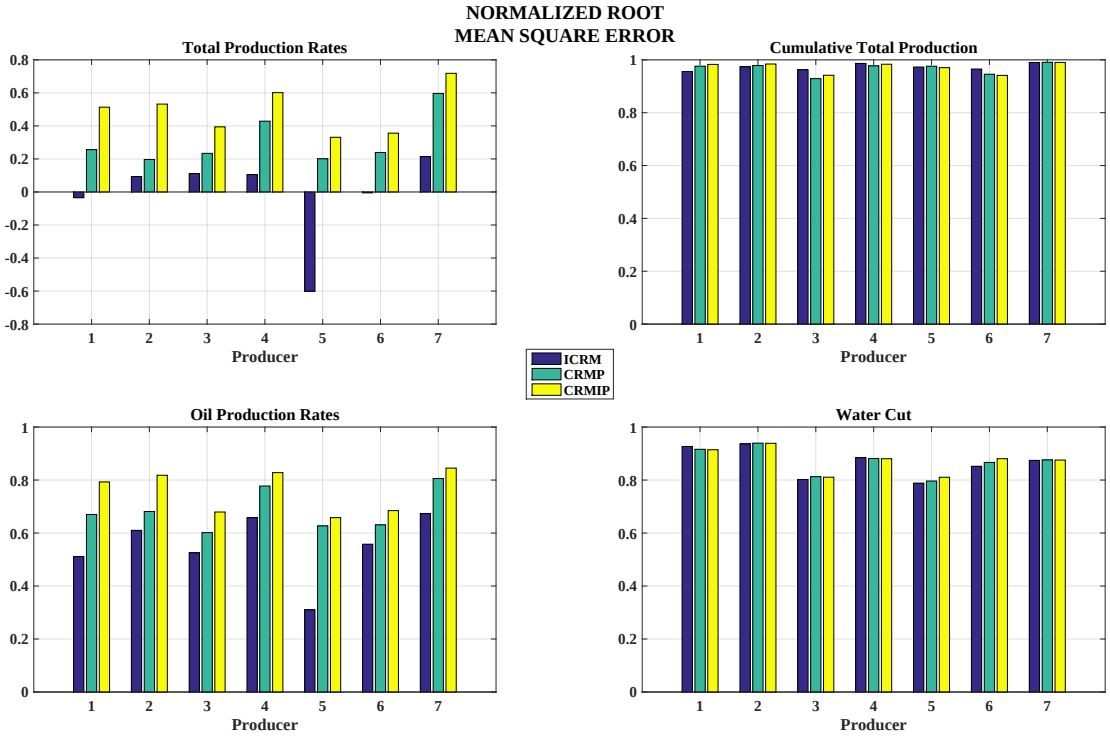

Figure B.12: Normalized root mean square error for ICRM, CRMP and CRMIP (case 2).

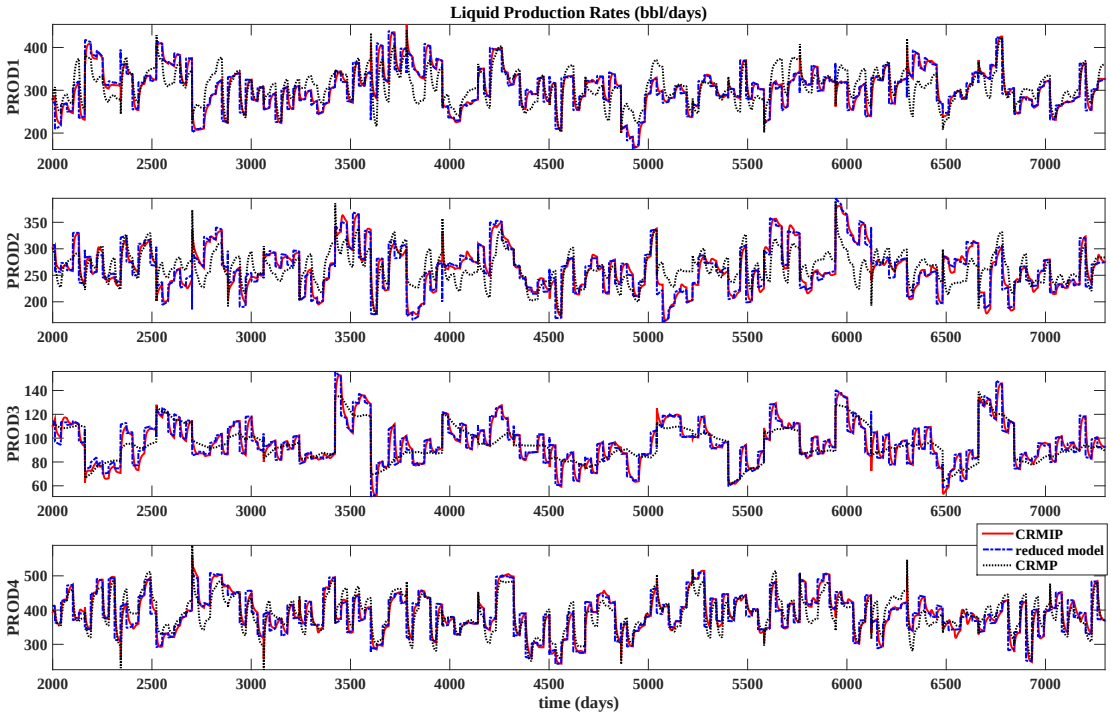

Figure B.13: Comparison between CRMP, CRMIP and reduced order model liquid production rates (bbl/days) for producer 1 to 4 (case 2).

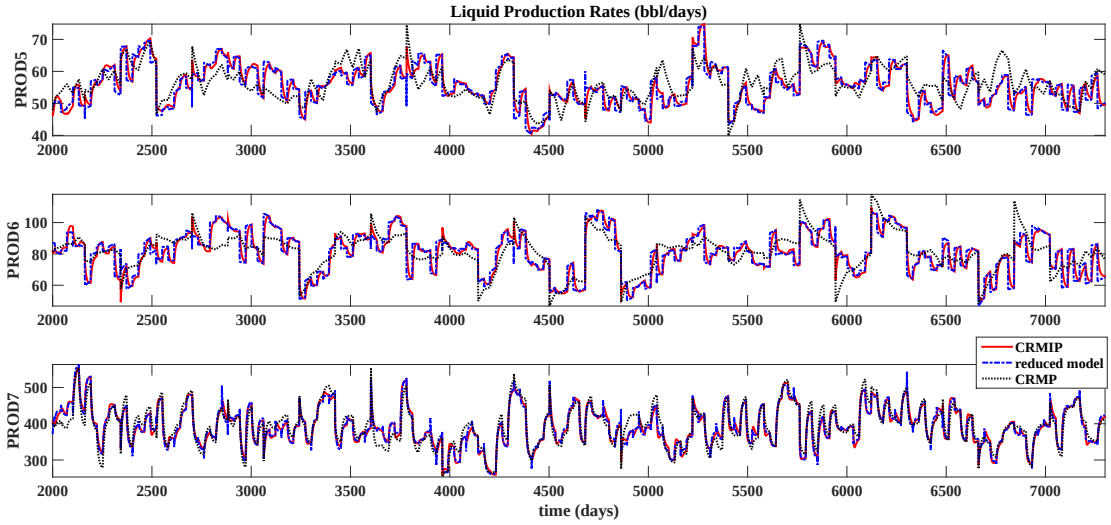

Figure B.14: Comparison between CRMP, CRMIP and reduced order model liquid production rates (bbl/days) for producer 5 to 7 (case 2).

Table B.3: Connectivity estimates (case 2).

	i \ j	1	2	3	4	5	6	7	8	sum
ICRM	1	0.039	0.000	0.915	0.000	0.000	0.000	0.539	0.000	1.493
	2	0.441	0.522	0.063	0.149	0.018	0.000	0.000	0.165	1.359
	3	0.177	0.202	0.018	0.000	0.098	0.000	0.000	0.000	0.495
	4	0.000	0.000	0.000	0.000	0.799	0.953	0.000	0.157	1.909
	5	0.197	0.045	0.000	0.008	0.043	0.000	0.000	0.000	0.293
	6	0.146	0.231	0.004	0.000	0.041	0.000	0.000	0.000	0.422
	7	0.000	0.000	0.000	0.843	0.000	0.047	0.461	0.678	2.029
	sum	1.000	1.000	1.000	1.000	1.000	1.000	1.000	1.000	
CRMP	1	0.525	0.387	0.373	0.096	0.000	0.000	0.190	0.000	1.572
	2	0.298	0.148	0.271	0.176	0.194	0.095	0.000	0.153	1.334
	3	0.000	0.232	0.062	0.000	0.000	0.180	0.000	0.000	0.474
	4	0.000	0.101	0.219	0.319	0.745	0.372	0.124	0.051	1.932
	5	0.072	0.016	0.043	0.113	0.041	0.004	0.000	0.000	0.288
	6	0.037	0.116	0.032	0.113	0.010	0.106	0.000	0.000	0.414
	7	0.069	0.000	0.000	0.183	0.010	0.243	0.686	0.796	1.987
	sum	1.000	1.000	1.000	1.000	1.000	1.000	1.000	1.000	
CRMIP	1	0.424	0.433	0.259	0.072	0.001	0.000	0.373	0.000	1.563
	2	0.409	0.224	0.178	0.236	0.075	0.072	0.000	0.157	1.351
	3	0.023	0.167	0.115	0.004	0.113	0.059	0.000	0.000	0.481
	4	0.000	0.149	0.207	0.323	0.664	0.449	0.000	0.151	1.943
	5	0.000	0.000	0.096	0.047	0.068	0.053	0.016	0.000	0.278
	6	0.000	0.028	0.145	0.040	0.053	0.137	0.000	0.000	0.404
	7	0.143	0.000	0.000	0.278	0.026	0.230	0.611	0.692	1.980
	sum	1.000	1.000	1.000	1.000	1.000	1.000	1.000	1.000	

Table B.4: Fractional flow parameters estimates for ICRM, CRMP and CRMIP (case 2).

Producer		1	2	3	4	5	6	7
ICRM	a	1.15E-06	2.40E-07	2.34E-10	4.77E-09	3.30E-12	2.93E-09	2.55E-06
	b	1.0908	1.2424	1.7752	1.4501	2.1328249	1.6420371	1.0231165
CRMP	a	5.43E-07	3.55E-07	3.82E-10	4.88E-09	5.97E-12	5.12E-09	2.61E-06
	b	1.1403	1.2151	1.7411	1.4496	2.0911196	1.6017791	1.02162
CRMIP	a	5.72E-07	2.96E-07	4.26E-10	4.38E-09	1.24E-11	8.51E-09	2.59E-06
	b	1.1376	1.2275	1.7312	1.4562	2.0336131	1.5621142	1.022304

APPENDIX C

DATA AND RESULTS FOR CASE 3

Table C.1: Productivity indices estimates (case 3).

	CRMIP								CRMP	ICRM
i / j	1	2	3	4	5	6	7	8		
1	0.0000	0.0000	0.1831	0.0000	0.0000	0.0000	0.0000	0.0000	0.19	0.42
2	0.0000	0.0000	0.0000	0.0000	0.0000	0.0000	0.0000	0.0618	0.06	0.00
3	0.0000	0.1255	0.0000	0.6373	0.2740	0.0000	0.0000	0.0000	0.77	0.56
4	0.0000	0.0000	0.0000	0.0000	0.0000	0.0000	0.3313	0.0000	0.33	0.00
5	0.0000	0.0426	0.0000	0.0000	0.1137	0.0085	0.0000	0.0000	0.11	6.07
6	0.0000	0.0000	0.1082	0.0000	0.0000	0.0022	0.0000	0.0000	0.11	0.04
7	0.0000	0.0026	0.0000	0.0000	0.0115	0.0258	0.0000	0.0000	0.03	0.00

Table C.2: Time constant estimates (case 3).

	CRMIP								CRMP	ICRM
i / j	1	2	3	4	5	6	7	8		
1	4.67	24.84	200.00	26.27	27.41	22.26	85.23	31.54	200.00	74.85
2	11.78	3.46	117.25	104.80	11.96	8.60	53.81	200.00	200.00	63.85
3	15.62	7.06	8.04	200.00	5.83	20.74	56.29	173.46	124.78	47.03
4	8.56	100.15	9.03	11.22	16.18	3.64	200.00	93.72	200.00	1.00
5	36.13	2.83	43.10	19.54	200.00	0.79	32.87	33.40	102.88	1.00
6	21.72	115.32	200.00	15.04	9.56	200.00	39.18	37.71	200.00	76.36
7	28.07	5.23	200.00	50.16	15.69	200.00	108.51	22.54	78.04	200.00

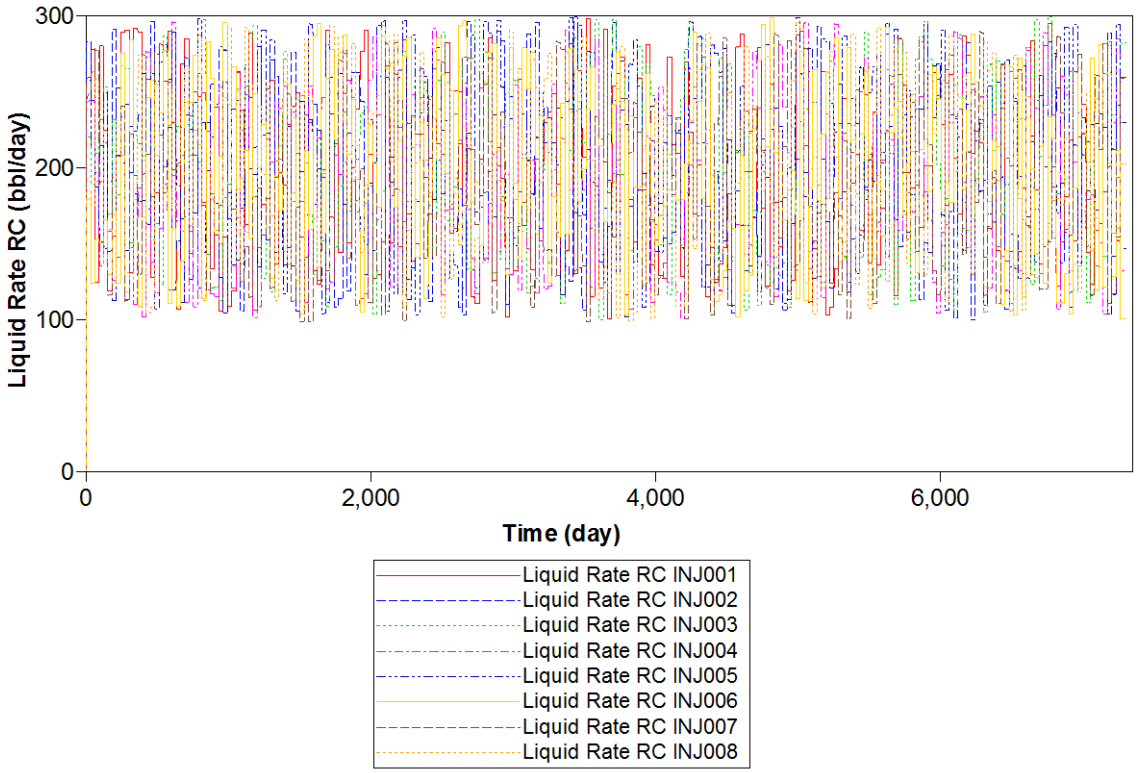

Figure C.1: Injection rates (bbl/day) for the eight injectors during the simulation time (days) in case 3.

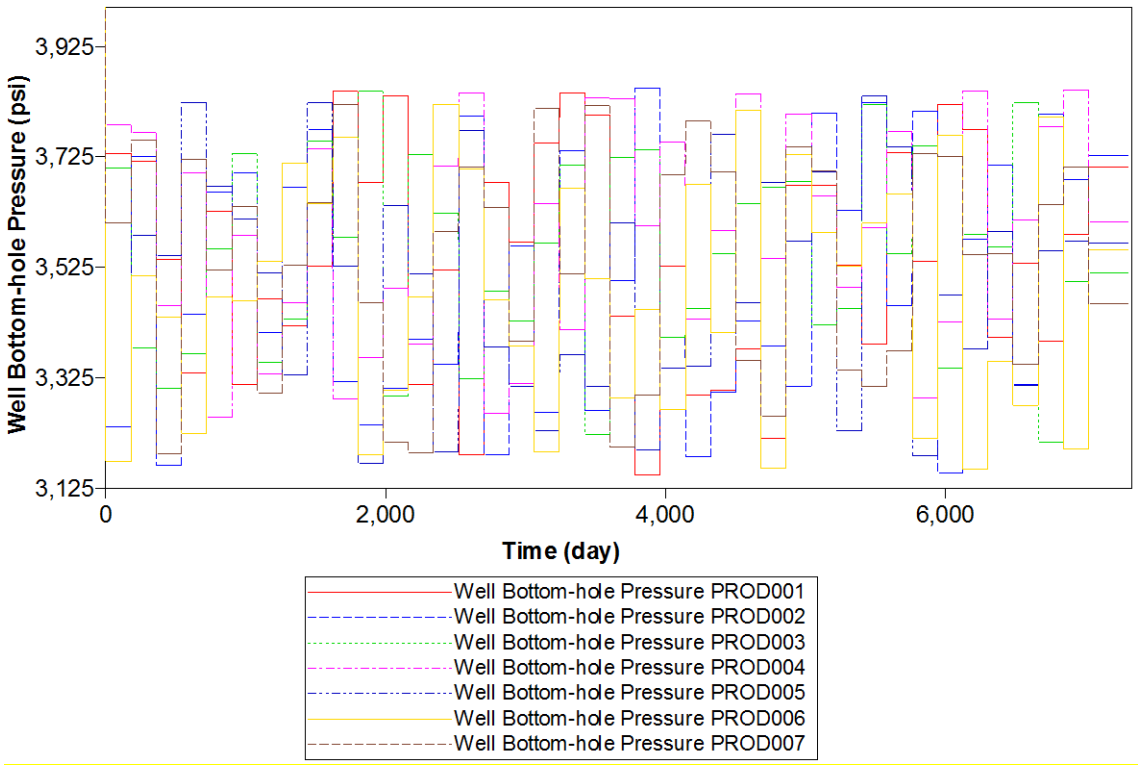

Figure C.2: Bottom hole pressures (psi) for the seven producers during simulation time (days) in case 3.

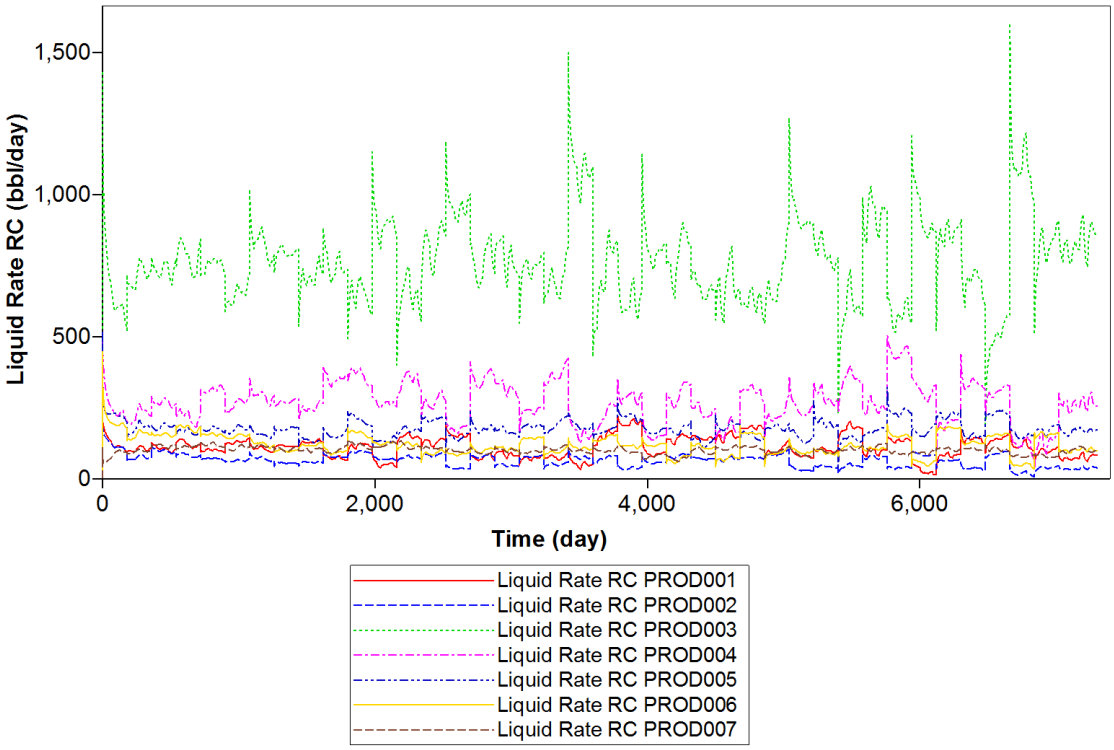

Figure C.3: Production rates (bbl/day) for the seven producers from production history (IMEX [36]) in case 3.

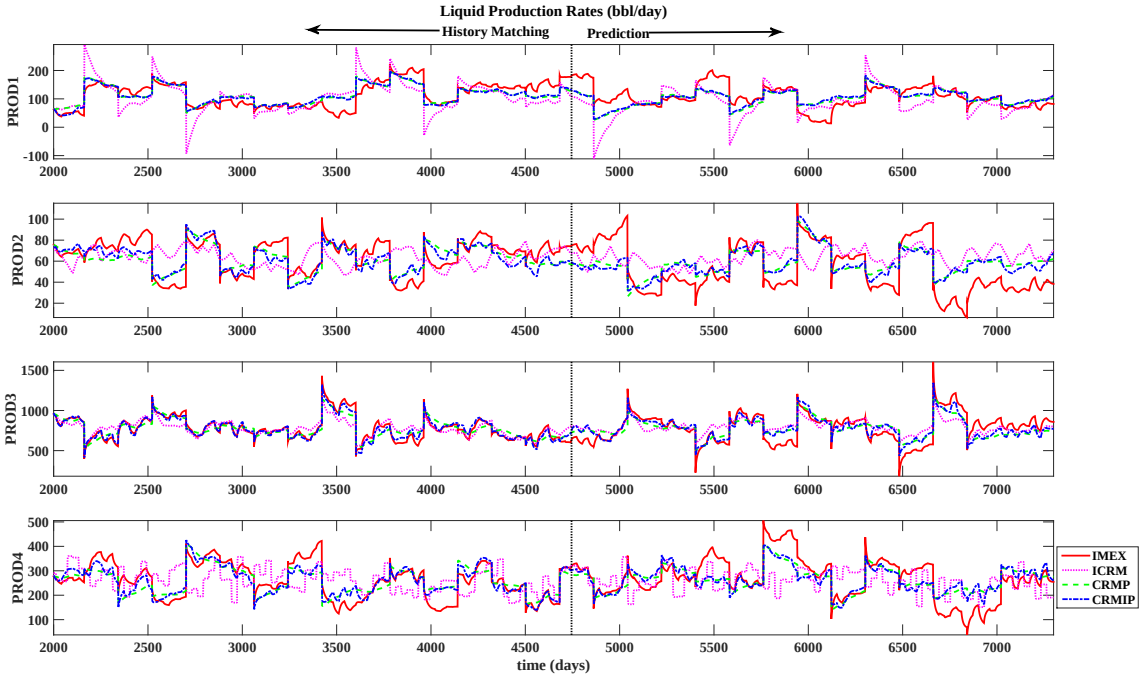

Figure C.4: Liquid production rates (bbl/days) for ICRM, CRMP and CRMIP compared to the production history for producers 1 to 4 (case 3).

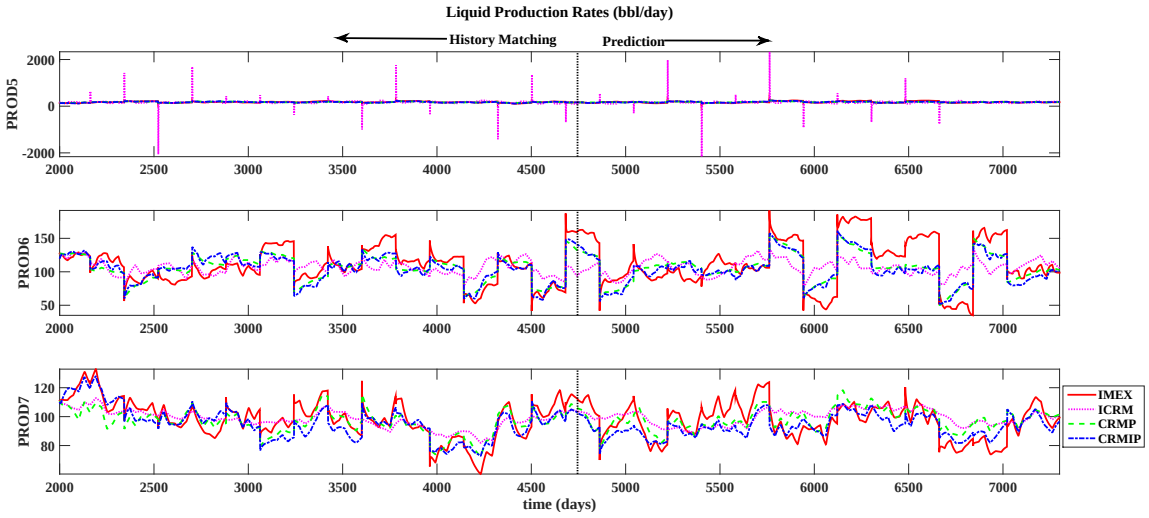

Figure C.5: Liquid production rates (bbl/days) for ICRM, CRMP and CRMIP compared to the production history for producers 5 to 7 (case 3).

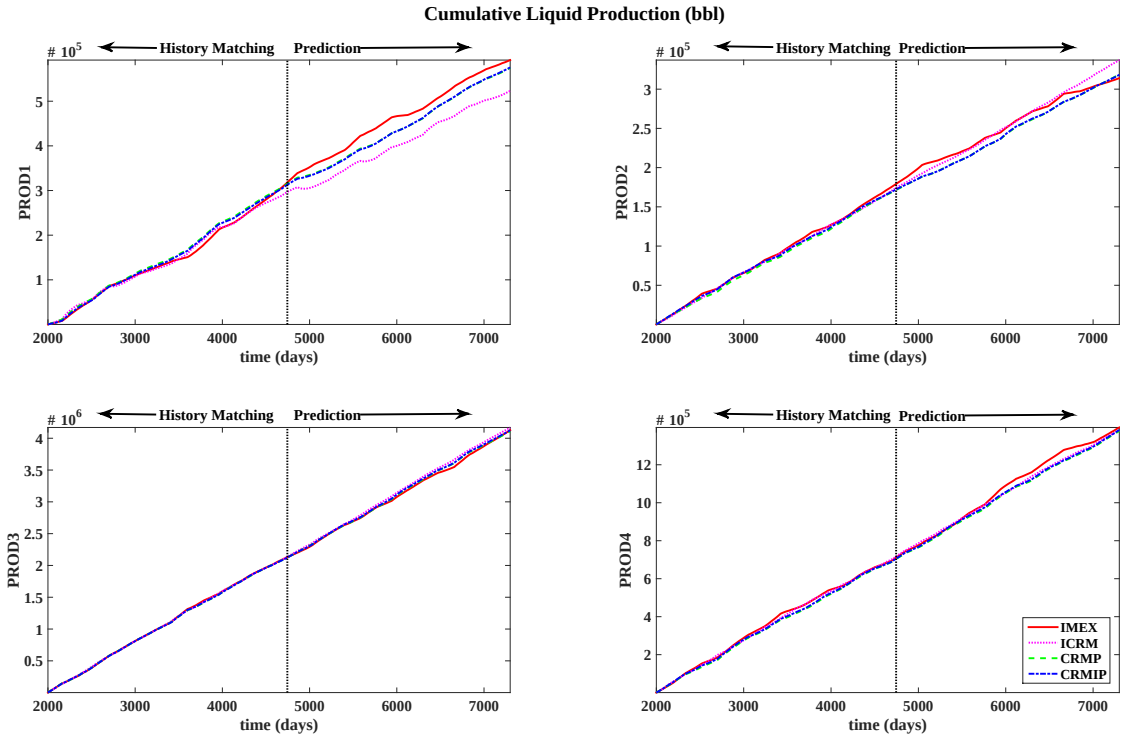

Figure C.6: Cumulative liquid production (bbl) for ICRM, CRMP and CRMIP compared to the production history for producers 1 to 4 (case 3).

Table C.3: Fractional flow parameters estimates for ICRM, CRMP and CRMIP (case 3).

Producer		1	2	3	4	5	6	7
ICRM	a	3.35E-06	8.83E-09	1.19E-06	1.23E-07	1.48E-10	1.16E-10	0.000104
	b	1.0900	1.5232	1.0521	1.2681	1.761504	1.774041	0.803848
CRMP	a	2.96E-06	6.47E-09	1.24E-06	1.24E-07	1.15E-10	1.27E-10	0.000108
	b	1.0933	1.5486	1.0496	1.2686	1.778902	1.76859	0.801542
CRMIP	a	2.68E-06	6.34E-09	1.26E-06	1.04E-07	1.17E-10	1.64E-10	0.000127
	b	1.1003	1.5518	1.0485	1.2802	1.776636	1.751157	0.791362

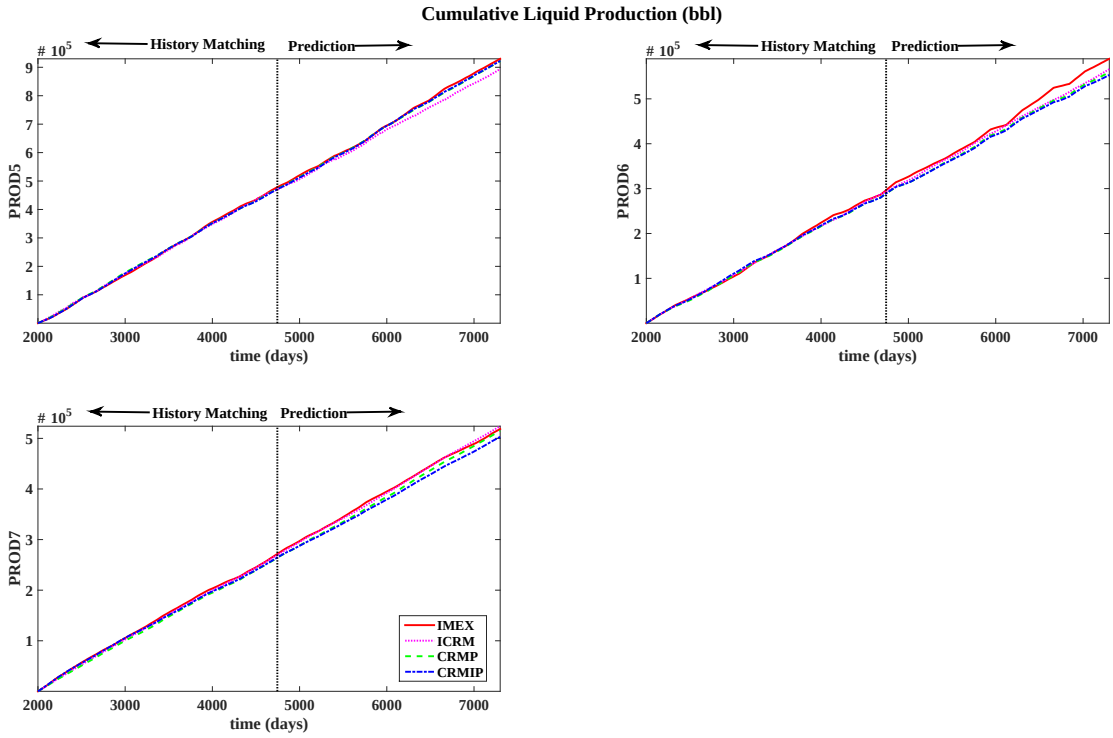

Figure C.7: Cumulative liquid production (bbl) for ICRM, CRMP and CRMIP compared to the production history for producers 5 to 7 (case 3).

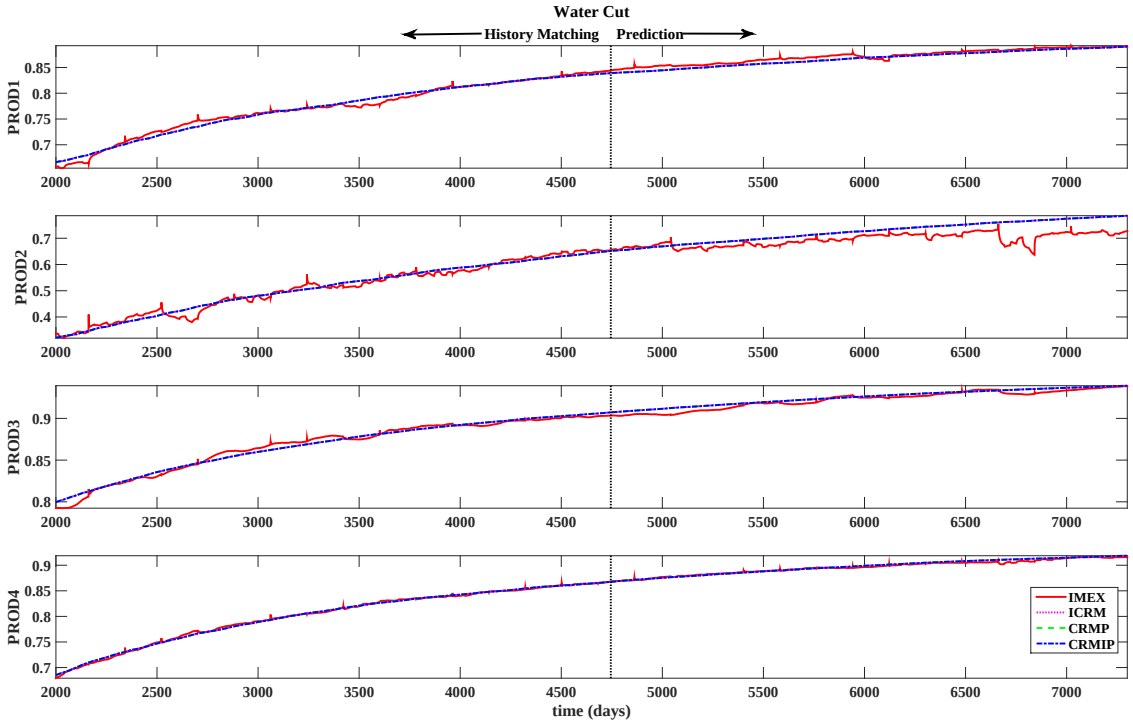

Figure C.8: Water cut for ICRM, CRMP and CRMIP compared to the production history for producers 1 to 4 (case 3).

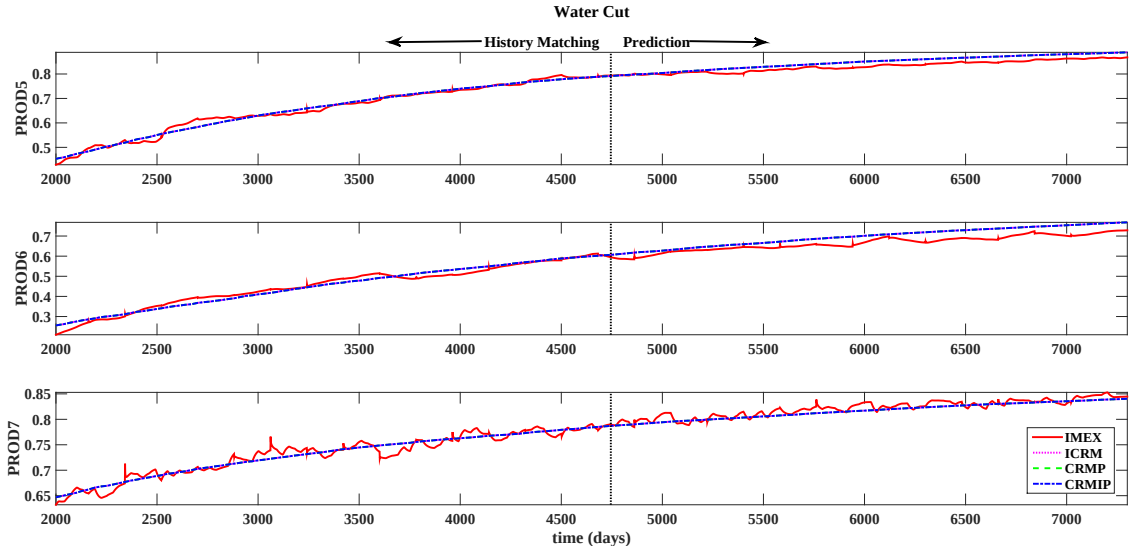

Figure C.9: Water cut for ICRM, CRMP and CRMIP compared to the production history for producers 5 to 7 (case 3).

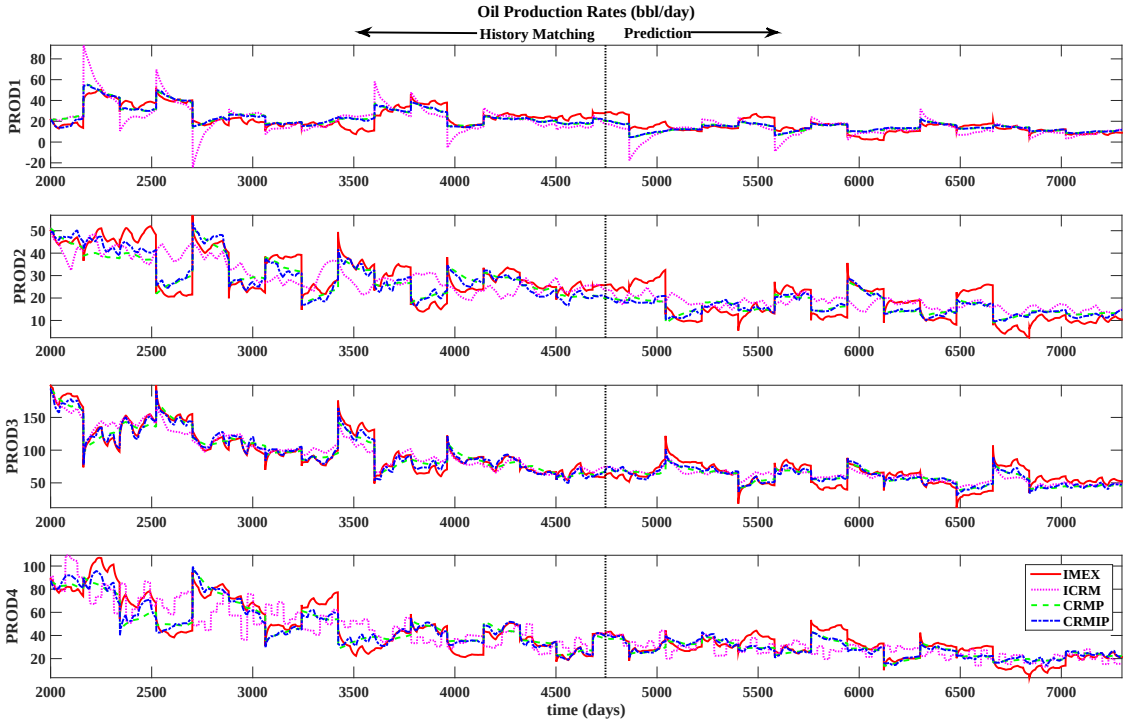

Figure C.10: Oil production rates (bbl/days) for ICRM, CRMP and CRMIP compared to the production history for producers 1 to 4 (case 3).

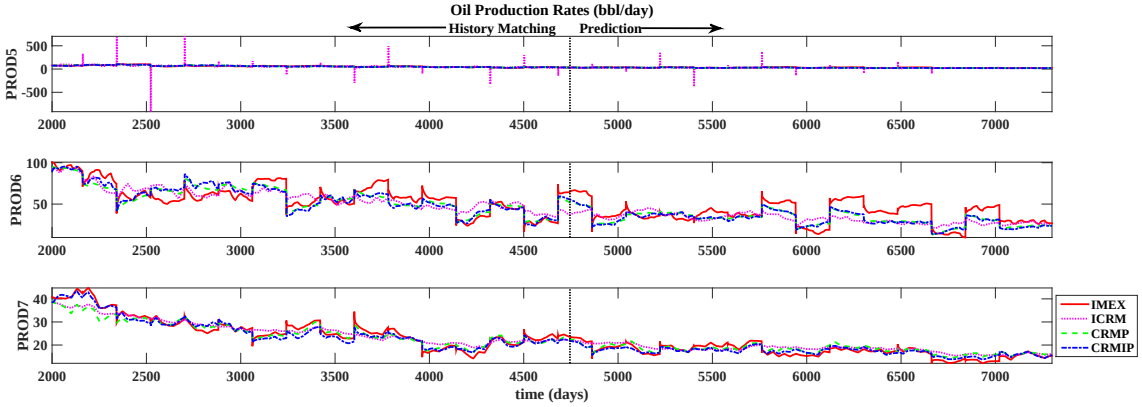

Figure C.11: Oil production rates (bbl/days) for ICRM, CRMP and CRMIP compared to the production history for producers 5 to 7 (case 3).

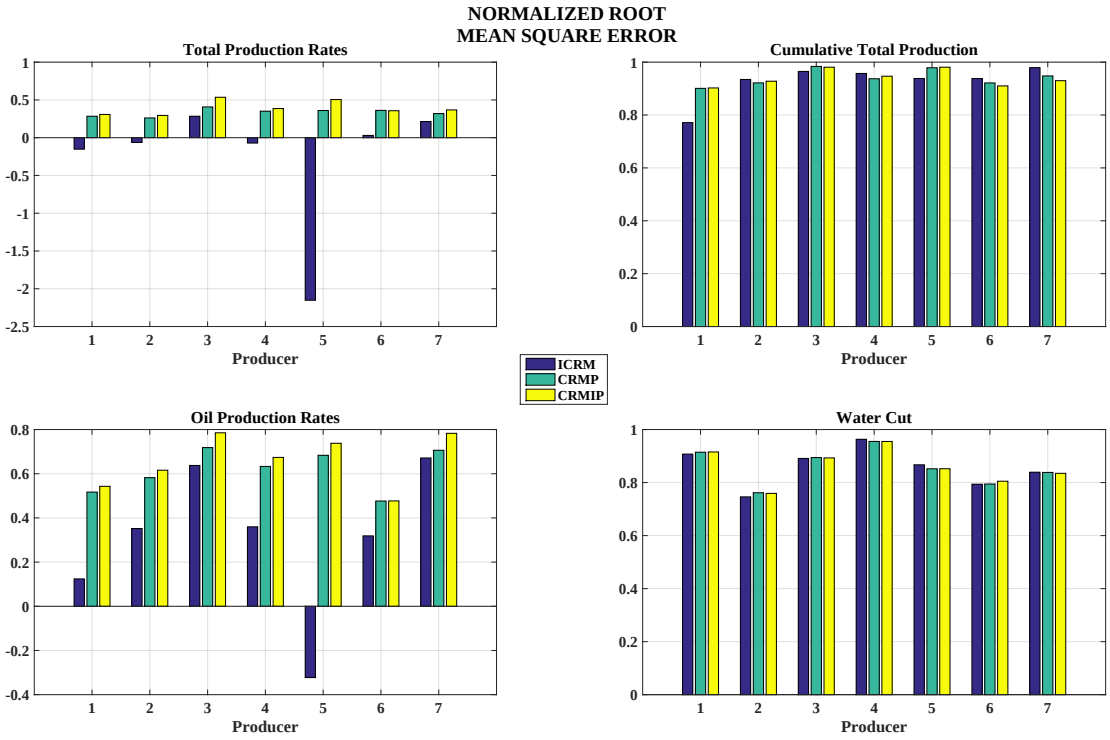

Figure C.12: Normalized root mean square error for ICRM, CRMP and CRMIP (case 3).

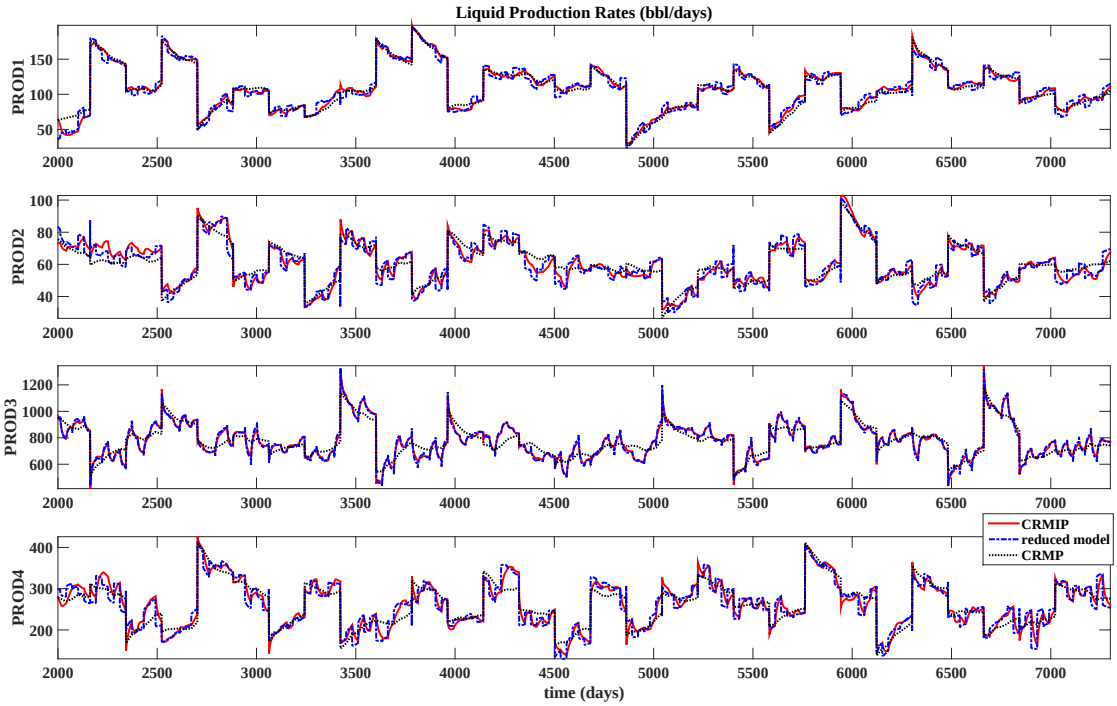

Figure C.13: Comparison between CRMP, CRMIP and reduced order model liquid production rates (bbl/days) for producer 1 to 4 (case 3).

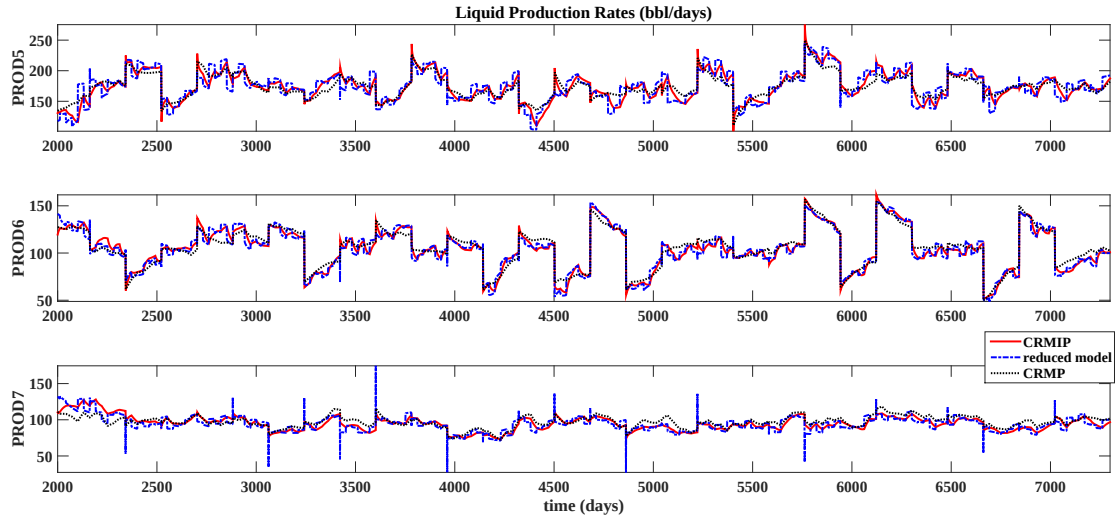

Figure C.14: Comparison between CRMP, CRMIP and reduced order model liquid production rates (bbl/days) for producer 5 to 7 (case 3).

Table C.4: Connectivity estimates (case 3).

	i \ j	1	2	3	4	5	6	7	8	sum
ICRM	1	0.000	0.000	0.476	0.000	0.000	0.000	0.015	0.000	0.491
	2	0.000	0.003	0.000	0.000	0.000	0.000	0.324	0.000	0.327
	3	1.000	0.329	0.074	1.000	0.775	0.262	0.286	0.282	4.008
	4	0.000	0.000	0.000	0.000	0.000	0.738	0.073	0.481	1.292
	5	0.000	0.232	0.450	0.000	0.157	0.000	0.001	0.000	0.840
	6	0.000	0.436	0.000	0.000	0.068	0.000	0.036	0.000	0.540
	7	0.000	0.000	0.000	0.000	0.000	0.000	0.265	0.237	0.502
	sum	1.000	1.000	1.000	1.000	1.000	1.000	1.000	1.000	
CRMP	1	0.000	0.000	0.287	0.000	0.000	0.000	0.264	0.000	0.551
	2	0.000	0.095	0.129	0.000	0.000	0.000	0.082	0.000	0.306
	3	0.837	0.415	0.544	0.678	0.000	0.877	0.000	0.575	3.926
	4	0.000	0.155	0.000	0.000	0.630	0.123	0.119	0.269	1.296
	5	0.163	0.013	0.040	0.088	0.267	0.000	0.313	0.000	0.885
	6	0.000	0.321	0.000	0.112	0.103	0.000	0.000	0.000	0.536
	7	0.000	0.000	0.000	0.121	0.000	0.000	0.222	0.156	0.499
	sum	1.000	1.000	1.000	1.000	1.000	1.000	1.000	1.000	
CRMIP	1	0.038	0.000	0.238	0.000	0.000	0.000	0.281	0.000	0.558
	2	0.062	0.008	0.115	0.000	0.029	0.000	0.089	0.000	0.303
	3	0.612	0.468	0.547	0.532	0.306	0.716	0.000	0.749	3.929
	4	0.038	0.375	0.000	0.285	0.321	0.126	0.000	0.176	1.321
	5	0.144	0.000	0.036	0.113	0.289	0.009	0.298	0.000	0.890
	6	0.082	0.150	0.063	0.056	0.055	0.069	0.049	0.000	0.524
	7	0.024	0.000	0.000	0.014	0.000	0.079	0.283	0.074	0.474
	sum	1.000	1.000	1.000	1.000	1.000	1.000	1.000	1.000	